STRUCTURE OF RNA TUMOR VIRUS GENOME

Thesis by Hsing-Jien Kung

In partial fulfillment of the requirements
for the degree of
Doctor of Philosophy

California Institute of Technology
Pasadena, California 91125

1976

(Submitted December 16, 1975)

To My Mother and My Wife

ACKNOWLEDGEMENTS

It is my great privilege to work under the direction of Professor Norman Davidson. I am most grateful for his close supervision and his skillful, patient guidance throughout all phases of my graduate studies. His continuous concern and encouragement have made my staying here both enlightening and enjoyable.

I would like to thank Dr. Shyam Dube for his valuable advice and infectious enthusiasm for science. The pleasant association with him has meant a great deal to me.

I also wish to thank the following colleagues:

Drs. Ming-Ta Hsu and Louise T. Chow, for teaching me the electron microscopic techniques during the initial stage of this work.

Dr. Jim Bailey, Welcome Bender and Sylvia Hu, for the pleasant collaborations we had.

Drs. Jim Casey, Dave Hershey, Tom Broker and Peter Chandler for the good times we shared together.

Drs. M. Nicholson, R. McAllister and P. Vogt are gratefully acknowledged for providing virus samples of the best quality for my studies.

Also, special thanks to Drs. A. Y. Lau and Y. C. Chien for their helpful discussions and suggestions during the preparation of Propositions IV and V.

ABSTRACT

Part I of the thesis describes the characterization of the RNA structure of the RNA tumor viruses.

The genome of type C RNA tumor viruses is an RNA complex which sediments at "50-60"S in a nondenaturing aqueous electrolyte. Upon exposure to denaturing conditions, it can be dissociated into subunits of "30-40"S plus small "4-10"S RNA's. The structure and molecular weight of the "50-60"S and "30-40"S RNA species have been studied by electronmicroscopy, gel electrophoresis and sedimentation analysis. It was found that type C viruses, isolated from different origins (feline, murine, simian and baboon) all contain as their genomes "50-60"S RNA species which have similar secondary structure patterns. The "50-60"S molecule has a molecular length about 16-20 Kb ($\sim 6 \times 10^6$ daltons) as measured by electronmicroscopy. It contains two characteristic secondary structure features (i) a central T-shaped structure (the dimer linkage structure) (ii) two loops symmetrically positioned on each side of the dimer linkage structure. Melting of the dimer linkage structure resulted in a concomitant dissociation of the 52S molecule into two half-size subunits, each about 8-10 Kb. PolyA mapping by electronmicroscopy shows that the "50-60"S molecules contain two polyA segments, one at each end.

These results suggest that the "50-60"S RNA consists of two 8-10 Kb or "30-40"S subunits, each with a characteristic secondary structure loop. These two subunits which are possibly identical are

joined at their 5' ends within the dimer linkage structure. The primary nucleotide sequence, the molecular weight and the stability of the "50-60"S RNA is different for each different virus. Yet, the finding that these different viral RNA's contain similar secondary structure patterns suggests that such features are functionally important. If this is true, it is possible that they are present in all type C virus genomes.

In part II, an electronmicroscopic technique for studying single-stranded RNA is described. This technique has been applied to determine the molecular weight, to study the secondary structure and to map the polyA sequence of RNA isolated from an arbovirus (Sindbis).

This spreading technique utilizes glyoxal as a denaturing agent. Glyoxal reacts preferentially with guanine residues of polynucleotides and blocks their hydrogen binding donor functions. Single-stranded RNA, after treatment with glyoxal, appears as an extended filament whose length can be accurately measured by electronmicroscopy. By this means, the molecular weight of Sindbis virus RNA is determined to be $4.7 \pm 0.4 \times 10^6$ daltons. Glyoxal treatment is useful for the electronmicroscopic mapping of polyA sequences on RNA molecules, since the RNA is extended without affecting the polydT binding which is the basis for polyA mapping. Using this method, a polyA sequence has been mapped at one end of Sindbis virus RNA. Many circular molecules are seen when Sindbis RNA is treated for only short periods with glyoxal, then spread for electron-

microscopy. Under more denaturing conditions, linear molecules are seen. It is proposed that the two ends of Sindbis viral RNA contain mutually complementary sequences which normally are base-paired to form circular molecules. Under the more denaturing conditions hydrogen bonding is disrupted, which produces linear molecules.

TABLE OF CONTENTS

Part I

Structure of RNA Tumor Virus Genome

Chapter 1

RSV (Avian Sarcoma Virus)

FeLV (Feline Leukemia Virus)

Electron Microscope Studies of Tumor Virus RNA*

HSING JIEN KUNG, JAMES M. BAILEY, AND
NORMAN DAVIDSON

Department of Chemistry
California Institute of Technology
Pasadena, California 91109

and

PETER K. VOGT, MARGERY O. NICOLSON, AND
ROBERT M. McALLISTER

University of Southern California School of Medicine
Los Angeles, California 90054

---

* Contribution number: 4925

ABSTRACT

The "50-60"S RNA's isolated from an avian sarcoma virus (RSV) and a feline leukemia virus (FeLV) were studied by electron-microscopy. When spread in low denaturing conditions, they appear as tangled complexes with a great deal of secondary structure. If treated with glyoxal which is quite effective in disrupting secondary structure of polynucleotide chains, the "50-60"S RNA's of both RSV and FeLV are dissociated into subunits with the appearance of well extended filaments. The molecular weights of the RNA subunits were determined to be 3.3 and 3.2 x 10^6 daltons for RSV and FeLV respectively, in good agreement with the sedimentation data. The RNA of a feline endogenous virus, RD-114 virus, has also been studied. After similar glyoxal treatment, RD-114 viral RNA has a molecular weight about 5 x 10^6 daltons, significantly larger than those observed for RSV and FeLV.

The principal component of the RNA of the RNA tumor viruses, as extracted from the virion, is a complex which sediments at 60-70S, and is estimated to have a molecular weight of approximately 10^7 daltons. When subjected to denaturing conditions, this complex dissociates to give several large components with sedimentation coefficients of ~ 35S and some lower molecular weight components with sedimentation coefficients in the range 4-10S. The mobilities in gel electrophoresis for these several large and small components are consistent with molecular weight estimates from their sedimentation coefficients (Temin, 1974; Bolognesi, 1974).

Electron microscopy has the potential of being a useful physical method for the study of the molecular structure of the 60-70S complex and of the several subunits of which it is composed. We report here on our initial studies of the RNA of several tumor viruses. We have been particularly concerned with length measurements of the large (~ 35S) subunits and with the question of whether the two or three large subunits that probably occur in a single 70S complex are identical in sequence or different.

In the formamide modification of the basic protein film technique using a spreading solution consisting of 50% formamide and 0.1 M Tris supporting electrolyte, single strands of DNA with a G+C content of less than about 60% appear as smooth, well extended filaments (Davis et al., 1971). Under similar spreading conditions, RNA molecules of similar base composition tend to be knobby, thick, and short.

Several modified techniques are useful for spreading RNA molecules: (a) the gene 32 procedure of Delius et al. (1973); this method has recently been used for studies of tumor virus RNA (Delius et al., 1974); (b) the glyoxal-formamide technique described by Hsu et al. (1973); see also Forsheit et al. (1974); (c) the urea-formamide spreading solution at low electrolyte concentration described by Robberson et al. (1971) and Wellauer and Dawid (1973). This technique appears to be particularly effective for revealing certain kinds of stable secondary structure features in RNA and DNA molecules. In the present studies, we have used methods (b) and (c).

Further electron microscope studies of viral RNAs by the urea-formamide technique (Weber et al., 1974) and by a formaldehyde-formamide method (Chi and Bassel, 1974) have appeared after the present experiments had been concluded.

Results

RSV and related viruses. RNA was extracted from the Prague strain of transforming Rous Sarcoma virus. The 70S complex was purified by sucrose gradient velocity sedimentation as described in the legend to Figure 1. When this RNA is spread from a 30% formamide, 0.1 M Tris solution, condensed, bush-like structures are seen. We believe these are undissociated 70S complexes. More extended molecules are seen in spreadings from 50% formamide, as shown in Figure 1a. The molecules are still tangled with considerable secondary structure, but they are sufficiently extended so that a very rough estimate of the total contour length and thus of the total mass per

Fig. 1. Electron micrograph of 70S RSV RNA spread by the formamide isodenaturing technique (Davis and Hyman, 1971), a) in 50% formamide; b) in 80% formamide; c) in 95% formamide.

Cell culture techniques followed published procedures (Vogt, 1969). Chick embryo fibroblasts were of the C/B phenotype and were free of endogenous helper factor activity. The Prague strain of Rous Sarcoma virus subgroup C (PR-C) which can produce infectious progeny viruses without the aid of either endogenous or exogenous helper viruses was used. Viruses were produced by inoculating chick embryo fibroblasts with live foci of PR-C transformed cells. Ten to fifteen individual foci were aspirated with a capillary pipet from a plate of chick embryo fibroblasts infected with a high dilution of virus. The foci were deposited in a roller bottle containing 10^8 normal C/B cells. After 3 to 4 days, the bottle showed heavy transformation, and virus was harvested every 2 hrs. Virus was labeled with ^{3}H uridine (New England Nuclear 20 ci/mmole as follows. The labeling medium contained only 2 instead of the usual 5% serum; the trypton phosphate broth was also reduced to 2%. The ^{3}H uridine was added to virus producing cells at 10 μci/ml. Viral harvests were initiated 12 to 18 hours after addition of the label. Infectivity titers in the viral harvests were usually 5×10^6 to 10^7 FFU/ml.

The collective cell culture fluid was centrifuged at 10 K RPM for 15 minutes to remove cell debris and then at 22 K RPM for 60

minutes to concentrate viruses in an SW 25.2 rotor. Viruses were purified by isopycnic banding in a 24-48% sucrose gradient in NTE buffer (0.1 M NaCl, 0.01 M Tris, pH 7.2, 1 mM EDTA) in an SW 50.1 tube for 3 hrs. at 44 K RPM. Virus fractions were pooled, diluted to less than 20% sucrose with NTE solution and centrigued in an SW 50.1 rotor for 3 hrs at 40 K RPM to pellet the viruses. Viral RNAs were isolated by dissolving the virus pellet in ~ 0.1 ml NTE solution containing 1% SDS and 1% mercapto ethanol, followed by repeated extraction with phenol. The 70S RNA complexes were isolated by centrifuging this extract through a 5 ml 10-30% sucrose gradient (NTE buffer) at 45 K RPM for 2 hrs.

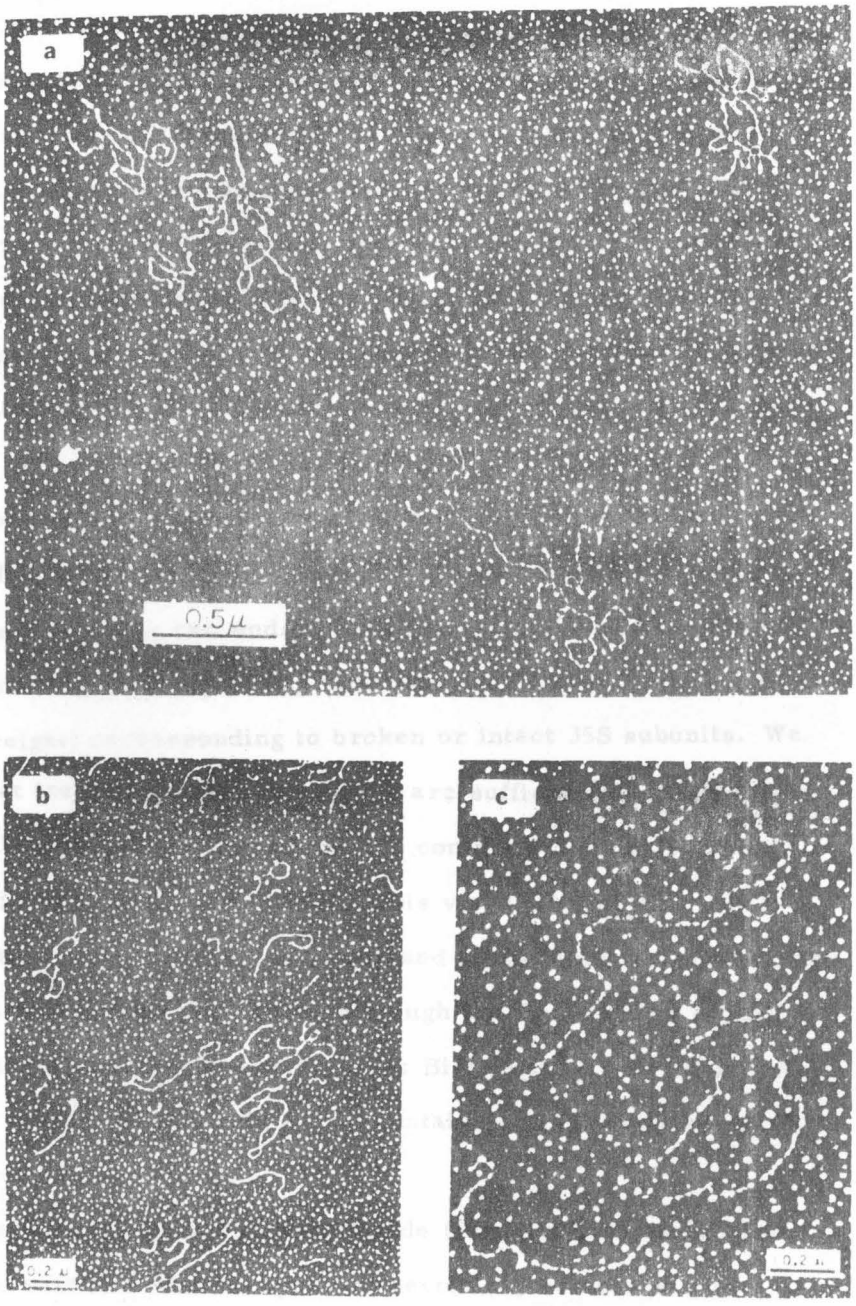
a
0.5μ
b
c

tangled unit can be made. (E. coli 23S rRNA, M = 1.08×10^6, is used as an external standard.) Some of these units have molecular weights substantially greater than 3×10^6 and are probably undissociated or incompletely dissociated 70S complexes. Others have molecular weights of 3×10^6 or slightly less. It appears that the denaturing conditions in the 50% formamide solvent at room temperature are such as to cause denaturation of some, but not all, of the 70S complexes into subunits. There are secondary structure features in these molecules, but we have not been able to discern any reproducible patterns.

In spreadings from 80% formamide (Fig. 1b), the molecules are more extended, although some secondary structure persists. Most of the molecules have only two ends. There is a distribution of contour lengths, from very short up to approximately 2.1 μm (~ 3×10^6 daltons molecular weight) corresponding to broken or intact 35S subunits. We conclude that these spreading conditions are sufficient to cause dissociation of the large subunits of the 70S complex. It may be noted that 16S and 23S E. coli rRNA and Sindbis virus (Hsu et al., 1973) are well extended with only a few knobs and kinks along the chain under these spreading conditions. Thus, although the G+C content of RSV (50 ± 2%) (Robinson and Duesberg, 1968; Bishop et al., 1970) is not higher than that of the other RNAs, it contains a higher degree of intramolecular base pairing.

In spreadings from 95% formamide (Fig. 1c), the molecules are stiff and extended with no apparent secondary structure. The

lengths correspond to 3×10^6 daltons or less in molecular weight. RNA molecules mounted under these conditions are stiffer and shorter than if mounted by the glyoxal-formamide or urea-formamide techniques. The variability in length for a homogeneous RNA preparation tends to be rather large, and there are some denatured cytochrome globs attached to the RNA molecules. We therefore prefer to use either glyoxal-formamide or urea-formamide spreading conditions, as described below, for molecular weight studies.

Glyoxal is a reagent which is useful for disrupting the secondary structure of RNA and DNA. It reacts with cytidine, adenosine, and guanosine. The formation constants for the reaction with cytidine and adenosine are low and the reaction is rapidly reversible. Because of ring formation, the reaction of glyoxal with guanosine has a larger equilibrium formation constant (10^3 $\underline{M}^{-1}$) and its rate of dissociation is slow (Broude and Budowsky, 1971). It is therefore possible to select conditions in which glyoxal reacts selectively with G residues and blocks their hydrogen bonding functionalities (Hsu et al., 1973). Isolated RSV RNA was treated with glyoxal as described in the legend to Figure 2 and examined by electron microscopy. The molecules are well extended with few or no remaining secondary structure features (Fig. 2a). A molecule with a length corresponding to a molecular weight of 3.0×10^6 is shown in Fig. 2b. The histogram of length measurements for all of the molecules in the sample from glyoxal treatment of total phenol extracted RNA (Fig. 3) reveals a broad size

Fig. 2. Electron micrograph of glyoxal treated RSV RNA as extracted from virions by phenol-SDS. a) total phenol-extracted RNA mixture; b) a 35S RNA molecule. The length marker is 0.2 μm.

Phenol-SDS extracted total RSV RNAs were dialyzed against 1 M glyoxal in 0.01 M phosphate buffer, pH 7.0, for 1 hr at 37°C, then dialyzed against 0.1 M glyoxal in the same buffer for approximately 30 minutes at 4°C to remove excess glyoxal which sometimes interferes with the EM spreadings. Samples thus treated were diluted ca. 10-fold into 50% formamide, 0.1 M Tris, 0.01 M EDTA, pH 8.5, 50 μg/ml cytochrome C and spread onto 20% formamide with one-tenth the electrolyte concentration.

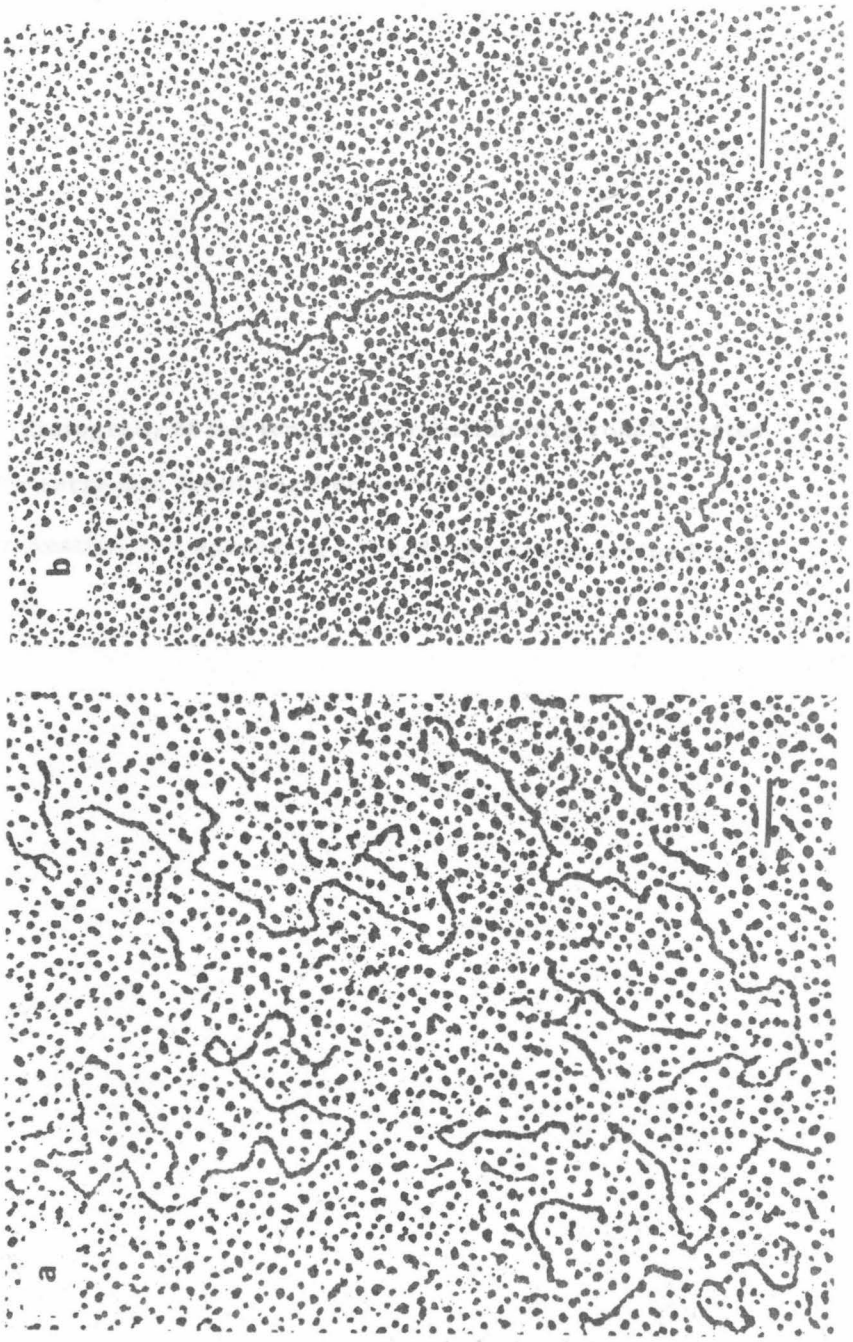
b
a

Fig. 3. Histogram of the length distribution of glyoxal treated total RSV RNAs extracted from purified viruses.

RNA purification and spreading procedures are described in the legend to Fig. 2.

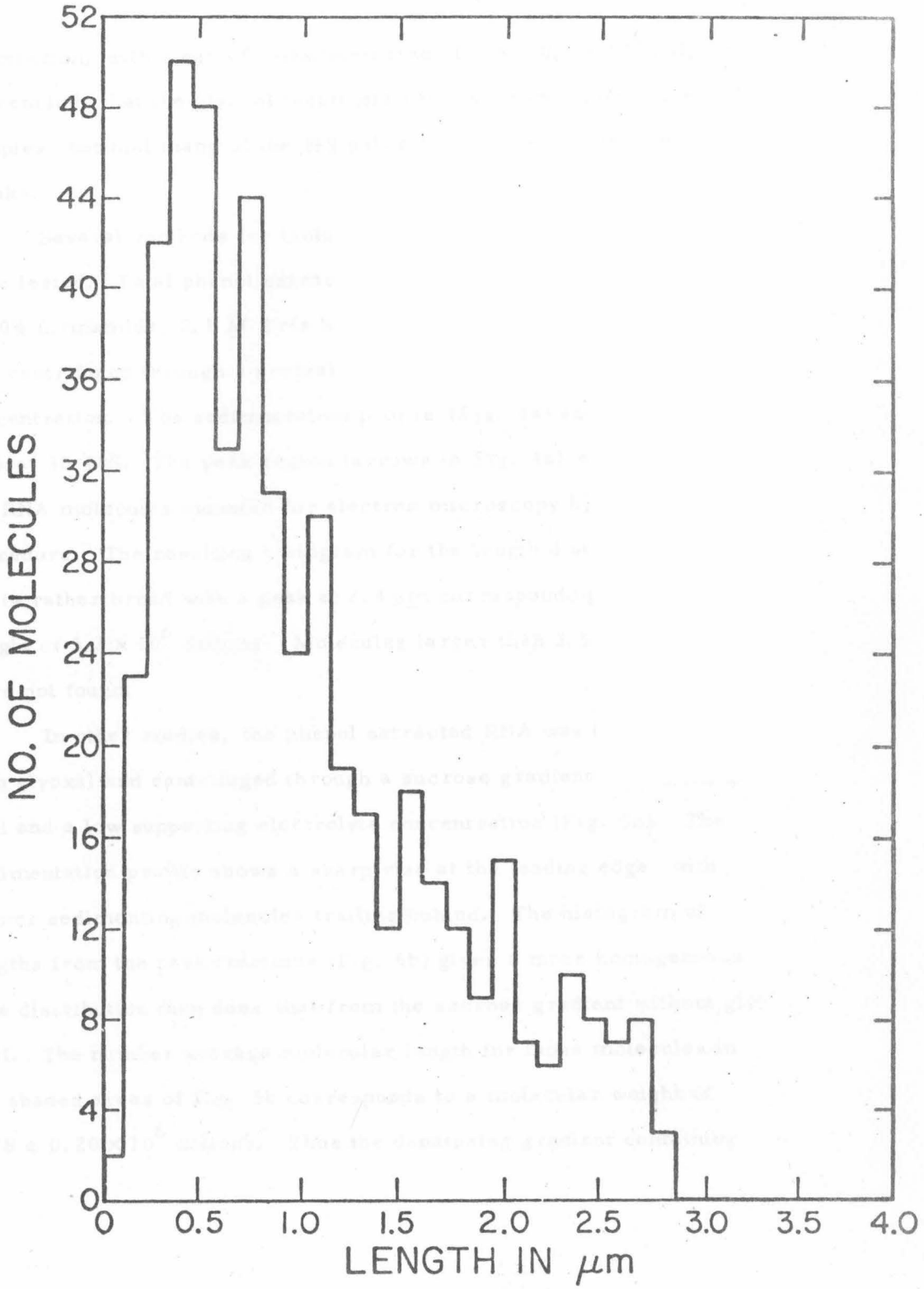
NO. OF MOLECULES
0
4
8
12
16
20
24
28
32
36
40
44
48
52
0
0.5
1.0
1.5
2.0
2.5
3.0
3.5
4.0
LENGTH IN μm

distribution, with a cut-off maximum size of $3.5 \pm 0.1 \times 10^6$ daltons. We conclude that the glyoxal treatment causes dissociation of the 70S complex, but that many of the 35S subunit molecules contain internal breaks.

Several methods for isolating the putative intact 35S subunits were tested. Total phenol extracted RNA from the virion was exposed to 50% formamide, 0.1 M Tris buffer at 37° for 10 min; the sample was centrifuged through a neutral sucrose gradient at low electrolyte concentration. The sedimentation profile (Fig. 4a) shows a broad peak at 30-40S. The peak region (arrows in Fig. 4a) was pooled, and the RNA molecules mounted for electron microscopy by the glyoxal procedure. The resulting histogram for the length distribution (Fig. 4b) is rather broad with a peak at 2.4 μm corresponding to a molecular weight of 3.2×10^6 daltons. Molecules larger than 3.5×10^6 daltons were not found.

In other studies, the phenol extracted RNA was treated directly with glyoxal and centrifuged through a sucrose gradient containing glyoxal and a low supporting electrolyte concentration (Fig. 5a). The sedimentation profile shows a sharp rise at the leading edge, with slower sedimenting molecules trailing behind. The histogram of lengths from the peak fractions (Fig. 5b) gives a more homogeneous size distribution than does that from the sucrose gradient without glyoxal. The number average molecular length for those molecules in the shaded areas of Fig. 5b corresponds to a molecular weight of $3.28 \pm 0.20 \times 10^6$ daltons. Thus the denaturing gradient containing

Fig. 4a. Sedimentation profile of the formamide-dissociated total RSV RNA in a low salt-sucrose gradient.

50 µl of a solution containing ~ 40 µg/ml RSV RNA phenol extract, 50% formamide in NTE was incubated at 37°C for 10 minutes. The reaction was then quickly quenched on ice. These conditions are sufficient to dissociate 70S complexes. After a four-fold dilution with double distilled water, the samples were loaded onto a 10-30% sucrose gradient containing 0.01 M Tris, 1 mM EDTA, pH 7.2. The centrifugation was done in an SW 50.1 rotor at 4°C, 44 K RPM for 2.5 hrs. ^{3}H labeled 23S E. coli rRNA was run in a separate tube at the same time.

b) Histogram of the length distribution of glyoxal treated 35S RSV RNA fractionated by the low salt-sucrose gradient. Samples taken from the peak fraction (as indicated by arrows in Fig. 4a) were treated with glyoxal and spread from 50% formamide as described in the legend to Fig. 2.

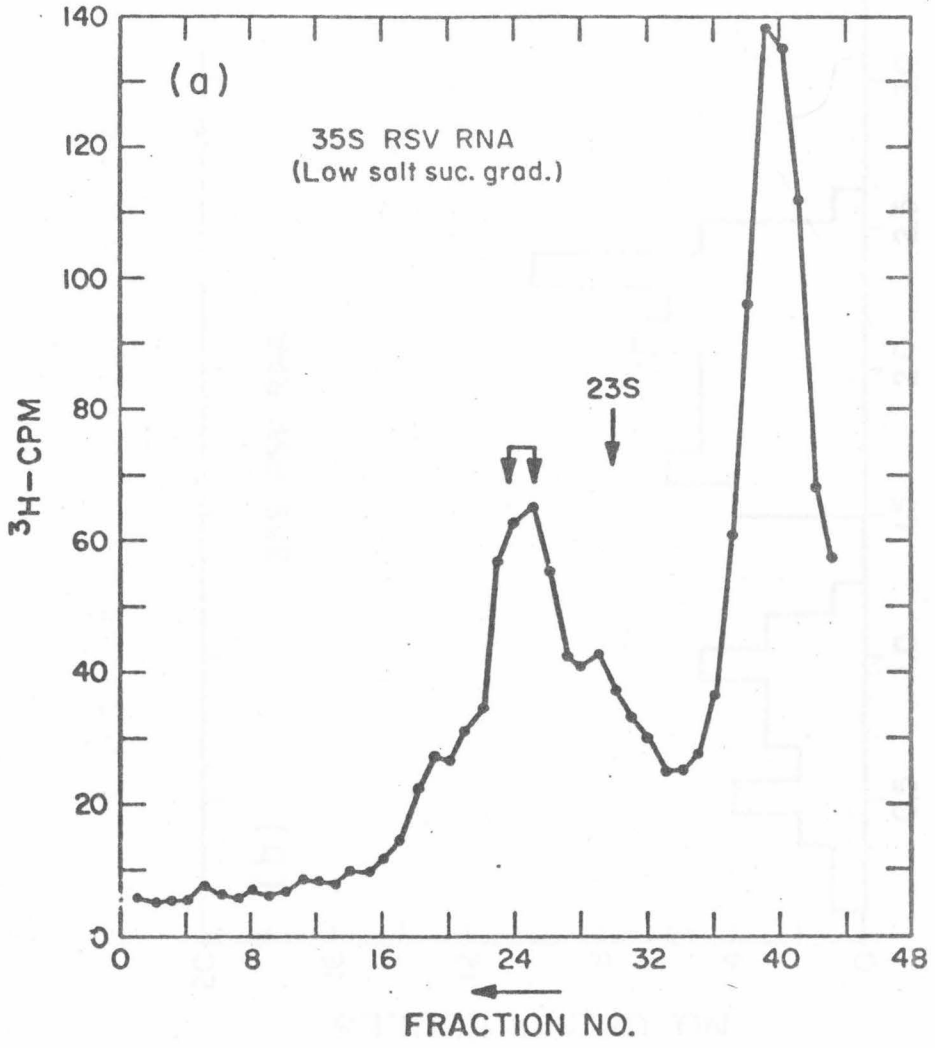
(a)
35S RSV RNA
(Low salt suc. grad.)
23S
^{3}H-CPM
FRACTION NO.
0
20
40
60
80
100
120
140
0
8
16
24
32
40
48

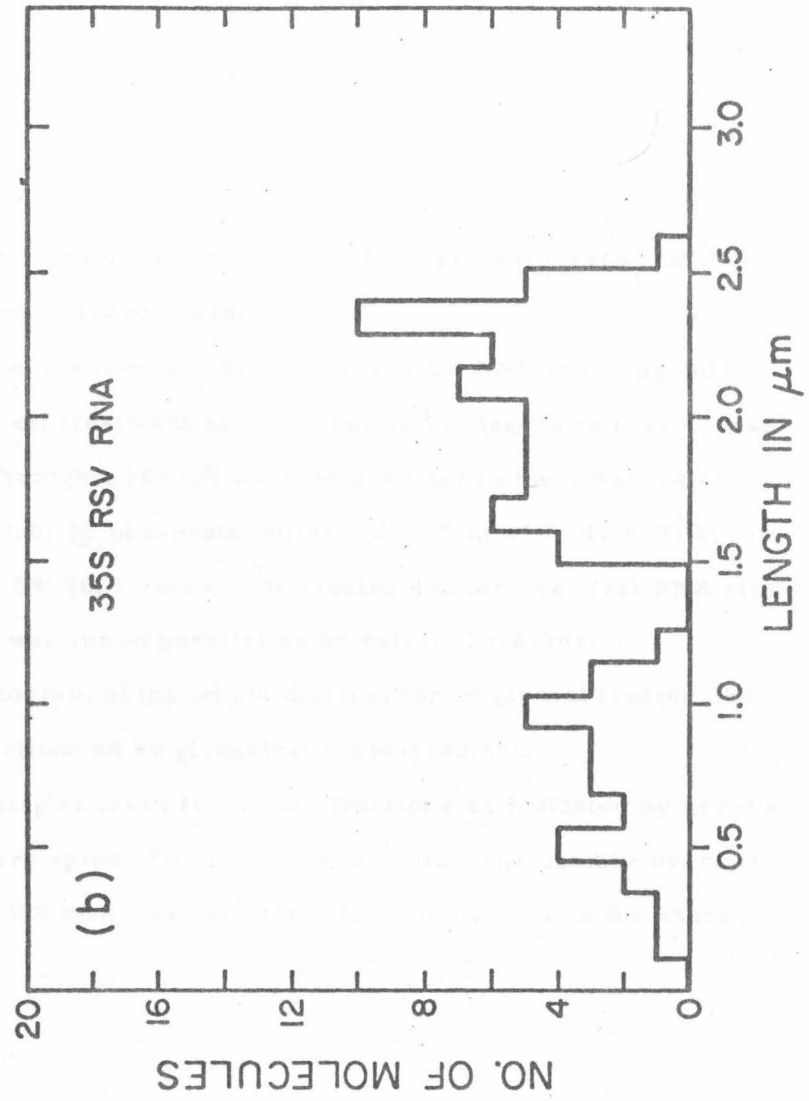
(b)
35S RSV RNA
NO. OF MOLECULES
0
4
8
12
16
20
0.5
1.0
1.5
2.0
2.5
3.0
LENGTH IN μm

Fig. 5a. Sedimentation profile of the glyoxal treated total RSV RNA in a glyoxal-sucrose gradient.

0.1 ml of the phenol extracted total RSV RNA (~ 100 μg/ml) after the glyoxal treatment as described in the legend to Fig. 1, was sedimented through a 10-30% sucrose gradient in the presence of 0.1 M glyoxal, 0.01 M phosphate buffer, pH 7.2 at 4°C, 44 K RPM for 5 hrs. in an SW 50.1 rotor. ^{3}H-labeled 49S Sindbis viral RNA similarly treated was run in parallel as an external marker.

b) Histogram of the length distribution of glyoxal treated 35S RSV RNA fractionated by glyoxal-sucrose gradient.

RNA samples taken from peak fractions as indicated by arrows in Fig. 5a were spread from 50% formamide. The number average length of the 35S RNA was calculated from molecules in the shaded area.

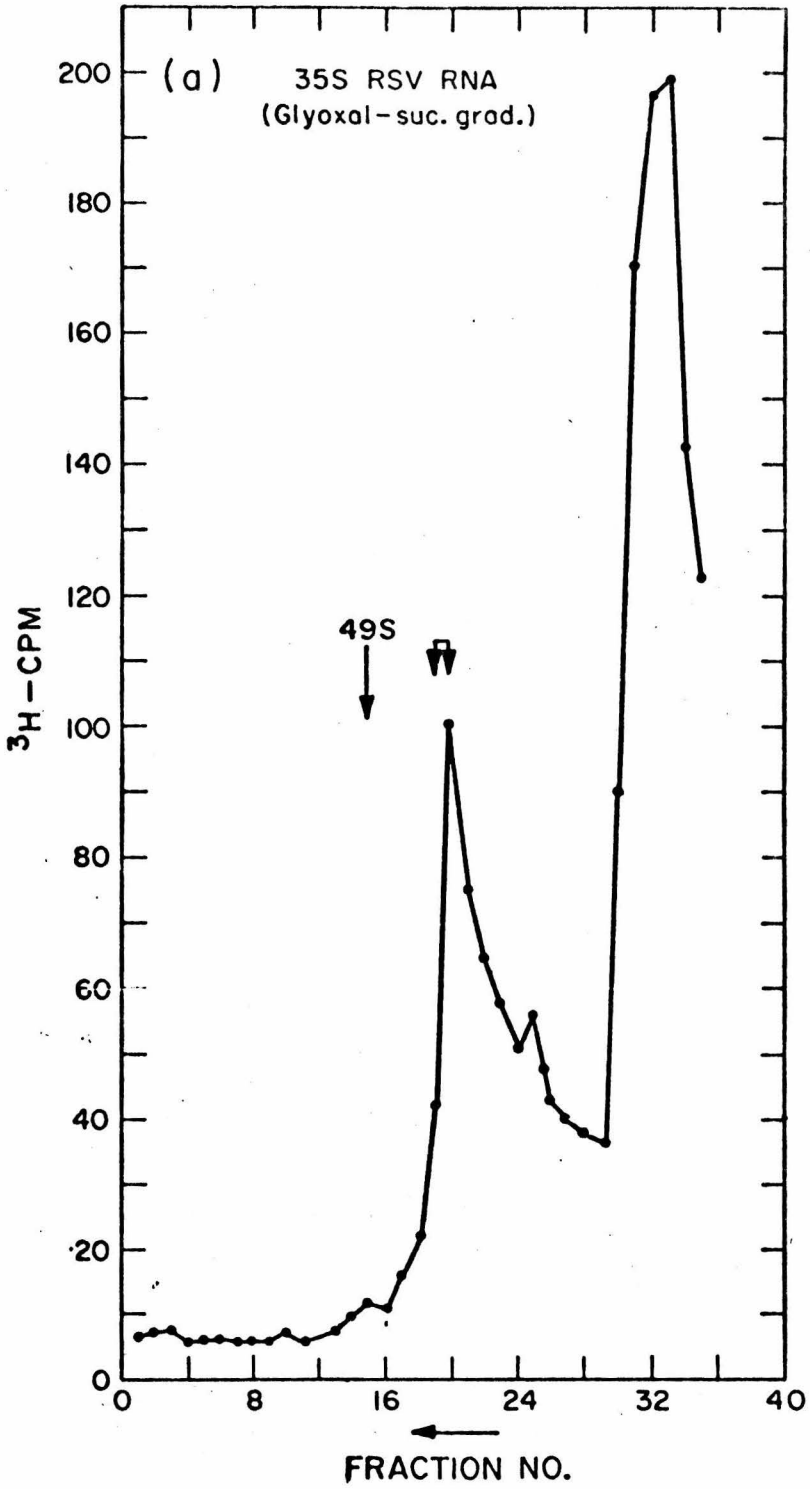
(a)
35S RSV RNA
(Glyoxal-suc. grad.)
49S
^{3}H-CPM
0
20
40
60
80
100
120
140
160
180
200
0
8
16
24
32
40
FRACTION NO.

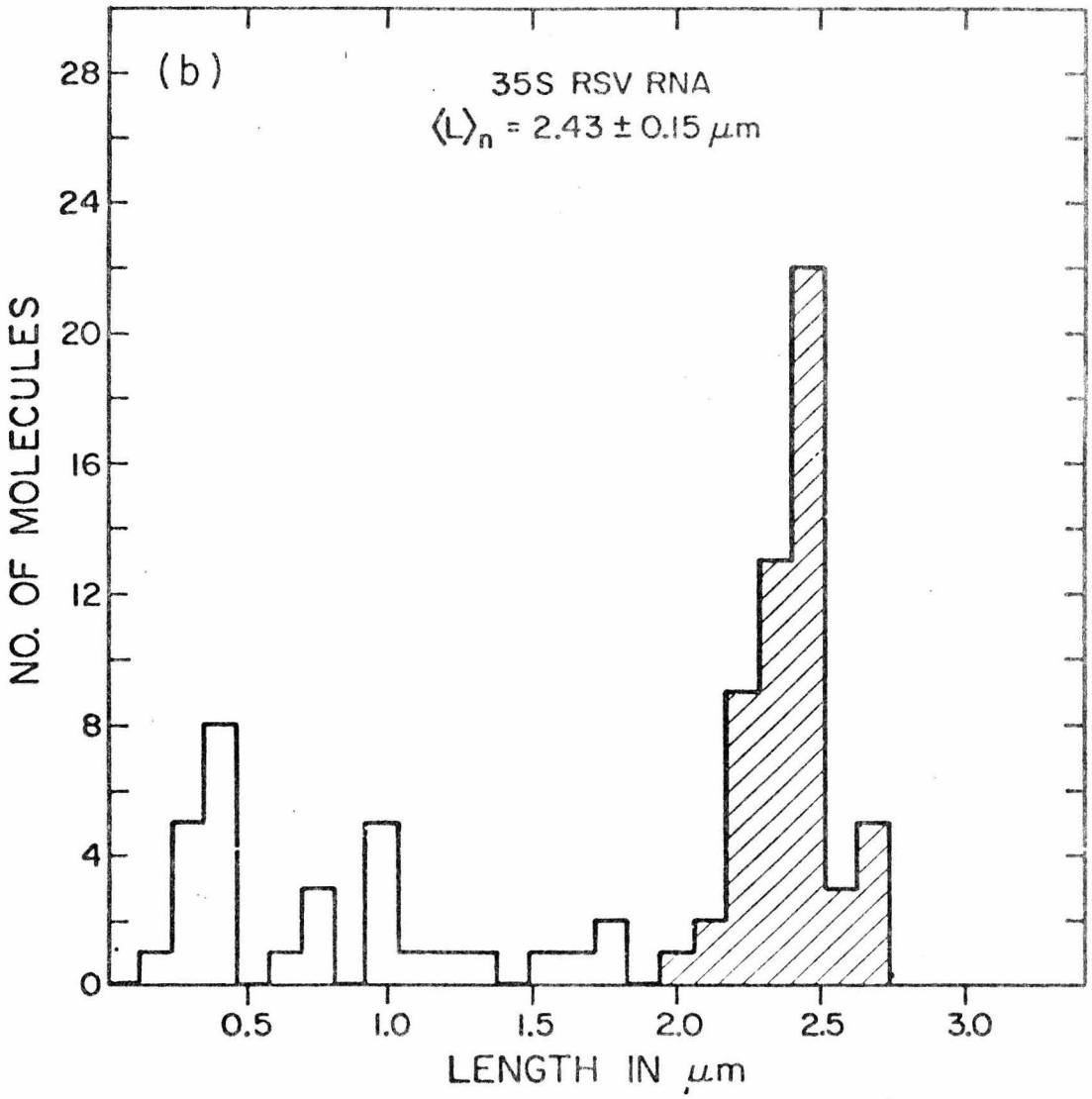
(b)
35S RSV RNA
⟨L⟩n = 2.43 ± 0.15 μm
NO. OF MOLECULES
0
4
8
12
16
20
24
28
0.5
1.0
1.5
2.0
2.5
3.0
LENGTH IN μm

glyoxal is more effective than a simple sucrose gradient in fractionating molecules according to size.

Feline leukemia virus RNA. The 70S complex from the Gardner-Arnstein strain of feline leukemia virus (FeLV) (McAllister et al., 1973) when denatured with glyoxal gave extended RNA molecules as illustrated in Fig. 6a, b. The length distribution (Fig. 7) is broad just as for RSV. When the phenol extracted total virion RNA is denatured with glyoxal and sedimented through glyoxal, sucrose (Fig. 8a), a sedimentation profile with a sharp rise at the leading edge is again seen. The peak fractions have a narrow length distribution (Fig. 8b) with a number average molecular weight of $3.27 \pm 0.22 \times 10^6$ daltons.

RD-114 RNA. The 70S RNA from RD-114 was isolated by sedimentation (Fig. 9a). The RNA was then denatured and spread by the urea-formamide (Fig. 10a, b) and the glyoxal technique (Fig. 10c, d). The resulting large components of RD-114 show several unusual features, when compared to the RNAs of RSV and FeLV.

The contour lengths of the molecules when spread by either method show a broad size distribution (Fig. 9b and c) with a peak close to the maximum corresponding to a molecular weight of 5.05×10^6 daltons.

In the otherwise smooth and well extended molecules in the urea- formamide spreading, there is a characteristic T or Y shaped secondary structure feature (SSF) close to the middle of the molecule (Fig. 10a and b). The SSF maps reproducibly at a position 0.46 ± 0.02 fractional lengths from one end of the molecule, for those mole-

Fig. 6. Electron micrograph of glyoxal treated FeLV RNA extracted from purified virions. a) total phenol-extracted RNA mixture; b) a 35S RNA molecule.

Growth and purification of the Gardner-Arnstein feline leukemia viruses from RD cells have been described (McAllister et al., 1973). The procedures for RNA extraction, glyoxal treatment and EM spreading were the same as those for RSV as described in the legend to Fig. 2. The length marker is 0.2 μm.

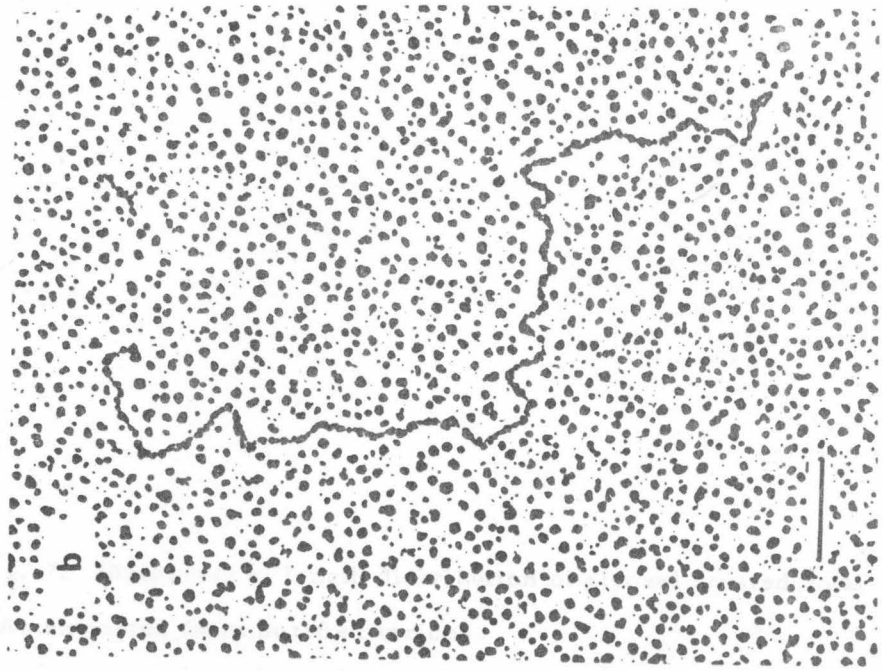
b

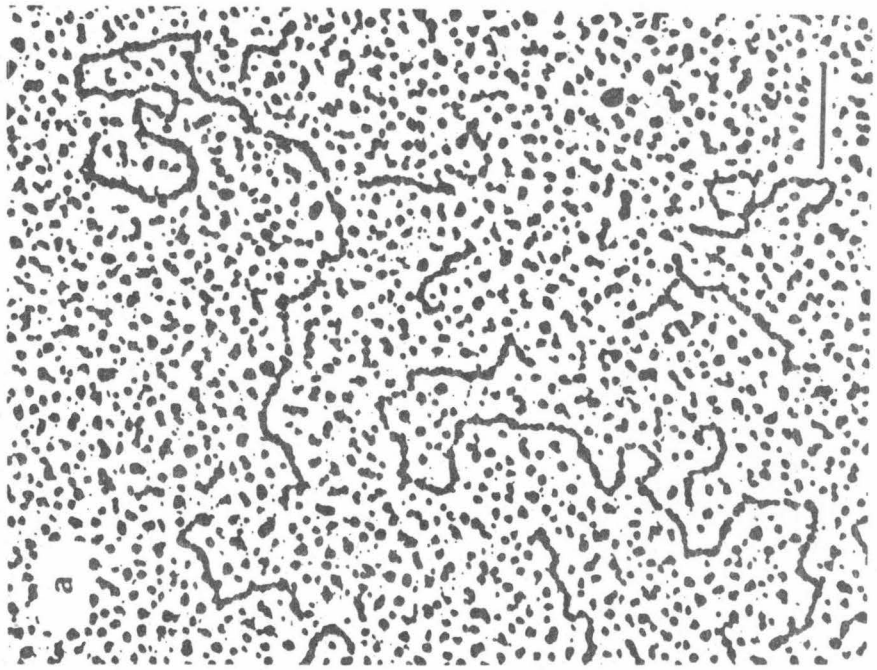
a

Fig. 7. Histogram of length distribution of glyoxal treated total FeLV RNAs extracted from purified virions.

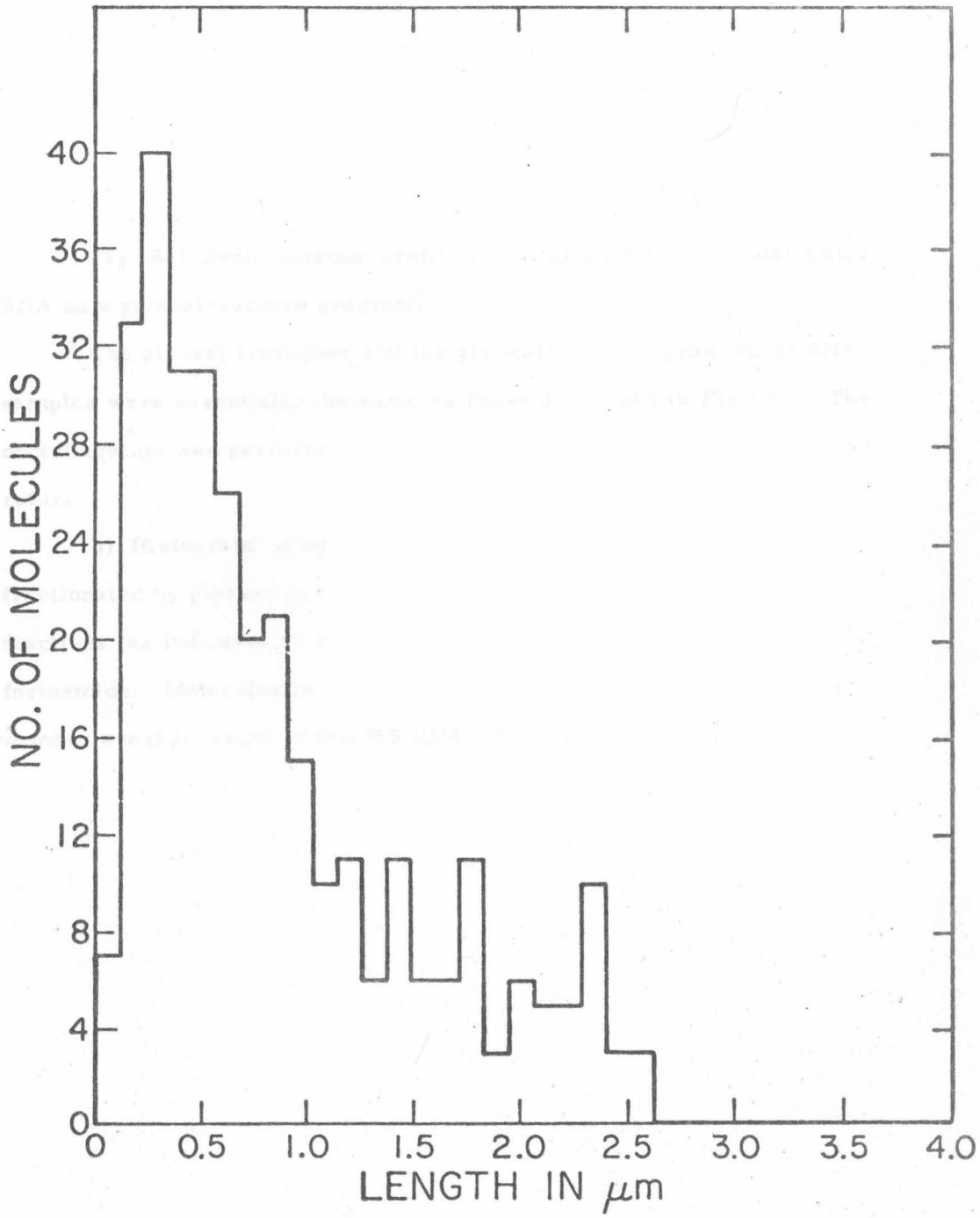
NO. OF MOLECULES
0
4
8
12
16
20
24
28
32
36
40
0
0.5
1.0
1.5
2.0
2.5
3.0
3.5
4.0
LENGTH IN μm

Fig. 8a) Sedimentation profile of the glyoxal treated total FeLV RNA on a glyoxal-sucrose gradient.

The glyoxal treatment and the glyoxal-sucrose gradient of RNA samples were essentially the same as those described in Fig. 5a. The centrifugation was performed at 44 K RPM, 4°C for 6 hrs, in an SW 50.1 rotor.

b) Histogram of lengths of glyoxal treated 35S FeLV RNA fractionated by glyoxal-sucrose gradient. Samples taken from peak fractions (as indicated by arrows in Fig. 8a) were spread from 50% formamide. Molecules in the shaded area were used to calculate the number average length of the 35S RNA.

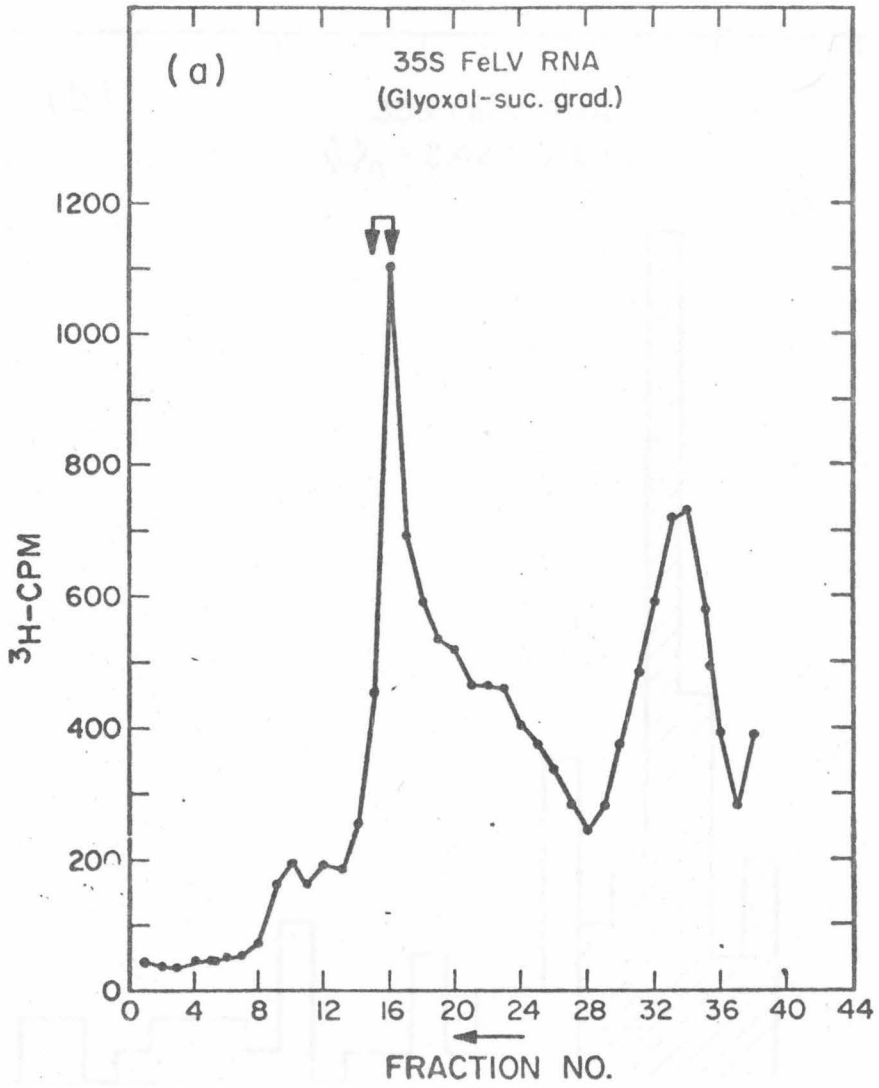
(a)
35S FeLV RNA
(Glyoxal-suc. grad.)
1200
1000
800
600
400
200
0
^{3}H-CPM
0
4
8
12
16
20
24
28
32
36
40
44
FRACTION NO.

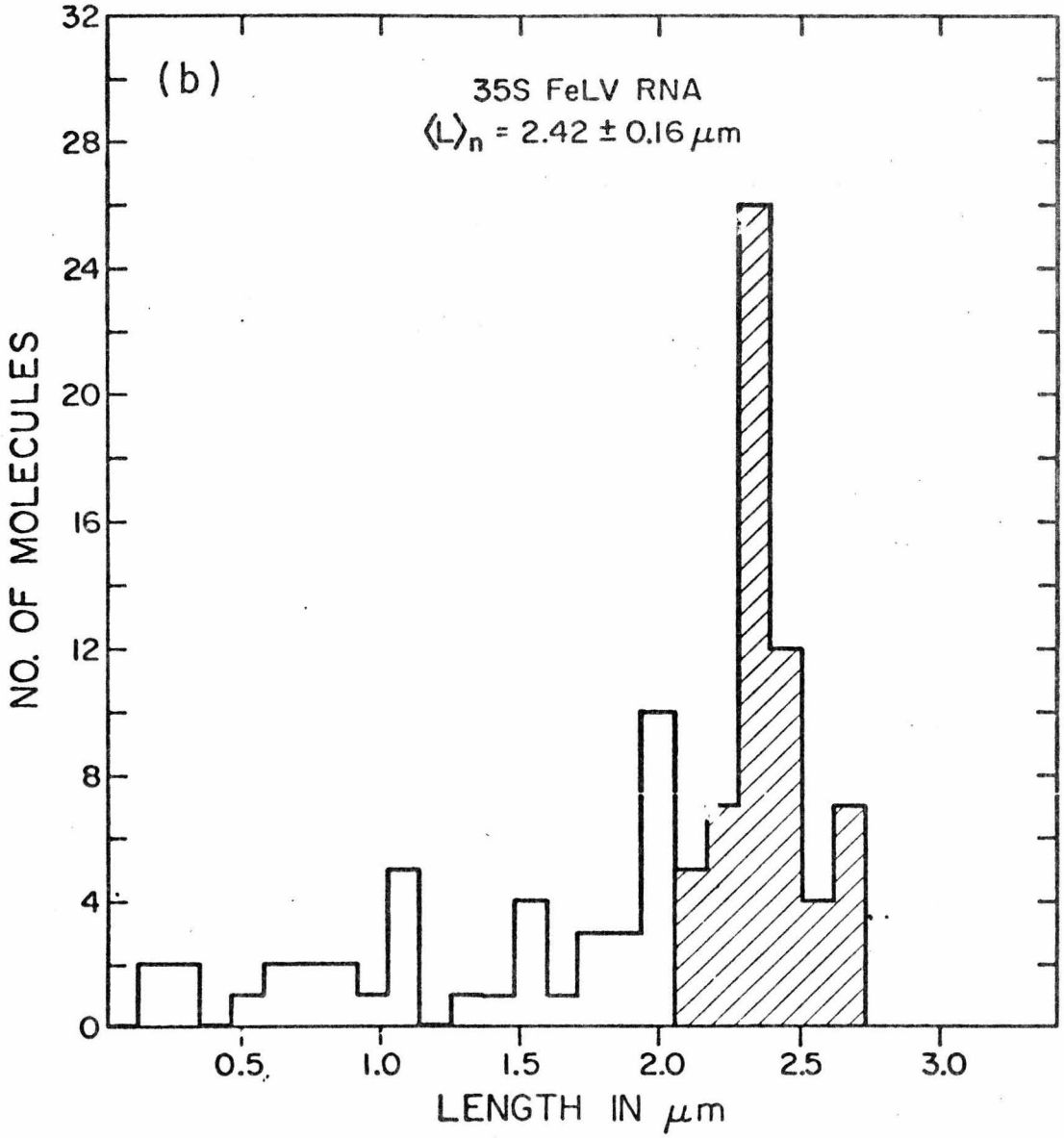
(b)
35S FeLV RNA
⟨L⟩n = 2.42 ± 0.16 μm
NO. OF MOLECULES
LENGTH IN μm
0
4
8
12
16
20
24
28
32
0.5
1.0
1.5
2.0
2.5
3.0

Fig. 9a) Sedimentation profile of the RD-114 RNA.

The RNA extraction procedure has been previously described (Kung et al., 1974). The pronase-digested RNA extract was layered directly onto a 5 ml 10-30% sucrose (in TNE) gradient in an SW50.1 tube and centrifuged at 45 K RPM, 5°C, for 2 hrs. Fractions from the 60-70S RNA region (as indicated by arrows) were used for electron microscopy.

b) Histogram of length distributions of the 70S RD-114 RNA from glyoxal-formamide spreadings.

The RNA in the 60 to 70S region (~ 10 μg/ml) was dialyzed against 0.5 M glyoxal, 0.01 M phosphate buffer, pH 7.2 at 37°C for 1 hr, then diluted ca 20-fold into 40% formamide, 0.1 M Tris, 0.01 M EDTA, pH 8.5, 50 μg/ml cytochrome C and spread onto a 10% formamide hypophase with one-tenth the electrolyte concentration. Molecules in the shaded area were used for calculating the number average length.

c) Histogram of length distributions of the 70S RD-114 RNA from urea-formamide spreadings.

5 μl of the 60 - 70S RNA samples (~ 10 μg/ml) was mixed with 40 μl of 8 M urea in pure formamide, 5 μl. 1 M Tris, 0.1 M EDTA, pH 8.5, 2.5 μl. Cytochrome C (1 mg/ml) and spread onto a hypophage containing 8 mM Tris and 0.8 mM EDTA, pH 8.5. Films were picked up within 10 seconds after spreading.

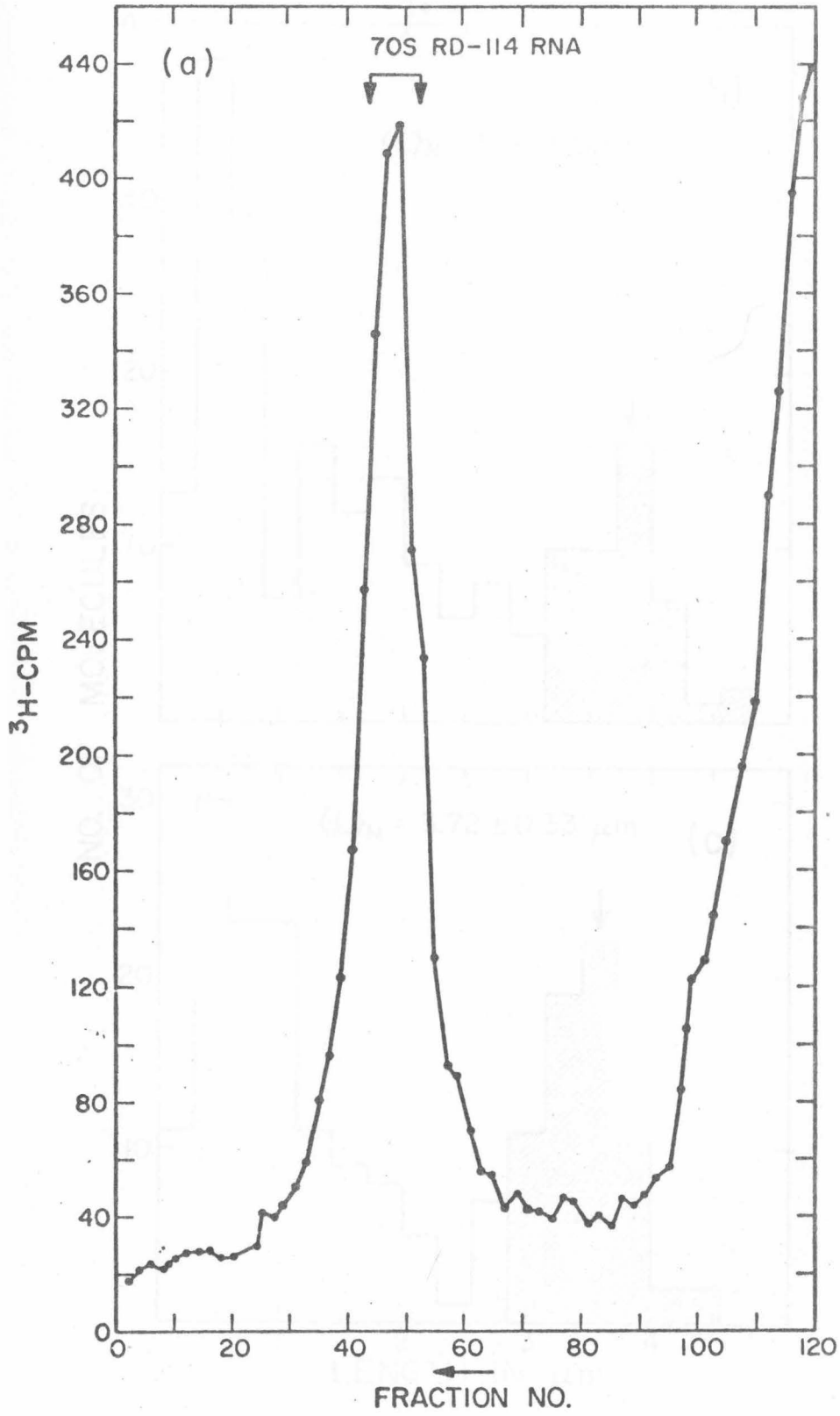
(a)
70S RD-114 RNA
440
400
360
320
280
240
200
160
120
80
40
0
^{3}H-CPM
0
20
40
60
80
100
120
FRACTION NO.

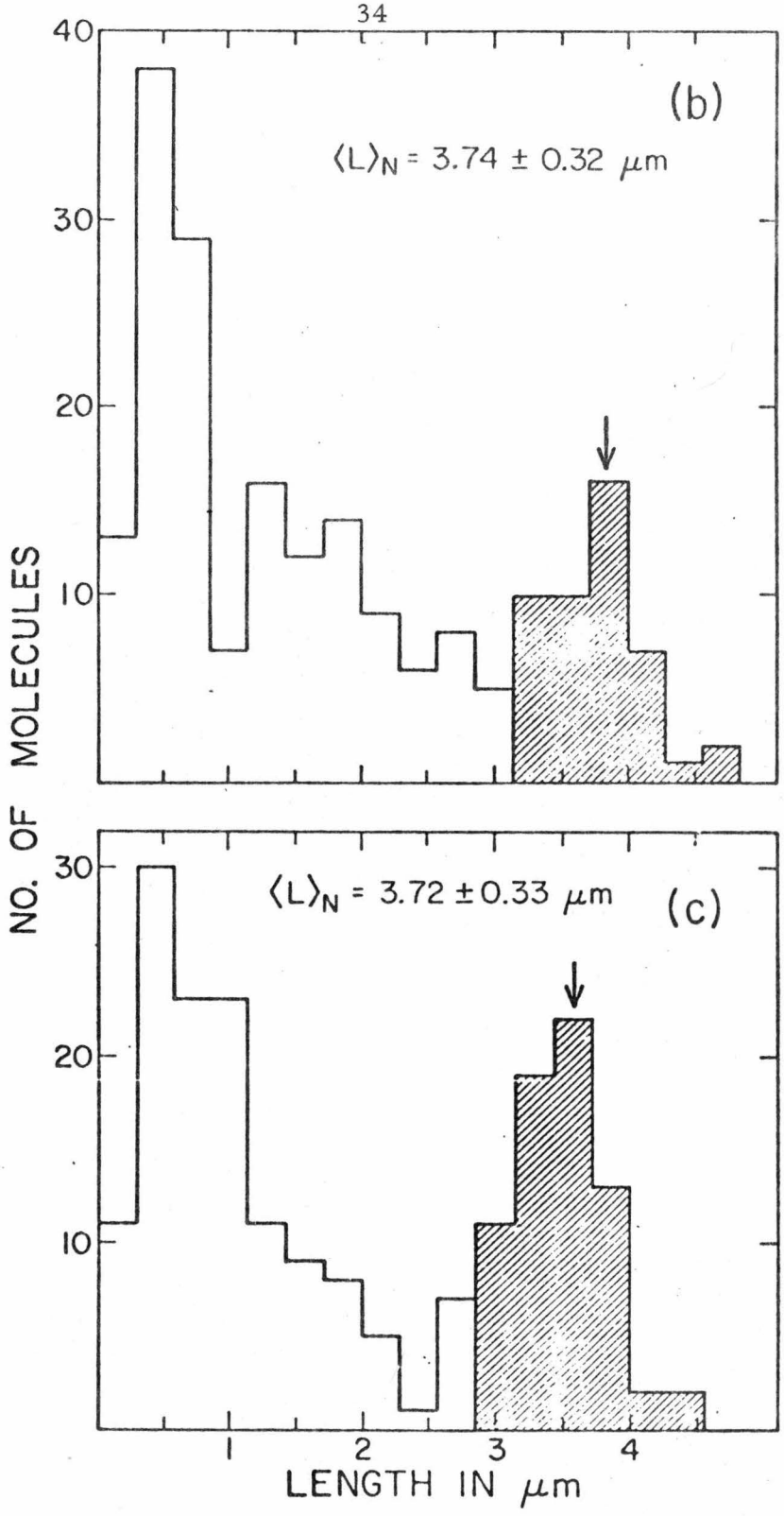
40
30
20
10
(b)
$\langle L \rangle_N$ = 3.74 ± 0.32 μm
NO. OF MOLECULES
30
20
10
$\langle L \rangle_N$ = 3.72 ± 0.33 μm
(c)
1
2
3
4
LENGTH IN μm

Fig. 10. Electron micrographs of RD-114 70S RNA spread by the urea, formamide and glyoxal, formamide techniques. a and b) urea-formamide spreadings; c and d) glyoxal-formamide spreadings. The spreading conditions are described in the legend to Figs. 9b and c. White arrows indicate the SSF. Fig. d shows 5×10^6 daltons molecules containing no SSF in the middle. The length marker is 0.2 µm.

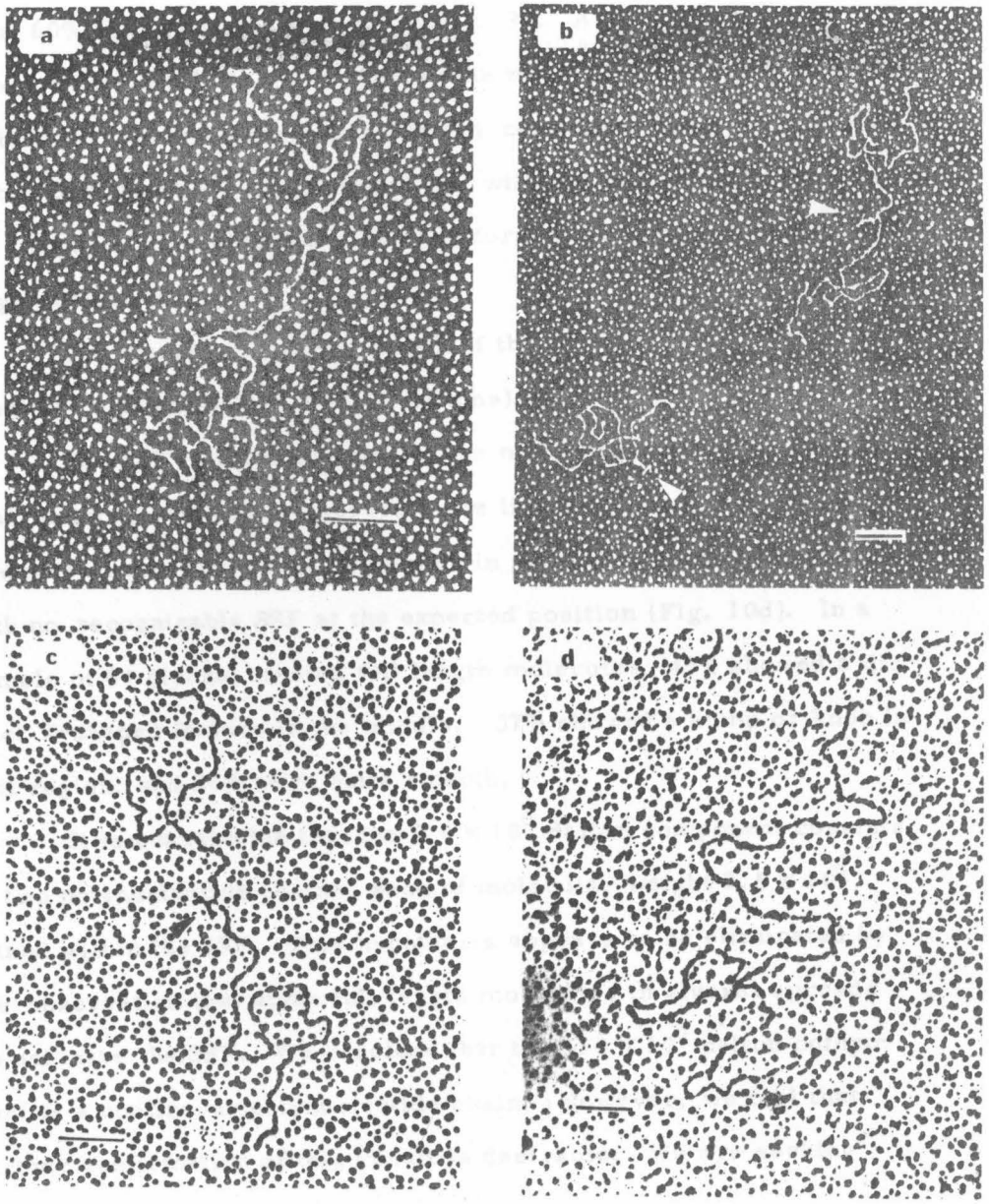
a
b
c
d

cules of full length (i.e., in the shaded area in Fig. 9c). The SSF occurs in over 90% of the molecules in this sample.

We have also examined the smaller molecules with lengths from 60% (2.2 μm) to full length in Fig. 9c. Almost all of these molecules contain the SSF. The shorter the molecule, the more off-center is the SSF. This suggests that RD-114 contains a 3.7 μ or 5.05×10^6 dalton component (or components), all with the SSF close to the center and that smaller molecules have been formed by cleavage of this large component.

The measured contour length of the SSF indicates that it contains about 900 nucleotides (3.1×10^5 daltons).

The SSF is found in some of the molecules spread by the glyoxal method, although it appears more like a V than a Y (Fig. 10c). However, some full length molecules in glyoxal spreads are smooth, with no recognizable SSF at the expected position (Fig. 10d). In a sample of 64 glyoxal treated full length molecules, 43% showed a distinct V-shaped feature in the middle. 37% showed a bump or knob in that region, and 20% were quite smooth.

It is conceivable that the 5.0×10^6 dalton component consists of two polynucleotide chains, each of molecular weight 2.5×10^6, joined within the SSF. This hypothesis appears to be eliminated by the observation that some full length molecules in glyoxal spreads do not have the SSF. We conclude that the 5.0×10^6 dalton component is a continuous polynucleotide chain. However, we feel that further confirmation of this result is desirable. We are seeking

conditions under which over 90% of the 5×10^6 dalton molecules will have no SSF and/or conditions under which the SSF can be reversibly denatured and renatured.

East et al. (1973) report that when the product of SDS disruption of RD-114 virions is heated to 100°C for 2 min, RNA molecules with a sedimentation coefficient of 28S are formed. This is the same as observed by them for FeLV RNA. If our conclusion that the 5.0×10^6 dalton component of RD-114 RNA is a single polynucleotide chain is correct, the smaller subunits observed by East et al. result from thermal scission. If their interpretation is correct, the 5.0×10^6 dalton component is held together by base pairs which are resistant to dissociation by the several denaturing conditions used by us.

Discussion

Electron microscopy is an independent method of estimating the lengths of the 35S subunits of RNA tumor viruses. Our results give molecular weights for this component of RSV and FeLV of $3.28 \pm 0.20 \times 10^6$ daltons and $3.27 \pm 0.22 \times 10^6$ daltons respectively. Thus, these two virions have almost identical molecular weights. Our electron microscope value for the molecular weight of RSV RNA agrees moderately well with the value determined by the gene 32 electron microscope technique (Delius et al., 1974) and is consistent with the values determined by sedimentation in DMSO (3.1×10^6, Duesberg, 1968) and by gel electrophoresis in formamide (2.4 to 3.4×10^6,

Duesberg and Vogt, 1973). Our value for FeLV is slightly higher than the 2.2 to 2.6 $\times 10^6$ value obtained by gel electrophoresis (Whalley, 1973).

Results reported elsewhere in this Symposium (Duesberg et al., 1974; Weissman et al., 1974; Balude et al., 1974) support the view that the several 35S subunits of the 70S complex of RSV have identical sequences. Thus, all of the viral information is encoded in a molecule of length 9.5×10^3 nucleotides. On the other hand, RD-114, which is also a feline C-type virus, has a genome consisting of one or more 1.5×10^4 nucleotide long molecules. It may therefore contain more genetic information.

There is no evidence as to the number of 5.0×10^6 components in the 70S complex of RD-114 RNA. If the usual correlations of sedimentation coefficient with molecular weight for RNA molecules apply to the complex, it has a molecular weight of ca. 10^7 daltons and contains two 5.0×10^6 dalton components. Alternatively, it may contain only a single 5.0×10^6 dalton component which is held in a compact rapidly sedimenting conformation by hydrogen bonding interactions with the small (4-7S) components.

Finally, if there are several 5.0×10^6 dalton components in the 70S complex of RD-114, there is no evidence as to whether they are identical or different in sequence. The result that the 5.0×10^6 dalton components of RD-114 all have the same secondary structure feature close to the middle is most simply consistent with the hypothesis that these molecules are identical. Alternatively, if they are different, the

common secondary structure feature must have a function needed by all the molecules.

Acknowledgments

This research has been supported by research grants, GM 10991 and CA 13213 from the United States Public Health Service, and by contracts PH 43-68-1030 and N01CP 43306 with the National Cancer Institute. JMB is the recipient of a Helen Hay Whitney fellowship.

References

BALUDA, M. A., M. SHOYAB, P. D. MARKHAM, R. EVANS, and W. N. DROHAN. 1974. Characterization of avian myeoblastosis virus genome by molecular hybridization. Cold Spring Harbor Symp. 39, in press.

BISHOP, J. M., W. LEVINSON, D. SULLIVAN, L. FANSHIER, N. KUINTRELL, and J. JACKSON. 1970. The low molecular weight RNAs of Rous sarcoma virus. II. The 7S RNA. Virology 42:927.

BOLOGNESI, D. P. 1974. Structural components of RNA tumor viruses. Advances in Virus Research. 19: 315.

BROUDE, N. E., and E. I. BUDOWSKY. 1971. The reaction of glyoxal with nucleic acid components. III. Kinetics of the reaction with monomers. Biochim. Biophys. Acta 254:380.

CHI, Y. Y., and A. R. BASSEL. 1974. Electron microscopy of viral RNA: Molecular weight determination of bacterial and animal virus RNAs. J. Virol. 13:1194.

DAVIS, R. W., M. SIMON, and N. DAVISON. 1971. Electron microscopic heteroduplex methods for mapping regions of base sequence homology in nucleic acids, p. 413. In Methods in enzymology, vol. 21, eds. L. Grossman and K. Moldave. Academic Press, New York.

DAVIS, R. W., and R. W. HYMAN. 1971. A study in evolution: The base sequence homology between coliphage T7 and T3. J. Mol. Biol. 61:287.

DELIUS, H., H. WESTPHAL, and N. AXELROD. 1973. Length measurements of RNA synthesized in vitro by E. coli RNA polymerase. J. Mol. Biol. 74:677.

DELIUS, H., P. DUESBERG, and W. MANGEL. 1974. Electron microscopic measurements of Rous sarcoma virus RNA. Cold Spring Harbor Symp. 39, in press.

DUESBERG, P. H. 1968. Physical properties of Rous sarcoma virus RNA. Proc. Nat. Acad. Sci. 60:1511.

DUESBERG, P. H., and P. K. VOGT. 1973. Gel electrophoresis of avian leukosis and sarcoma viral RNA in formamide: Comparison with other viral and cellular RNA species. J. Virol. 12:594.

DUESBERG, P. H., P. K. VOGT, M. LAI, and K. BEEMAN. 1974. Studies on genetic recombination between avian tumor viruses. Cold Spring Harbor Symp. 39, in press.

EAST, J. L., J. E. KNESEK, P. T. ALLEN, and L. DMOCHOWSKI. 1973. Structural characteristics and nucleotide sequence analysis of genomic RNA from RD-114 virus and feline RNA tumor viruses. J. Virol. 12:1085.

FORSHEIT, A. B., N. DAVIDSON, and D. B. BROWN. 1974. An electron microscope heteroduplex study of the ribosomal DNAs in xenopus laevis and xenopus mulleri. J. Mol. Biol. in press.

HSU, M. T., H. J. KUNG, and N. DAVIDSON. 1973. An electron microscope study of Sindbis virus RNA, p. 943. in Cold Spring

Harbor Symposia on Quantitative Biology, vol. 38, ed. Nancy Ford. Cold Spring Harbor, N. Y.

KUNG, H. J., J. M. BAILEY, N. DAVISON. M. O. NICOLSON, and R. M. McALLISTER. 1974. Structure and molecular length of the large subunits of RD-114 viral RNA. J. Virol. 13, in press.

McALLISTER, R. M., M. NICOLSON, M. B. GARDNER, S. RASHEED, R. W. RONGEY, W. D. HARDY, and R. V. GILDEN. 1973. RD-114 virus compared with feline and murine type-c viruses released from RD cells. Nature New Biol. 242:75.

ROBBERSON, D., Y. ALONI, G. ATTARDI, and N. DAVIDSON. 1971. Expression of the mitochondrial genome in HeLa cells. XI. Size determination of mitochondrial ribosomal RNA by electron microscopy. J. Mol. Biol. 60:473.

ROBINSON, W. S., and P. H. DUESBERG. 1968. The chemistry of the RNA tumor viruses. p. 306. In Molecular basis of virology. ed. H. Fraenkal-Conrat. Reinhold Book. Corp., New York.

RYMO, L., J. T. PARSONS, J. M. COSSIN, and C. WEISSMANN. 1974. In vitro synthesis of Rous sarcoma RNA. Cold Spring Harbor Symp. 39, in press.

TEMIN, H. M. 1974. The cellular and molecular biology of RNA tumor viruses, especially avian leukosis-sarcoma viruses, and their relatives. Advances in Cancer Research 19:47.

VOGT, P. K. 1969. Focus assay of Rous sarcoma virus, p. 198. In Fundamental techniques in virology. eds. K. Habel and N. P. Salzman. Academic Press, New York.

WEBER, G. H., U. HEINE, M. COTTLER-FOX, and G. S. BEAUDREAU. 1974. Visualization of single-stranded nucleic acids of RNA tumor virus with the electron microscope. Proc. Nat. Acad. Sci. 71:887.

WELLAUER, P. K., and I. DAWID. 1973. Secondary structure maps of RNA: processing of HeLa ribosomal RNA. Proc. Nat. Acad. Sci. 70:2827.

WHALLEY, J. M. 1973. Size difference in the ribonucleic acids of feline leukemia viruses. J. Gen. Virol. 21:39.

Chapter 2

RD114 (Feline Endogenous Virus)

Structure and Molecular Length of the Large Subunits of RD-114 Viral RNA*

HSING-JIEN KUNG, JAMES M. BAILEY, and NORMAN DAVIDSON

Department of Chemistry, California Institute of Technology, Pasadena, California 91109

MARGERY O. NICOLSON and ROBERT M. McALLISTER

Department of Pediatrics
University of Southern California School of Medicine
Childrens Hospital of Los Angeles
Los Angeles, California 90054

Abstract

By electron microscopy, the large subunits of RD114 RNA have a molecular weight of 5.0×10^6; they all have a characteristic secondary structure feature close to the middle.

* * * * * *

* Contribution No. : 4848

RD-114 is an endogenous feline type C virus that is immunologically and biochemically distinct from the conventional feline leukemia-sarcoma viruses (1-10). We wish to report here on our preliminary electron microscope studies of the properties of the large molecular weight subunits of the 60-70S RNA complex of this virus.

Virus was grown as described previously (11). Heavily grown monolayers of RD-114 cells were labeled with uridine-5-^{3}H (28 ci/mMole, 40 μc/ml) and the culture medium harvested at 3-hour intervals. Virions were isolated and the 60-70S RNA complex extracted and purified as described in the legend to Fig. 1.

When the 60-70S complex is mounted for electron microscopy under the more or less standard spreading conditions involving 50-60% formamide that are effective for extending single strands of DNA (12), the RNA is collapsed into a "bush-like" structure due to intramolecular base pairing, and it is impossible to study the topology of the molecules. If the formamide concentration is raised to 80%, molecules are more extended but still not traceable. We therefore treated the 60-70S complex with glyoxal under conditions previously described (13) (see also legend to Fig. 1). Glyoxal is a reagent which disrupts the secondary structure of a polynucleotide by selective reaction with the guanine residues in such a way as to block their hydrogen bonding functions. The resulting molecules were well spread and suitable for length measurement. An example is shown in Fig. 1a. A histogram of the length distribution is given in Fig. 2a. It may be seen that the 60-70S complex is dissociated

Legends to Figures

Fig. 1 Electron micrographs of the large molecular weight subunits of RD114-70S RNA Arrows indicate the secondary structure feature.

^{3}H-labelled viruses in culture medium were loaded on SW27 tubes underlayered with 5 ml 20% TNE (0.1 M NaCl, 0.01 M tris, 1 mM EDTA, pH 7.2) and 0.5 ml 65% sucrose in TNE. After centrifugation at 20Krpm for 2 hrs, the upper layer was carefully removed, the bottom 1 to 1.5 ml, corresponding to the virus band, was gently dispersed with a syringe. The virus concentrate was then diluted with TNE to 20% sucrose or less and pelleted by centrifugation at 27Krpm for 90 min. RNA was extracted by adding 0.2 – 0.4 ml self-digested pronase (2 hr, 37°C, 0.02 M tris, pH 7) 500 μg/ml containing 0.5% SDS to the virus pellet and incubating at 37°C for 30 min. The RNA extract was layered directly onto a 5 ml 10-30% sucrose (in TNE) gradient in a SW50.1 tube and centrifuged at 45 Krpm, 5°C for 2 hrs. Fractions from the 60-70S RNA region were used for electron microscopy.

1a) Glyoxal-formamide spreading:

The RNA (~10 μg/ml) was dialyzed against 0.5 M glyoxal 0.01 M PO_4, pH 7 at 37°C for 1 hr, then diluted ca. 20-fold into 40% formamide, 0.1 M EDTA, pH 8.5, 50 μg/ml

cytochrome c and spread onto a 20% formamide hypophase with one-tenth the electrolyte concentration.

1b). Urea-formamide spreading:

5 λ of the RNA sample (~10 μg/ml) was mixed with 40 λ of pure formamide to which urea is added to 8M, 5 λ 1 M tris-0.1 M EDTA, pH 8.5, 2.5 λ cytochrome c (1 mg/ml) and spread onto a hypophase containing 0.083 M tris and 0.00083 M EDTA, pH 8.5. Films were picked up within 10 seconds after spreading.

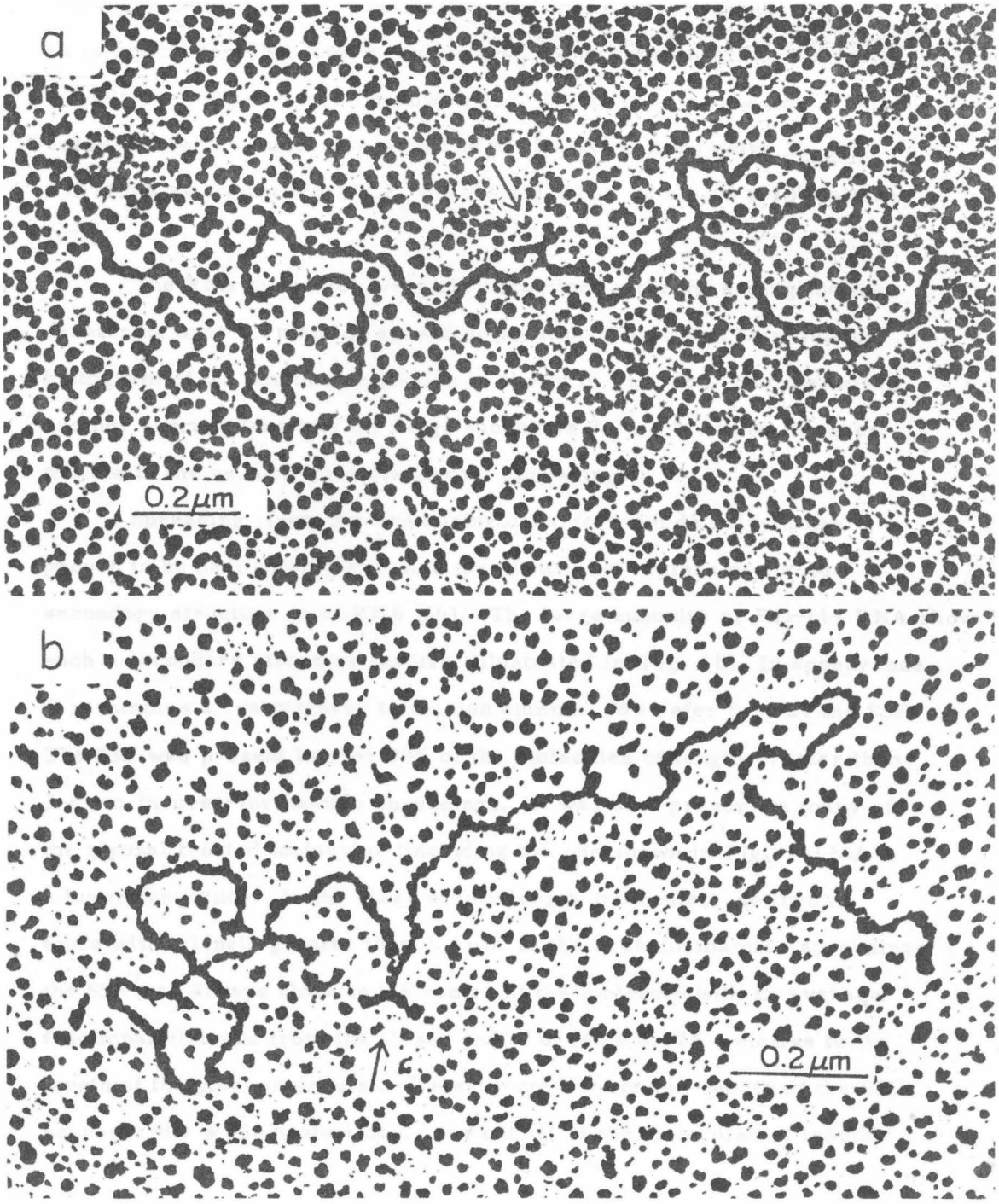
a
0.2μm
b
0.2μm

into large subunits plus some smaller and more heterogeneous RNA's as is typical for RNA tumor viruses (14). The mean length of the large subunit, as indicated by an arrow in Fig. 2a, is 3.74 ± 0.32 μm. This corresponds to a molecular weight of 5.03×10^6 daltons using E. coli 23S rRNA as a standard [$\langle L \rangle_n = 0.80 \pm 0.05$ μ, $M = 1.08 \times 10^6$ daltons (13)].

The RNA molecules were also examined after spreading from a denaturing urea-formamide spreading solution (15, 16). The resulting histogram of the length distribution is shown in Fig. 2b. The measured number average length of the large subunit is 3.72 ± 0.33 μm in agreement with the results from the glyoxal spreadings.

Spreading from the denaturing urea-formamide solvent has proven to be particularly effective for identifying regions of stable secondary structure in an RNA (16). The large subunits of RD-114 RNA show such a secondary structure feature (illustrated in Fig. 1b). In appearance, it resembles a "rabbit-ear" television antenna. We refer to it as the SSF. The SSF was present in over 90% of the molecules of length greater than 3.4 μm in urea-formamide spreadings. It was also present in many of the glyoxal treated molecules (including the one shown in Fig. 1a) but at a lower frequency. In the class of full-length molecules, defined as those with a length greater than 3.4 μm in the urea-formamide spreadings, the SSF was always close to the center of the molecule with an average fractional distance from the closer end of 0.443 ± 0.025 (relative to the length of the given molecule). We estimate the contour length of the SSF as about 900 ± 150 nucleotides. Almost all of the molecules of length

Fig. 2. Histograms of the length distributions of the RNA from the RD-114 70S complex.

Average lengths and standard deviations reported in the text for the large subunits were calculated from the lengths of all molecules in the shaded areas in the two histograms. Arrows indicate the number average lengths.
(a) Length distribution obtained by the glyoxal-formamide method;

(b) Length distribution obtained by spreading from urea-formamide.

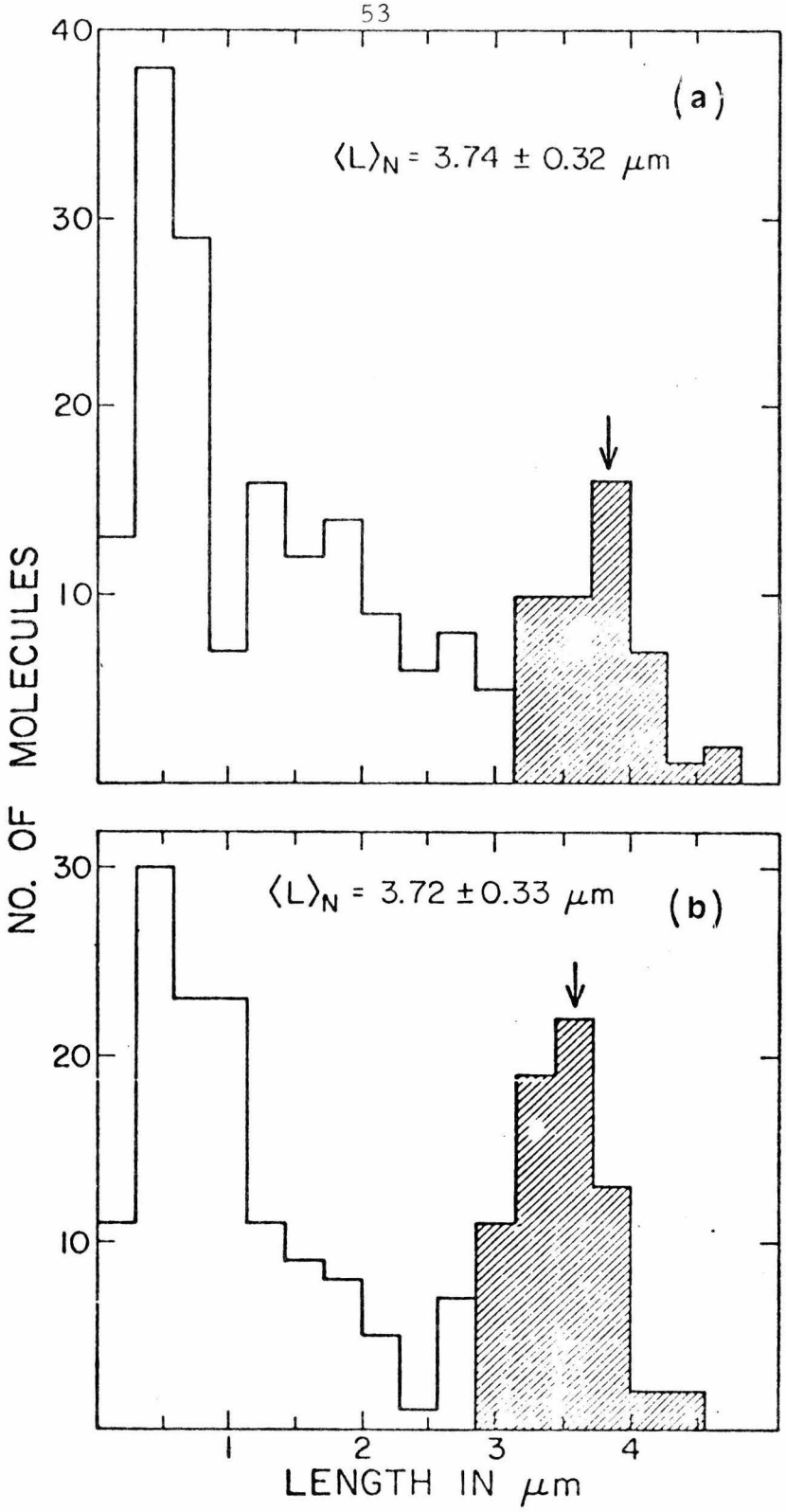
40
30
20
10
(a)
⟨L⟩N = 3.74 ± 0.32 μm
30
20
10
⟨L⟩N = 3.72 ±0.33 μm
(b)
NO. OF MOLECULES
1
2
3
4
LENGTH IN μm

greater than 2.0 μm have the SSF, but the shorter the molecule the more is this feature off center. The obvious interpretation of this result is that the intermediate length molecules are breakdown products of a full-length 3.7 μm subunit.

It is conceivable that the strand of molecular weight 5.03×10^6 daltons consists of two subunits of molecular weight 2.2×10^6 and 2.8×10^6 joined by base-pairing within the SSF. We believe this is unlikely because over 50% of the full length molecules in the glyoxal spreads were quite smooth or showed only small residual bumps in the middle. Therefore we believe the 5.0×10^6 strand is, most probably, a single covalent chain.

In collaboration with Dr. Peter Vogt, we are studying the molecular lengths of the large subunits of PR. RSV-C RNA. Our preliminary result is that this length corresponds to a molecular weight of 3.2×10^6, in approximate agreement with values deduced from sedimentation and electrophoresis studies (17). The molecular weights of the large subunits of Kirsten murine sarcoma and leukemia viruses and of a number of feline leukemia viruses lie in the range 2.0 to 2.5×10^6 (18, 19). It thus appears that the large subunit of RD-114 viral RNA has a molecular length that is considerably larger than that of other common type C viruses.

The stable secondary structure feature is due to a region which has a high G+C content and/or a rather perfect inverted repeat sequence. It occurs in all of the large subunits of the RD-114 60-70S RNA complex. This result is consistent with the hypothesis that the subunits are identical in sequence. If they are not identical, they all have the same kind of strongly base-paired sequence in the middle.

It should be noted that Granboulan et al. observed that long strands with estimated molecular weights of 10^7 daltons were seen when purified RNA from avian myleoblastosis virus was spread for electron microscopy under less denaturing conditions than used here (20).

This research is supported by a research grant GM 10991 from the United States Public Health Service and by contract PH 43-68-1030 within the Virus-Cancer Program of the National Cancer Institute, NIH, PHS. We are grateful to Dr. Peter Vogt for advice and discussion. JMB is the recipient of a Helen Hay Whitney Fellowship.

Literature Cited

1. McAllister, R. M., Nicolson, M., Gardner, M. B., Rongey, R. W., Rasheed, S., Sarma, P. S., Huebner, R. J., Hatanaka, M., Oroszlan, S., Gilden, R. V., Kabigting, A., and Vernon, L.: C-type virus released from cultured human rhabdomyosarcoma cells. Nature New Biol. 235: 3-6, 1972.
2. Livingston, D. M., and Todaro, G. J.: Endogenous type C virus from a cat cell clone with properties distinct from previously described feline type C virus. Virology 53: 142-151, 1973.
3. Sarma, P. S., Tseng, J., Lee, Y. J., and Gilden, R. V.: Virus similar to RD-114 virus in cat cells. Nature New Biol. 244: 56-59, 1973.
4. Fischinger, P., Peebles, P. T., Nomura, S., and Haapala, D.: Isolation of an RD-114-like oncornavirus from a cat cell line. J. Virol. 11: 978-985, 1973.
5. Gillespie, D., Gillespie, S., Gallo, R. C., East, J. L., and Dmochowski, L.: Genetic origin of RD114 and other RNA tumor viruses assayed by molecular hybridization. Nature New Biol. 244: 51-54, 1973.
6. Okabe, H., Gilden, R. V., and Hatanaka, M.: RD-114 virus-specific sequences in feline cellular RNA: Detection and characterization. J. Virol. 12: 984-994, 1973.
7. Baluda, M. A., and Roy-Burman, P.: Partial characterization of RD-114 virus by DNA-RNA hybridization studies. Nature New Biol. 244: 59-62, 1973.

8. Neiman, P. E.: Measurement of RD-114 virus nucleotide sequences in feline cellular DNA. Nature New Biol. 244: 62-64, 1973.

9. Ruprecht, R. M., Goodman, M. C., and Spiegelman, S.: Determination of natural host taxonomy of RNA tumor viruses by molecular hybridization: Application to RD-114, a candidate human virus. Proc. Nat. Acad. Sci. 70: 1437-1441, 1973.

10. McAllister, R. M., Nicolson, M., Gardner, M. B., Rasheed, S., Rongey, R. W., Hardy, W. D., Jr., and Gilden, R. V.: RD-114 virus compared with feline and murine type-C viruses released from RD cells. Nature New Biol. 242: 75-78, 1973.

11. Filbert, J. E., McAllister, R. M., Nocolson, M. O., and Gilden, R. V.: RD-114 virus infectivity assay by measurements of DNA polymerase activity and virus group specific antigen. Proc. Soc. Exp. Biol. Med.: in press.

12. Davis, R., Simon, M., and Davidson, N. "Electron microscopic heteroduplex methods for mapping regions of base sequence homology," in Grossman, L., and Moldave, K. (eds.): Methods in Enzymology, New York: Academic Press, 1971, vol. XXI, pp. 413-428.

13. Hsu, M.-T., Kung, H. J., and Davidson, N.: An electron microscope study of sindbis virus RNA. Cold Spring Harbor Symp., 1974. In press.

14. Duesberg, P. H., and Vogt, P. K.: Gel electrophoresis of avian leukosis and sarcoma viral RNA in formamide: Comparison with other viral and cellular RNA species. J. Virol. 12: 594-599, 1973.

15. Martin, G. S., and Duesberg, P. H. The α subunit in the RNA of transforming avian tumor viruses: I. Occurrence of different virus strains. II. Spontaneous loss resulting in nontransforming variants. Virology 47: 494-497, 1972.

16. Robberson, D., Aloni, Y., Attardi, G., and Davidson, N.: Expression of the mitochondrial genome in HeLa cells. XI. Size determination of mitochondrial ribosomal RNA by electron microscopy. J. Mol. Biol. 60: 473-484, 1971.

17. Wellauer, P. K., and Dawid, I. B.: Secondary structure maps of RNA: Processing of HeLa ribosomal RNA. Proc. Nat. Acad. Sci. 70; 2827-2831, 1973.

18. Maisel, J., Klement, V., Lai, M.-C., and Duesberg, P.: Ribonucleic acid components of murine sarcoma and leukemia virus. Proc. Nat. Acad. Sci. 70, 3536-3540, 1973.

19. Whalley, J. M.: Size differences in the ribonucleic acids of feline leukaemia viruses. J. gen. Virol. 21: 39-46, 1973.

20. Granboulan, N., Huppert, J., and Lacour, F.: Examen au microscope electronique du RNA du virus de la myeloblastose aviare. J. Mol. Biol. 16: 571-575, 1966.

Structure, Subunit Composition, and Molecular Weight of RD-114 RNA[1]

HSING-JIEN KUNG, JAMES M. BAILEY, NORMAN DAVIDSON, MARGERY O. NICOLSON*, and ROBERT M. McALLISTER*

Department of Chemistry, California Institute of Technology, Pasadena, California 91125, and *Department of Pediatrics, University of Southern California School of Medicine, Childrens Hospital of Los Angeles, Los Angeles, California 90054

Received for publication

[1]Contribution no. 5076 from the Department of Chemistry, California Institute of Technology

ABSTRACT

The properties and subunit composition of the RNA extracted from RD-114 virions have been studied. The RNA extracted from the virion has a sedimentation coefficient of 52S in a nondenaturing aqueous electrolyte. The estimated molecular weight by sedimentation in nondenaturing and weakly denaturing media is in the range 5.7 to 7.0 × 10^6 daltons. By electron microscopy, under moderately denaturing conditions, the 52S molecule is seen to be an extended single strand with a contour length of ca. 4.0 μm corresponding to a molecular weight of 5.74 × 10^6 daltons. It contains two characteristic secondary structure features: (a) a central Y or T shaped structure (the "rabbit ears") with a molecular weight of 0.3 × 10^6; (b) two symmetrically disposed loops on each side of and at equal distance from the center. The 52S molecule consists of two half-size molecules, with molecular weight 2.8 × 10^6, joined together within the central rabbit ears feature. Melting of the rabbit ears, with concomitant dissociation of the 52S molecule into subunits, has been caused by either one of two strongly denaturing treatments: incubation in a mixture of CH_3HgOH and glyoxal at room temperature, or thermal dissociation in a urea-formamide solvent. When half-size molecules are quenched from denaturing to nondenaturing temperatures, a new off-center secondary structure feature termed the BLS is seen. The dissociation behavior of the 52S complex and the molecular weight of the subunits have been confirmed by gel electrophoresis studies. The loop structures melt at fairly low temperatures; the dissociation of the 52S

molecule into its two subunits occurs at a higher temperature corresponding to a base composition of about 63% G+C.

Poly-A mapping by electron microscopy shows that the 52S molecule contains two poly-A segments, one at each end. It thus appears that 52S RD-114 RNA consists of two 2.8×10^6 dalton subunits, each with a characteristic secondary structure loop, and joined at the 5′ ends to form the rabbit ears secondary structure feature. The observations are consistent with but do not require the conclusion that the two 2.8×10^6 dalton subunits of 52S RD-114 RNA are identical.

The organization of RNA extracted from RNA tumor viruses has been extensively studied during the past few years. In most instances, the principal RNA species isolated from the virion is a complex sedimenting at 60-70S with a molecular weight of approximately 10^7 daltons. Upon exposure to denaturing conditions, this complex dissociates into a major component with a sedimentation coefficient of ca. 35S (and a molecular weight of $2.5 - 3.3 \times 10^6$ daltons) and into several small (4-10S) species.

In an earlier Note we described our preliminary electron microscope characterization of total RNA from the endogenous feline type-C virus, RD-114 (11). We reported that the major RNA component, when mounted for electron microscopy by procedures which extend the RNA sufficiently well for tracing, is a molecule of 3.7 μm contour length, corresponding to a molecular weight of 5.0×10^6 daltons. Furthermore, these molecules all contained a characteristic Y or T-shaped secondary structure feature near the middle of the molecule. Such an observation is consistent with the hypothesis that all 5×10^6 dalton molecules are identical in sequence. However, the molecular weight of this molecule is quite high in comparison to that of the major RNA component of other RNA tumor viruses. The presence of the characteristic secondary structure feature at the middle of the molecule therefore raises the possibility that the 5.0×10^6 dalton molecule is not a continuous polynucleotide chain but is instead two ca. 2.5×10^6 dalton molecules joined by base pairing within the central secondary structure feature.

We were initially inclined to reject this hypothesis because in electron microscope spreadings of RNA molecules exposed to rather strongly denaturing conditions, we were able to identify full length (3.7 μm) molecules in which the secondary structure feature appeared to be absent. We stated at the time that we felt that this evidence was not conclusive since only 50% of the full length molecules were in this class.

We have accordingly continued these studies and searched for denaturing conditions which would either denature the secondary structure feature in all molecules or cause dissociation into smaller subunits. Our further electron microscope, sedimentation, and gel electrophoresis investigations of the structure and subunit composition of RD-114 RNA are reported here.

MATERIALS AND METHODS

Virus and RNA preparations. RD-114 virus and Sindbis virus were prepared as previously described (12). RSV was a gift from Dr. Peter Vogt. Viral RNAs were concentrated by ethanol precipitation. HeLa 28S rRNA was generously provided by Dr. James Casey.

Sedimentation. (1) NTE-sucrose gradient. A solution (100 λ) of phenol-extracted ^{3}H-labeled RD-114 RNA (in NTE) was layered directly onto a 5 ml 10-30% sucrose gradient in NTE buffer (0.1 M NaCl, 0.01 M Tris, pH 7.0, 0.001 M EDTA). Centrifugation was carried out in an SW50.1 rotor at 45 K rpm at 4°C for 1¾ hrs. Sindbis RNA and 28S HeLa rRNA were run in parallel as external markers.

(2) Glyoxal-sucrose gradient. The phenol-extracted ^{3}H-labeled RD-114 RNA was dialyzed against 1 M glyoxal in 0.01 M phosphate buffer, pH 7.0 for 1 hr at 37°C, then dialyzed against 0.1 M glyoxal in the same buffer for approximately 30 min at 4°C, all as previously described (8, 12). The sample thus treated was sedimented through a 10-30% sucrose gradient in the presence of 0.1 M glyoxal, 0.01 M phosphate buffer, pH 7.2 at 4°C, 45 K rpm for 5 hr in an SW50.1 rotor. The peak fractions were used for electron microscope studies. Sindbis and RSV RNAs were similarly treated and run in parallel as external markers.

(3) Low salt-sucrose gradient. Phenol-extracted RD-114 RNA samples were incubated in 50% formamide, 50% NTE at 37°C for 10 min. This treatment was designed to expose the hidden nicks of the RNA complex so as to give a better fractionation. After removal of the formamide by dialysis at 4°C, RNA samples were loaded onto a 10-30% sucrose gradient containing 1 mM Tris, 0.2 mM EDTA, pH 7.2. Centrifugation was done in an SW50.1 rotor at 4°C, 41 K rpm for 3½ hrs. Peak fractions were pooled for other studies. RSV 60-70S RNA was similarly treated and run in parallel.

Electron microscopy. (1) Drop and high temperature spreading. In the present study, both the standard "dish" spreading technique described by Davis et al. (2) and a drop spreading technique were applied. The latter is a modification of the method described by Inman and Schnös (9). This technique requires only 1-5 ng RNA sample per spreading and is

thus useful for studying small quantities of nucleic acids. It is also convenient in that it allows a spreading to be performed at a uniform high temperature in an oven. A 10 cm × 10 cm × 1.2 cm Teflon block which contains nine evenly spaced indentations (1.9 cm in diameter and 0.1 cm deep) was prepared. One drop of hypophase (~ 0.9 ml) was placed on one of the indentations. A Pasteur pipet with the narrow end sealed was inserted at an angle of 60°C into the hypophase. Five µl of the spreading solution was then applied through the outer surface of the narrow end of the Pasteur pipet onto the hypophase. Samples were picked up by touching a parlodion coated grid to the surface of the drop within 30 seconds after spreading. The grid was then rinsed in 95% ethanol and rotary shadowed with platinum-palladium alloy.

For high temperature spreading, the Teflon block, the Pasteur pipet, the micropipets and the hypophase solution were all pre-equilibrated in an oven at the desired temperature for at least 30 minutes. The RNA sample was heated for 30 seconds to 1 minute by immersing 10 µl of spreading solution in a beaker of water pre-equilibrated in the oven. After heat treatment, 0.5 µl of cytochrome C solution (1 mg/ml) was added to the spreading solution, which was incubated in the hot water bath for another 30 seconds. The spreading was quickly performed inside the oven, with the door partially opened. The whole procedure from applying the spreading solution onto the hypophase until picking up the the film took approximately 30 seconds.

For experiments to study the reassociated secondary structure, the spreading solution after heat treatment was quickly chilled on ice for 15 to 30 seconds. The cytochrome C was added and the solution was spread at room temperature.

(2) Preparation for spreading. (a) Glyoxal-formamide method: RNA samples taken from the glyoxal-sucrose gradient peak fraction were diluted into the spreading solution to give a final concentration of 0.2 - 0.5 μg/ml RNA, 40% formamide, 0.1 M Tris, pH 8.2, 0.01 M EDTA and ~30 μg/ml cytochrome C. Five μl of the above spreading solution was used in one drop spreading, whereas 50 μl was required in the conventional dish spreading. The hypophase contained 10% formamide, 0.01 M Tris, pH 8.2, and 0.001 M EDTA.

(b) Urea-formamide method: RD-114 RNA samples purified either by NTE or low salt-sucrose gradient centrifugation were used. The RNA samples were diluted into the spreading solution which contained ~ 30 μg/ml cytochrome C, the desired concentration of urea-formamide and electrolyte.

The urea-formamide solvents used for electron microscope spreadings and for other denaturation studies were prepared as follows. Formamide (MCB) was purified by recrystallization (13). A solution was prepared by dissolving 480 grams (8 moles) of urea (Schwarz-Mann Ultra-pure grade) per liter of formamide. The conductance of this solution at 4°C was 200 μmho, corresponding to an estimated electrolyte concentration of ca. 6 mM. We observe a 1.35-fold volume increase of the solution relative to the formamide. (Thus, the estimated concentrations of components in the solvent are 74% volume percent formamide and 5.9 M urea, but this calculation is not used in characterizing the mixed urea, formamide, aqueous solutions as discussed below.) A solution prepared from p volumes of the urea-formamide and (100-p) volumes of aqueous solution is

described as a p% (U+F) solution. Unless otherwise specified, the aqueous electrolyte mixed with urea-formamide contained y M (Tris·OH+HCl), pH 8.5, 0.1 y M Na_3EDTA, with an estimated univalent cation concentration of 0.6 y M. The cation concentration, after dilution with urea-formamide, is reported for each experiment.

The 100% (U+F) solvent had an A_{275} of 0.5. The denaturing power of the solvent was determined by optical melting experiments with calf thymus DNA in aqueous U+F solutions containing the standard 0.06 M electrolyte. We observe that

$$T_m = 73° - 0.65° \times p(U+F).$$

For electron microscope spreading from (U+F) solutions, the hypophase was distilled water.

(c) CH_3HgOH-glyoxal-formamide: We have also used a modification of the glyoxal technique which very effectively extends RNA. This procedure consists of the dialysis of the RNA against 1 M glyoxal, 0.045 M sodium phosphate buffer, pH 8, and 10 mM methylmercuric hydroxide for 1 hr at room temperature, followed by dialysis against 0.1 M glyoxal, 0.045 M sodium phosphate buffer and 0.05 M NaCl for 1 hr at room temperature. Methylmercuric hydroxide is an effective denaturant that disrupts secondary structure features at room temperature (7, 15). The CH_3HgOH extended RNA is easily "fixed" by glyoxal treatment and the CH_3HgOH is then removed by the second dialysis against NaCl and glyoxal.

Agarose gel electrophoresis. Gels (10 cm × 0.8 cm) were formed by melting 0.8% or 1.0% agarose in E buffer [0.05 M boric acid, 0.005 M sodium borate ($Na_2B_4O_7 \cdot 10\ H_2O$), 0.01 M sodium sulfate, and 0.001 M EDTA, pH 8.2] and pouring the hot solution into an 11 cm glass tube covered at one end with dialysis membrane. To conduct electrophoresis under conditions which are denaturing for RNA, methylmercuric hydroxide was added to the hot gel solution to the desired concentration. This technique will be described in detail elsewhere (J. Bailey, personal communication).

After solidification of the agarose, the gels were electrophoresed in a vertical tube apparatus containing E buffer in both the upper and lower chambers (the denaturing gel system used in this study does not require the presence of methylmercuric hydroxide in the buffer chambers). The samples were applied in 50 λ of a twofold dilution of E buffer containing 10% glycerol, and 5 mM CH_3HgOH for denaturing gel electro-

phoresis. For other experiments, the samples were applied in an electron microscope spreading solution containing 65% (U+F), 0.026 M NaCl, 0.042 M Tris, pH 7.9, and 0.5 mM EDTA (the total cation concentration is 0.06 M). Electrophoresis at room temperature was performed at 5 ma per tube for periods of 2-3 hours. With radioactive RNA, the gels were sliced into 2 mm fractions with a nickel gel slicer and each fraction was incubated under 10 ml Aquasol for 16 hrs. Radioactivity was determined in a Beckman LS-250 liquid scintillation counter. In several experiments unlabeled RNA was used, in which case bands were located by ethidium bromide staining (15). After electrophoresis gels were incubated in 1γ/ml ethidium bromide, 0.5 M NH_4Ac (to remove CH_3HgOH and enhance the dye binding) for 30 minutes and then examined by illumination with short wavelength UV light.

RESULTS

Sedimentation analysis of RD-114 RNA. The sedimentation properties of the high molecular weight RNA component extracted from the RD-114 virion has been studied in sucrose gradients in nondenaturing (high salt, NTE), moderately denaturing (low salt), and more strongly denaturing (glyoxal) solvents. As shown in Fig. 1a, there is a high molecular weight RD-114 RNA complex which has a sedimentation coefficient of 52S relative to markers of Sindbis RNA (43S) and HeLa (28S rRNA) in the nondenaturing NTE solvent. A plot of log M vs. log (distance sedimented) in these experiments is shown in Fig. 2. If a linear relation between these two variables is assumed, the molecular weight of the RD-114 RNA complex is calculated by extrapolation to be $7.0(\pm 0.6) \times 10^6$ daltons.

Fig. 1. Sedimentation profiles of RD-114 RNA as extracted from the virion in (a) NTE-sucrose gradient; (b) glyoxal-sucrose gradient; (c) low salt-sucrose gradient. All procedures are described in MATERIALS and METHODS.

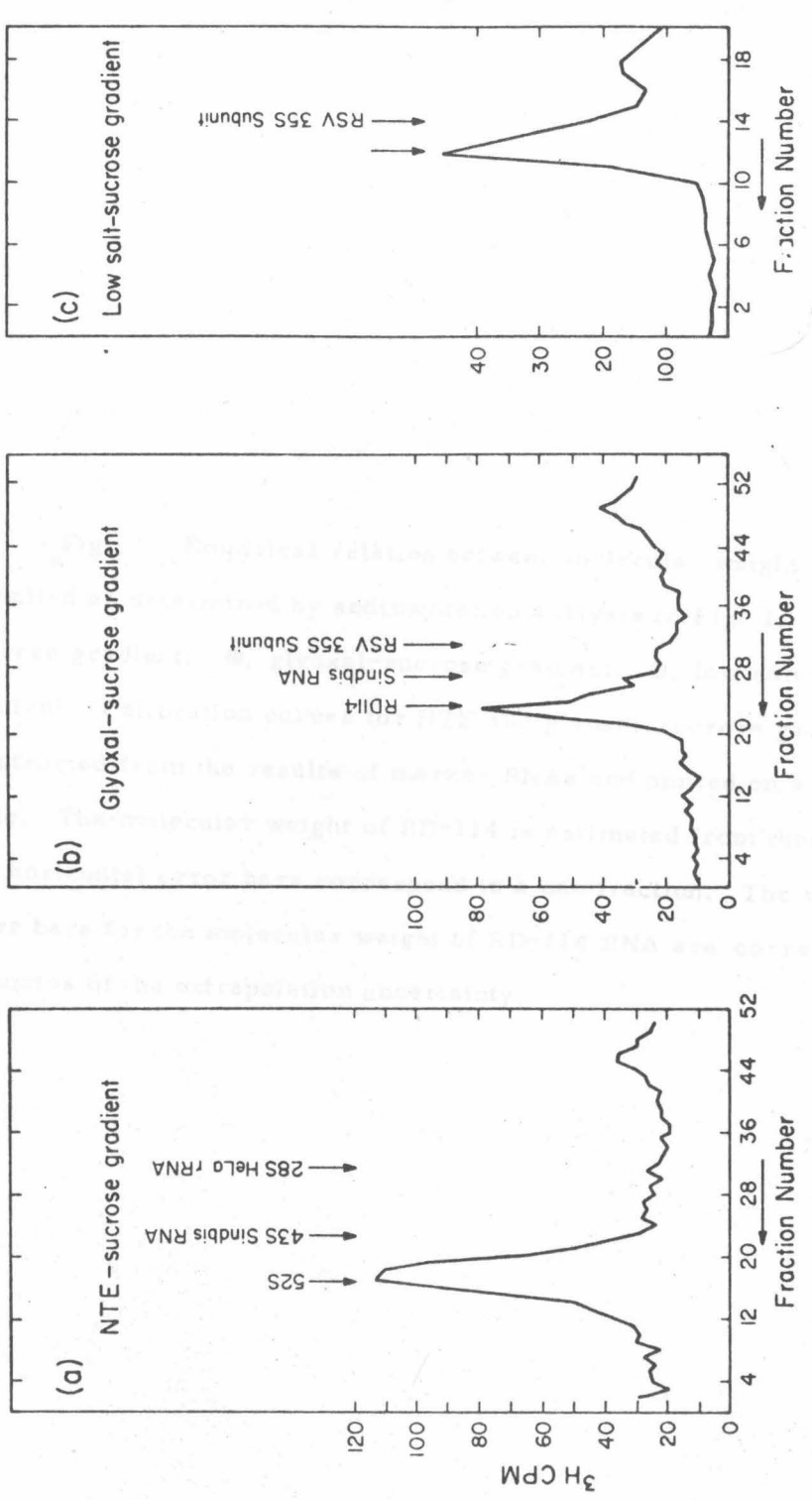
(a)
NTE-sucrose gradient
52S
43S Sindbis RNA
28S HeLa rRNA
^{3}H CPM
Fraction Number
(b)
Glyoxal-sucrose gradient
RDIIA
Sindbis RNA
RSV 35S Subunit
Fraction Number
(c)
Low salt-sucrose gradient
RSV 35S Subunit
Fraction Number

Fig. 2. Empirical relation between molecular weight and distance travelled as determined by sedimentation analysis in Fig. 1. ▲, NTE-sucrose gradient; ●, glyoxal-sucrose gradient; O, low salt-sucrose gradient. Calibration curves for NTE and glyoxal-sucrose gradient were constructed from the results of marker RNAs and plotted on a log-log scale. The molecular weight of RD-114 is estimated from these curves. The horizontal error bars correspond to ± one fraction. The vertical error bars for the molecular weight of RD-114 RNA are corresponding estimates of the extrapolation uncertainty.

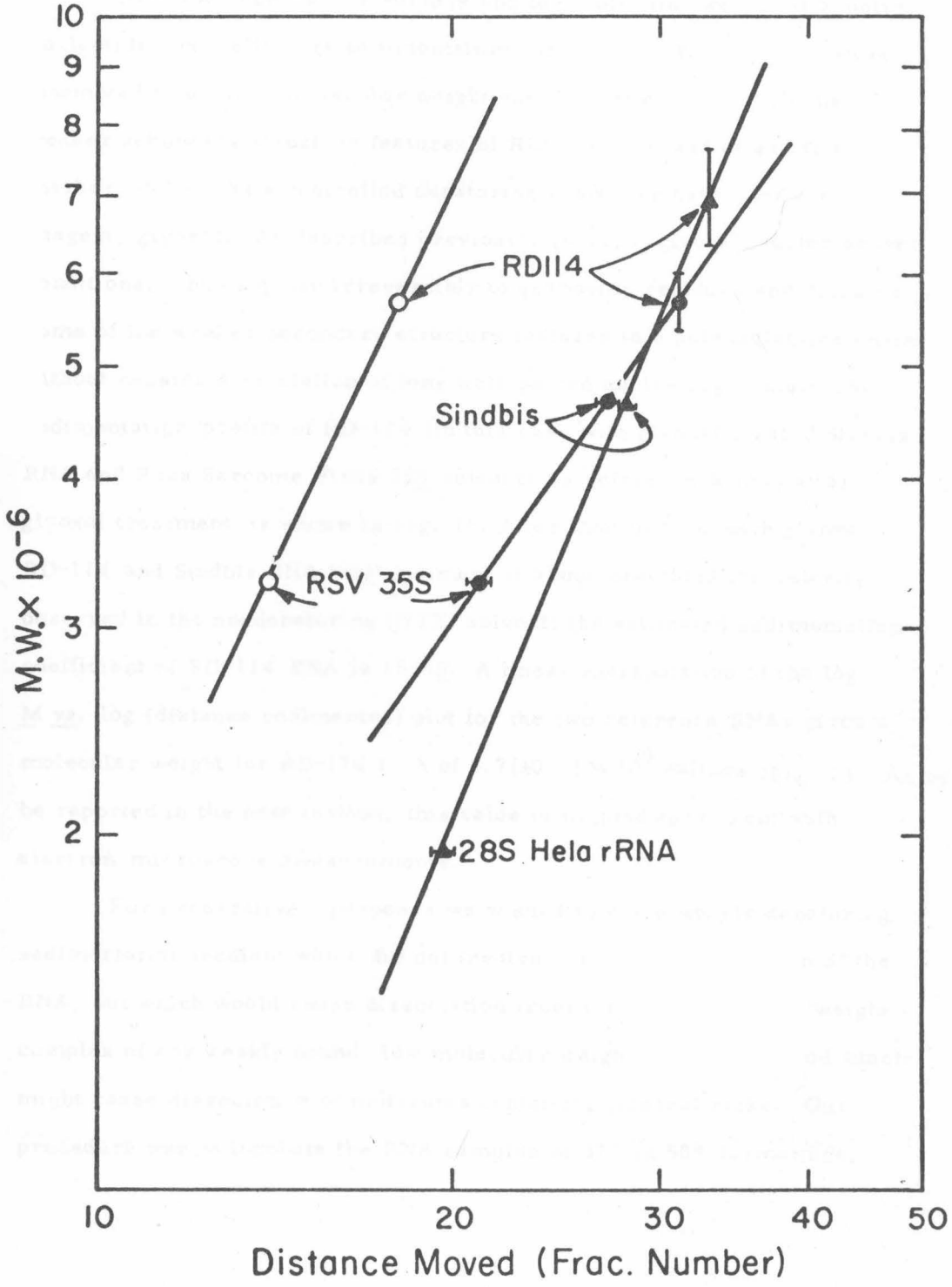
M.W. X 10⁻⁶
10
9
8
7
6
5
4
3
2
RDII14
Sindbis
RSV 35S
28S Hela rRNA
10
20
30
40
50
Distance Moved (Frac. Number)

Both the secondary structure and the molecular weight of a polynucleotide chain affect its sedimentation coefficient. We have therefore attempted to obtain a molecular weight estimate after disrupting the weaker secondary structure features of RD-114 RNA and of suitable marker RNAs. As a controlled denaturing agent, we have used the reagent, glyoxal. As described previously (8, 12, 6) glyoxal, under proper conditions, binds quasi-irreversibly to guanosine residues and disrupts some of the weaker secondary structure features in a polynucleotide chain without causing dissociation of long well-paired duplex segments. The sedimentation profile of RD-114 (in this case with glyoxal treated Sindbis RNA and Rous Sarcome Virus 35S subunits as reference RNAs) after glyoxal treatment is shown in Fig. 1b. After modification with glyoxal, RD-114 and Sindbis RNA both sediment at about one-third the velocity observed in the nondenaturing (NTE) solvent; the estimated sedimentation coefficient of RD-114 RNA is 15.6S. A linear extrapolation of the log M vs. log (distance sedimented) plot for the two reference RNAs gives a molecular weight for RD-114 RNA of $5.7(\pm 0.3) \times 10^6$ daltons (Fig. 2). As will be reported in the next section, this value is in good agreement with electron microscope measurements.

For preparative purposes we wished to use a weakly denaturing sedimentation medium which did not involve chemical modification of the RNA, but which would cause dissociation from the high molecular weight complex of any weakly bound, low molecular weight components and which might cause dissociation of molecules containing internal nicks. Our procedure was to incubate the RNA samples at 37° in 50% formamide,

50% NTE and to sediment the product through a low salt (1 mM Tris, pH 7.0) aqueous sucrose gradient. The peak fractions from these preparative runs were pooled for other studies. As shown in Fig 1c, RD-114 RNA again sediments at a position expected for a 5-6 $\times 10^6$ dalton RNA species.

We presume that essentially the same high molecular weight complex is being observed by sedimentation in the three different systems described above. We refer to this entity as the 52S RD-114 RNA complex. It may be noted that incubation at 37° in 50% formamide, 50% NTE causes dissociation of 60-70S avian RNA tumor virus RNA into 35S subunits (12, 16). However, the 52S RD-114 RNA is not dissociated by this treatment.

Electron microscope studies. We have studied the molecular weight, the secondary structure, and the subunit composition of the RD-114 52S RNA complex by electron microscopy in experiments in which the RNA is exposed to a set of conditions of increasing denaturing power. It may be recalled that single-strand RNA molecules are not well extended under the usual 40-60% formamide, 0.1 M Tris electrolyte, spreading conditions that are effective for extending single-strand DNA (2).

Several different solvent systems that are effective for extending RNA have been used in the present studies.

(a) Urea-formamide spreadings. A spreading solution containing urea, formamide, and a low electrolyte concentration is useful for extending RNA molecules under controlled denaturing conditions (17, 18). In the present instance, we have used a series of solutions with a fixed aqueous electrolyte solution, as described in MATERIALS and METHODS.

When 52S RD-114 RNA is spread from 30% formamide (0.06 M univalent cations, no urea) it has a highly condensed structure as illustrated in Fig. 3a and the detailed topology of the molecules cannot be discerned. In spreadings from 55% (U+F) (with 0.12 M univalent cations), the RNA is, in general, still very tangled. However, in some molecules, such as those shown in Fig. 3b, the secondary structure features described in detail below can be recognized. When the (U+F) concentration is raised to 70% (0.06 M cations), many of the molecules are sufficiently well extended so that they can be traced. There are two characteristic secondary structure features which are present in almost all of the full length traceable molecules: (a) a Y (or T) shaped structure located close to the middle, which we refer to as the "rabbit ears" structure or RE; (b) two symmetrically disposed loops, on each side of and at equal distances from the central rabbit ears feature. The micrograph in Fig. 3c illustrates such a molecule.

If the RNA is spread from 80% (U+F) (0.05 M cations), all of the molecules are extended and suitable for length measurements (Fig. 3d). A histogram of these length measurements is shown in Fig. 4a, with the number average length of 3.98 ± 0.21 μm.

We believe that the molecule of molecular length 3.98 μm with the RE and the two loops is the 52S RD-114 RNA complex. The length measurements correspond to a molecular weight of ca. 5.7×10^6. However, we defer a detailed discussion of lengths and molecular weights and of the positions of the several secondary structure features until a later section.

Among full length molecules (shaded area in Fig. 4a) over 97% contained the RE. Of these, 46% had one loop and 28% had both loops at

Fig. 3. Electron micrographs of RD-114 spread by the urea-formamide technique. (a) in 30% formamide (no urea, 0.06 M cations) at 20°C; (b) in 55% (U+F) (0.12 M cations) at 20°C; (c) in 70% (U+F) (0.06 M cations) at 20°C; (d) in 80% (U+F) (0.05 M cations) at 20°C; (e) in 65% (U+F) (0.06 M cations) at 80°C. Arrows indicate the central RE structure. Triangles point to the loop features. The urea-formamide and high temperature spreading technique are described in MATERIALS and METHODS. The length marker is 0.2 μm.

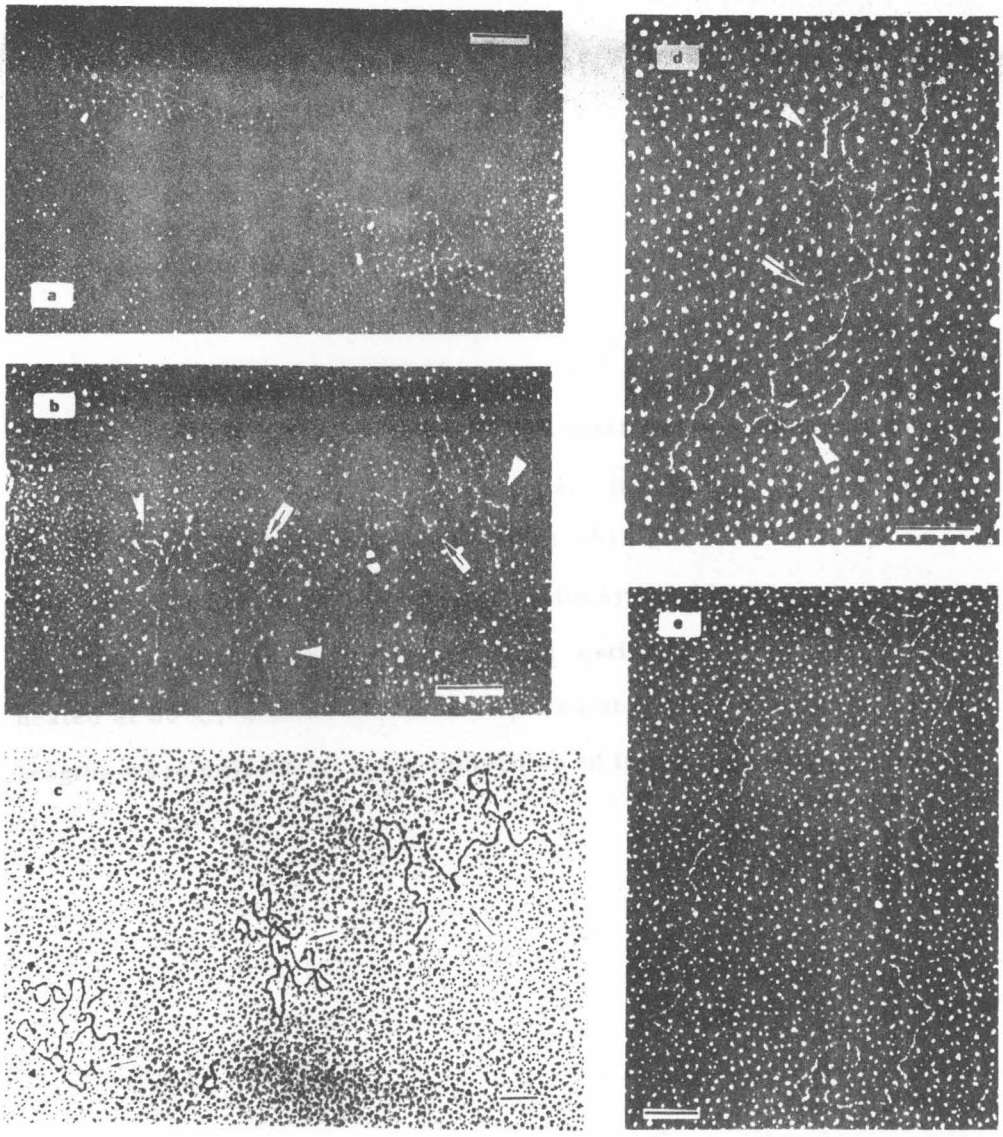
a
b
c
d
e

Fig. 4. Histogram of the length distribution of RD-114 RNA spread by the urea-formamide technique. (a) RD-114 RNA spread in 80% (U+F) (0.05 M cations) at 20°C; (b) RD-114 RNA spread in 65% (U+F) (0.06 M cations) at 80°C; (c) RD-114 RNA in 65% (U+F) (0.06 M cations), heated at 80°C, chilled on ice and spread at 20°C. The number average lengths were calculated from molecules in the shaded area.

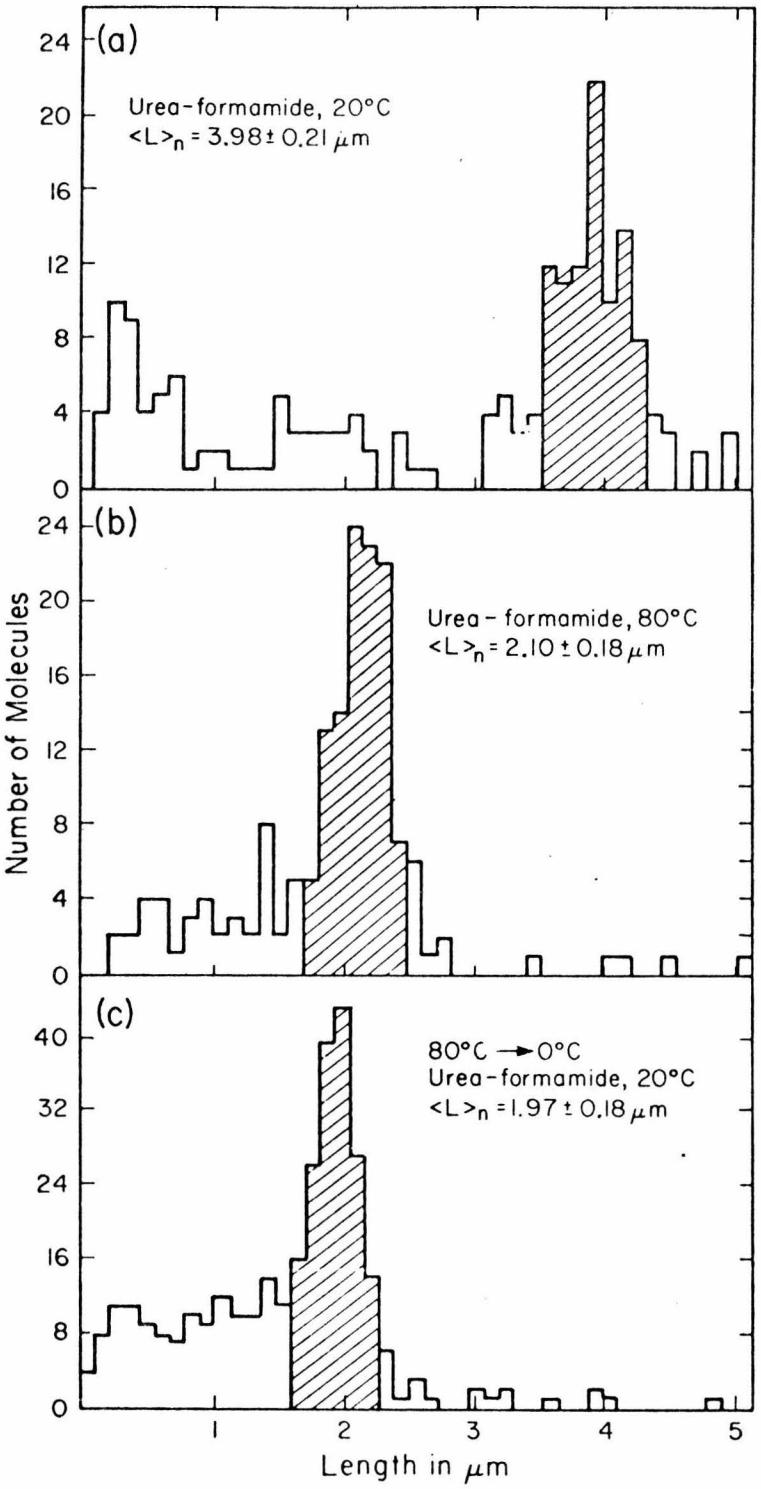
(a)
Urea-formamide, 20°C
<L>n = 3.98 ± 0.21 μm
(b)
Urea - formamide, 80°C
<L>n = 2.10 ± 0.18 μm
(c)
80°C → 0°C
Urea-formamide, 20°C
<L>n = 1.97 ± 0.18 μm
Number of Molecules
Length in μm

symmetrical positions. These observations, and others reported below, are consistent with the view that the two loops and the RE are native secondary structure features of 52S RD-114 RNA. Spreading conditions, such as those used in Fig. 3d, which are useful for extending the molecules for good length measurements, are sufficiently denaturing to cause dissociation of about 50% of the loops but not the RE. It should also be noted that the RE in RD-114 RNA was described in our preliminary papers (11, 12) but the reproducible loop structures were not recognized.

We wished to ask whether the RD-114 RNA molecule of molecular weight 5.7×10^6 is one continuous polynucleotide chain or consists of two subunits, each of molecular weight approximately 2.8×10^6, held together by some sort of cohesion within the rabbit ears. We therefore sought procedures to expose the RNA to strongly denaturing conditions while minimizing the risk of covalent chain breakage.

As reported in this and following sections, we have found two different denaturing treatments which cause the 52S RD-114 RNA molecule to be dissociated into two half-size molecules, with a concomitant disappearance of the RE.

The structure of the RNA was observed when spread from 65% (U+F) (0.06 M univalent cations), onto distilled water at several elevated temperatures as described in MATERIALS and METHODS. Below 50°C, 3.98 mμ molecules with an RE are observed. At 60° and above, many half-size molecules without an RE are observed. A histogram of the size distribution from an 80° experiment is shown in Fig. 4b. The average molecular length was 2.10 μm. Over 98% of the molecules observed were smooth and extended without any secondary structure feature,

as shown in the examples in Fig. 3e. About 2% of the molecules were undissociated, with a length of ca. 4.0 μm and an RE.

A solution of RD-114 RNA in the urea-formamide solvent was heated to 60° or 80°, quenched in ice water, and promptly spread at room temperature. The resulting molecules were half size without an RE. The length distribution presented in Fig. 4c corresponds to an average length of 1.97 μm, in good agreement with the lengths observed in the high temperature spreadings. There was a new secondary structure feature illustrated in the micrographs in Fig. 5. The structure can be described as having an unsymmetrical branch over its stem, and is referred to as a BLS (branch-like structure). It is morphologically quite different in appearance from the RE. The contour length of this feature (traced assuming it is duplex) is 0.31 ± 0.06 μm and it occurs at a distance of 0.21 ± 0.05 μm from one end of the otherwise linear 1.97 μm molecules. About 30% of the half size molecules in the quenched sample had the BLS; the remaining 70% were extended, although slightly knobby.

Between 1 and 2% of the molecules were full size (4.0 μm) with an RE. A representative molecule is shown in Fig. 5a. It contains two BLS, symmetrically disposed at a distance of 0.2 μm from the RE. This result strongly supports the model that RD-114 RNA consists of two chains of molecular weight 2.8×10^6 joined together within the RE. The BLS appears to be a base paired structure due to sequences extending from a point close to the RE to a point slightly within the loop structure. It is formed after quenching when the loop structures seen in the native 52S RNA complex are dissociated.

(b) Glyoxal-formamide spreading. Reaction with glyoxal under the conditions in MATERIALS and METHODS modifies single-strand RNA so

Fig. 5. Electron micrographs of heated and chilled RD-114 RNA spread by urea-formamide technique. 52S RD-114 RNA samples in 65% (U+F) were heated to 80°C, then quickly quenched on ice and spread at 20°C. (a) An undissociated 5.7×10^6 dalton RD-114 RNA. The molecule contains the RE (arrow) and the two BLS (triangles) symmetrically located on each side of the RE. (b and c) Each show a 2.8×10^6 dalton RD-114 RNA with the BLS (triangle). The length marker is 0.2 μm.

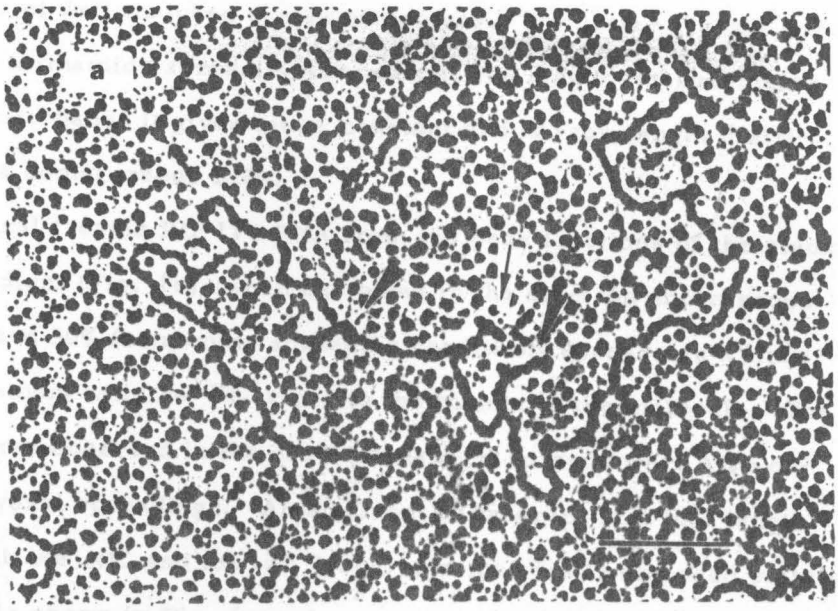
a

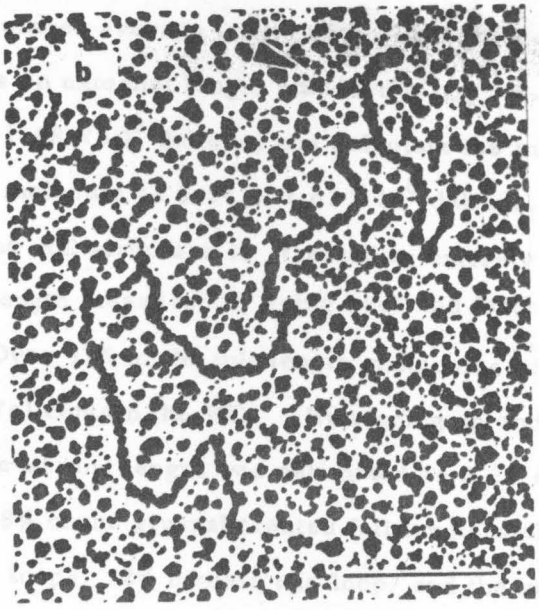
b

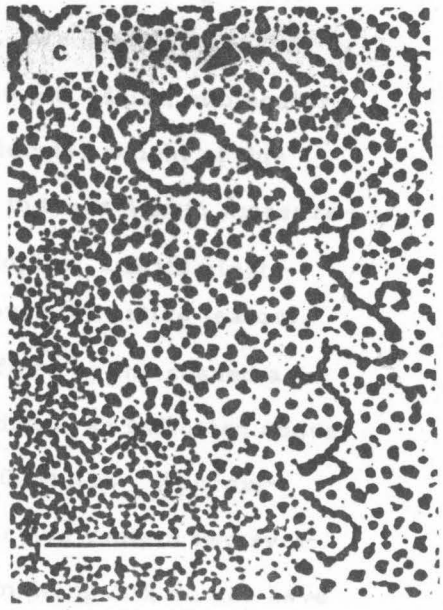
c

that it is well extended in formamide spreadings, but does not cause denaturation of well matched duplex structures. We prefer glyoxal spreading to urea-formamide spreading for quantitative length measurements because in our hands it gives more constant and narrow length distributions for a homogeneous RNA.

Glyoxal treated RD-114 RNA from the peak fractions of the glyoxal-sucrose gradient (Fig. 1b), when examined in the electron microscope under standard 50% formamide spreading conditions, appears as a linear extended filament with the RE close to the middle of the molecule. The loop structures observed in the urea-formamide spreads were also observed in glyoxal spreadings. An electron micrograph of a full length molecule with the RE and the two loops, symmetrically disposed relative to the RE, is shown in Fig. 6a. As shown in the histogram in Fig. 7a, the size distribution of the RNA molecules is reasonably homogeneous with a number average length of 4.27 ± 0.17 μm. We use E. coli 23S rRNA as an external length standard ($\langle L \rangle_n = 0.80 \pm 0.04$ μm, molecular weight $= 1.08 \times 10^6$ daltons) and calculate the molecular weight of this RD-114 molecule as $5.74 \pm 0.23 \times 10^6$ daltons. In these length measurements the RE structure is treated as entirely duplex, and its single-strand length measured by going back and forth over the entire feature.

Over 97% of the full length molecules (defined by the shaded area in Fig. 7a) contain the RE. By tracing up and down, as indicated above, its single-strand length was estimated as 0.21 ± 0.04 μm. Approximately 28% of the glyoxal treated full length molecules contain two symmetrical loops, 52% contain one loop, and the remaining 20% do not have any. As shown by the histogram in Fig. 7d, these loops are mapped reproducibly at a distance 0.44 ± 0.06 μm from the RE and have a

Fig. 6. Electron micrographs of RD-114 RNA spread by the glyoxal-formamide technique. (a) glyoxal treated RD-114 RNA; (b) CH_3HgOH-glyoxal treated RD-114 RNA. An arrow indicates the central RE structure. Triangles point to the two loop features. Procedures for RNA treatment and EM spreading are detailed in MATERIALS and METHODS. The length marker is 0.2 μm.

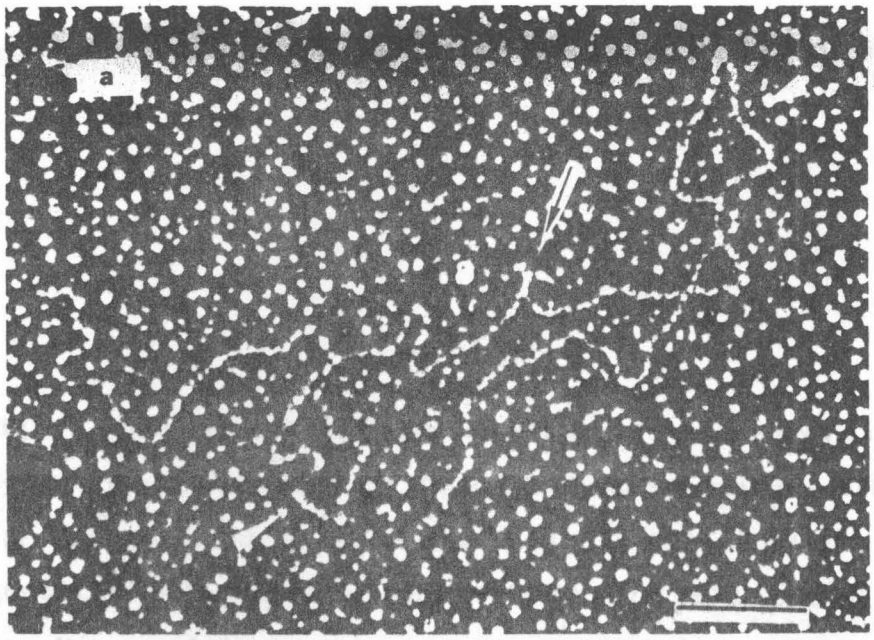
a

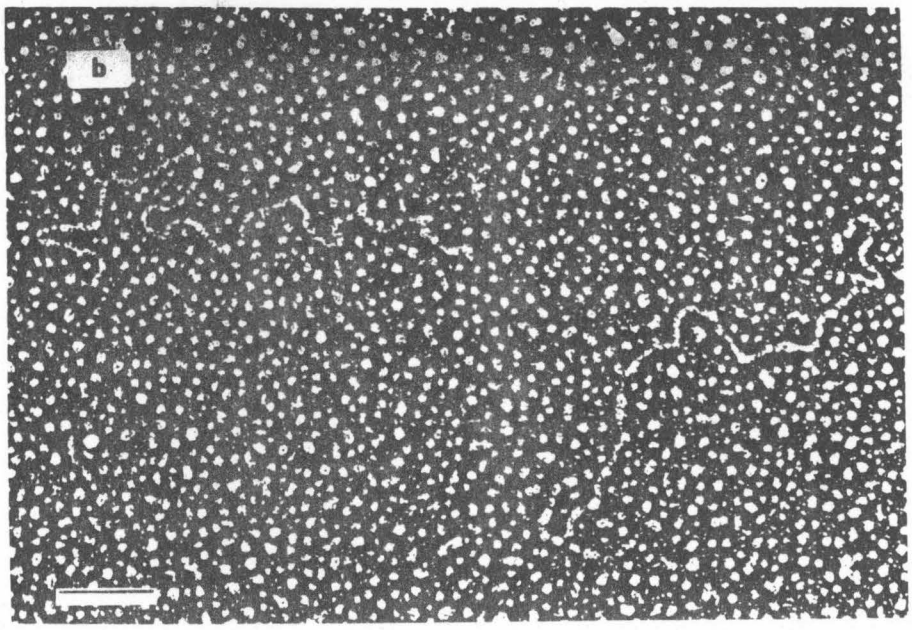
b

Fig. 7. Histogram of the length distribution of RD-114 RNA as studied by the glyoxal-formamide and CH_3HgOH-glyoxal-formamide techniques. (a) the total length of glyoxal treated RD-114 RNA; (b) the total length of CH_3HgOH-glyoxal treated RD-114 RNA; (c) end to central RE structure distance of glyoxal treated RD-114 RNA; (d) the loop joint to central RE structure distance and the loop size of glyoxal treated RD-114 RNA.

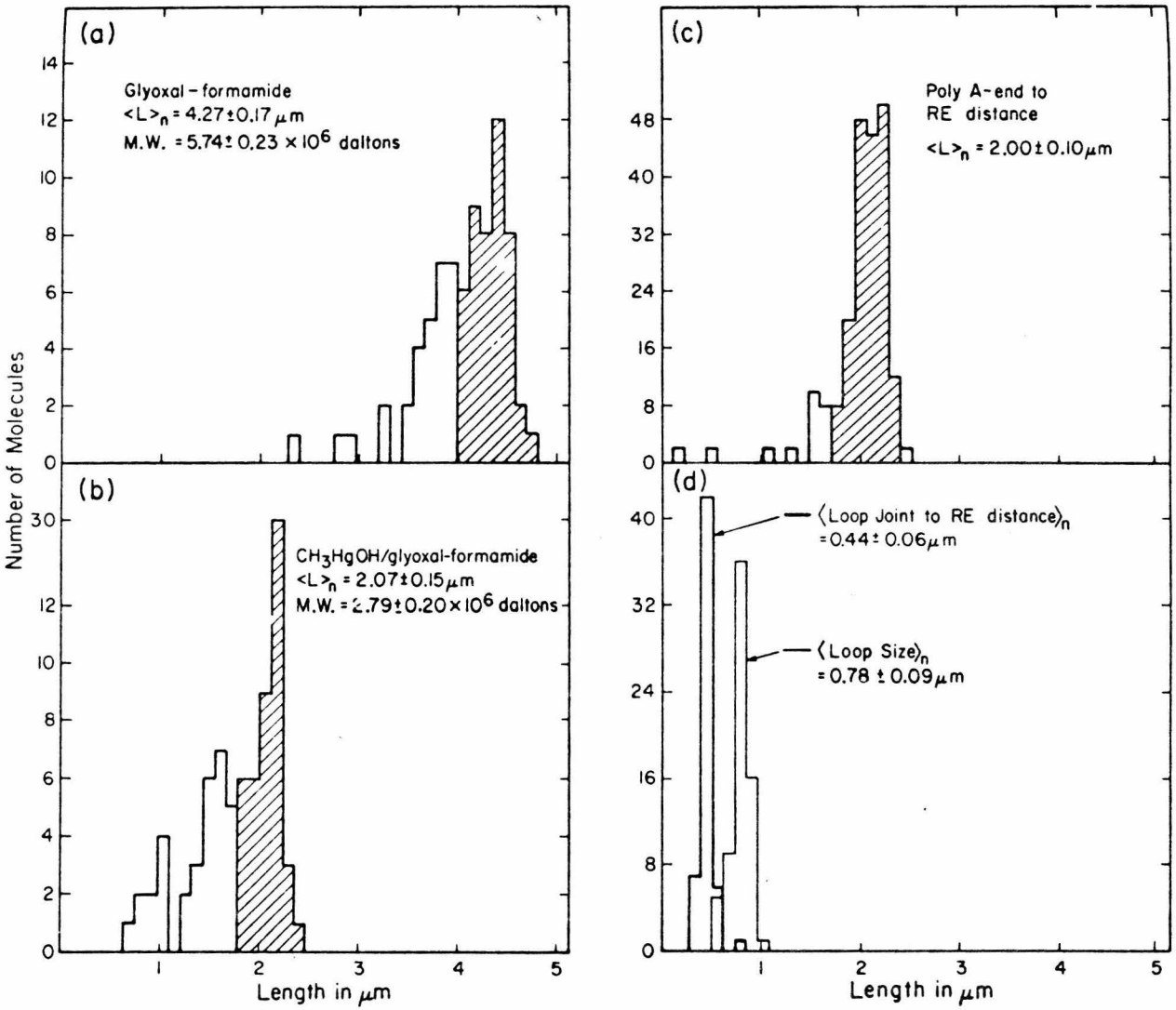
(a)
Glyoxal – formamide
<L>n = 4.27±0.17 μm
M.W. = 5.74± 0.23 × 10^6 daltons
(b)
CH3HgOH/glyoxal-formamide
<L>n = 2.07±0.15 μm
M.W. = 2.79±0.20×10^6 daltons
Number of Molecules
Length in μm
(c)
Poly A-end to
RE distance
<L>n = 2.00±0.10 μm
(d)
⟨Loop Joint to RE distance⟩n
= 0.44 ± 0.06 μm
⟨Loop Size⟩n
= 0.78 ± 0.09 μm
Length in μm

homogeneous loop length of 0.78 ± 0.09 μm. One would suspect that the loop structures are due to short complementary sequences at the base of the loop. If so, the length of this duplex segment appears to be less than 200 nucleotide pairs and thus too short to be positively identified as such in the electron micrographs. (One can, however, imagine that such a duplex segment does exist on examining micrographs such as that shown in Fig. 6a.) The observation that not all molecules contain the loop structure suggests that the glyoxal denaturing conditions frequently cause denaturation of the short sequence of base pairs involved.

Thus, the results from the glyoxal spreadings confirm the structures observed in urea-formamide spreadings and support the view that 52S RD-114 RNA isolated either by NTE gradients or by glyoxal gradients has essentially the same structure; i.e., a molecule of molecular weight 5.7×10^6 daltons, with the central rabbit ears structure and the two symmetrically disposed loop structures

We wish to ask whether the RE is actually in the center or slightly off-center of the molecule. Let L_2 and L_1 be distance from hypothetical left and right ends of an asymmetrical molecule of molecular weight 5.7×10^6 with an RE feature close to but not necessarily at the center. We cannot a priori distinguish L_2 from L_1 for any molecule measured. We have calculated the root mean square value of the observed distribution of values of the intrinsically positive (and measurable) quantity, $|L_2 - L_1|$, and find that it is 0.16 μm. For the same sample, the standard deviation of the distribution of values of $(L_1 + L_2)$ was measured as 0.17 μm. If the RE were at the center of the molecule, the average value of the

unobservable quantity ($\underline{L}_2 - \underline{L}_1$) would be zero and the root mean square value of $|\underline{L}_2 - \underline{L}_1|$ is predicted to have the same value as the standard deviation in values of ($\underline{L}_1 + \underline{L}_2$). Thus, the observations support the view that the RE is at the center of the molecule.

(c) Methylmercury-glyoxal spreadings. We wished to study the possible dissociation of the 52S RNA complex into its two subunits by a strongly denaturing treatment which did not involve elevated temperatures as in the urea-formamide thermal dissociation procedures. We have found that treatment with glyoxal in the presence of methylmercuric hydroxide is effective for this purpose.

CH_3HgOH is a reversible denaturing reagent for nucleic acids because it reacts with the imino NH bonds of G, U, and T (7, 15). It is a powerful denaturant. For example, at room temperature in 0.1 M Na_2SO_4 at pH 8.65 M. luteus DNA which has a G+C content of 72% is denatured at a CH_3HgOH concentration of 2.9 mM (7). We therefore anticipated that a sufficiently high concentration of CH_3HgOH would denature any base pairing within the RE. As described in MATERIALS and METHODS the G residues exposed by denaturation were then fixed in the non-hydrogen bonding state by treatment with glyoxal. Accordingly, 52S RD-114 RNA was treated with glyoxal in the presence of 10 mM methylmercuric hydroxide, as described in MATERIALS and METHODS. Note that the methylmercuric hydroxide is removed before spreading. Fig. 6b shows an electron micrograph of the resulting RD-114 RNA molecules. As shown by the histogram in Fig. 7b, the resulting molecules have an average length of 2.07 ± 0.15 μm corresponding to a molecular weight of $2.8 \pm 0.2 \times 10^6$ daltons. They do not have any of the characteristic

secondary structure features of the 5.7×10^6 dalton molecules. It therefore appears that the treatment described dissociates the 5.7×10^6 dalton RD-114 RNA into two subunits, each of molecular weight one-half the value for the starting molecule.

Gel electrophoresis of RD-114 RNA. The dissociation of 52S RD-114 RNA into two half-size subunits under suitable denaturation conditions has been confirmed by gel electrophoresis in several denaturing solvent systems.

We have recently developed a methylmercuric hydroxide-agarose gel system for electrophoresis under denaturing conditions. (Bailey and Davidson, personal communication). 52S RD-114 RNA electrophoreses through a 1% agarose gel containing 5 mM CH_3HgOH in the borate buffer electrolyte described in MATERIALS and METHODS at a velocity that is greater than that of Sindbis RNA but less than that of 28S HeLa rRNA, and 23S E. coli rRNA. Typical gel patterns are illustrated in Fig. 8a. The log M vs. (distance migrated) plot for several reference RNAs in this gel system is linear (Fig. 9) from which we interpolate the molecular weight of RD-114 RNA as $2.64(\pm 0.1) \times 10^6$ daltons. J. Bailey has observed that nicked circular duplex PM2 DNA is dissociated into single-strand components in the agarose gel-methylmercury system at methylmercury hydroxide concentrations greater than 3mM. Therefore, the concentration of 5mM used in the RD-114 RNA experiments is strongly denaturing. The observed molecular weight is approximately one-half of that (5.7×10^6) of the 52S RD-114 complex. Therefore we conclude that RD-114 RNA is dissociated into half-size subunits in the denaturing mercurial gel.

Fig. 8. Electrophoretic gel patterns. Electrophoresis is from left to right. (a) RD-114 RNA in a 5 mM CH_3HgOH agarose gel. The arrow marks the position of Sindbis 43S RNA; (b) gel patterns after heating to 55°C and to 60°C. Electrophoresis is in E buffer at 22°C. The arrow is the migration position of unlabeled 52S RD-114 directly from an NTE gradient, as detected by ethidium bromide staining.

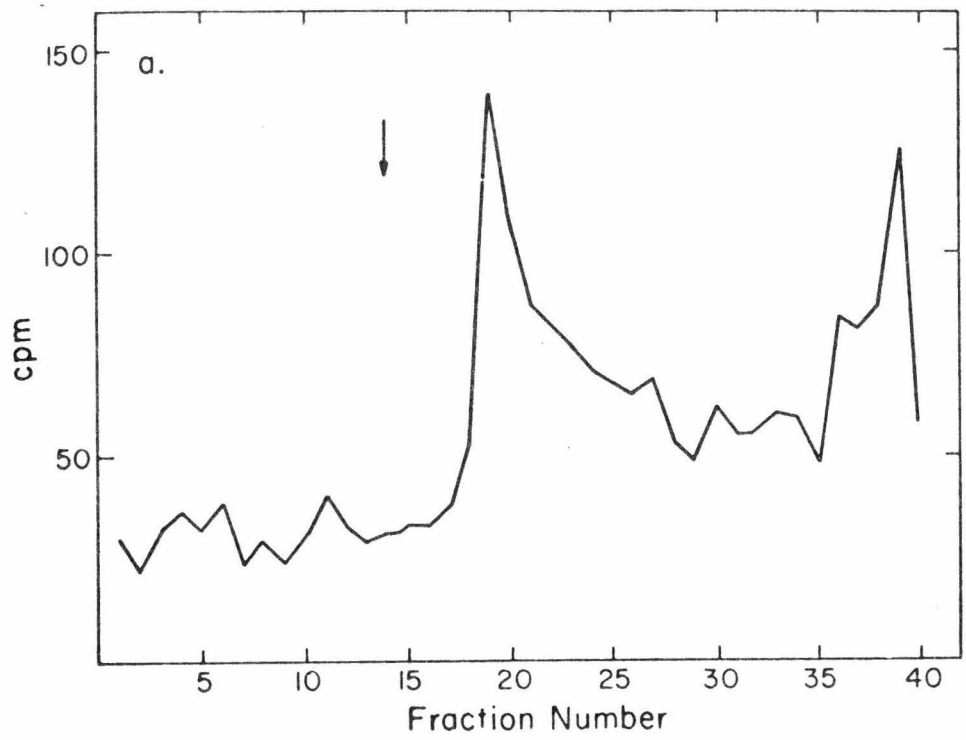
a.
150
100
50
cpm
5
10
15
20
25
30
35
40
Fraction Number

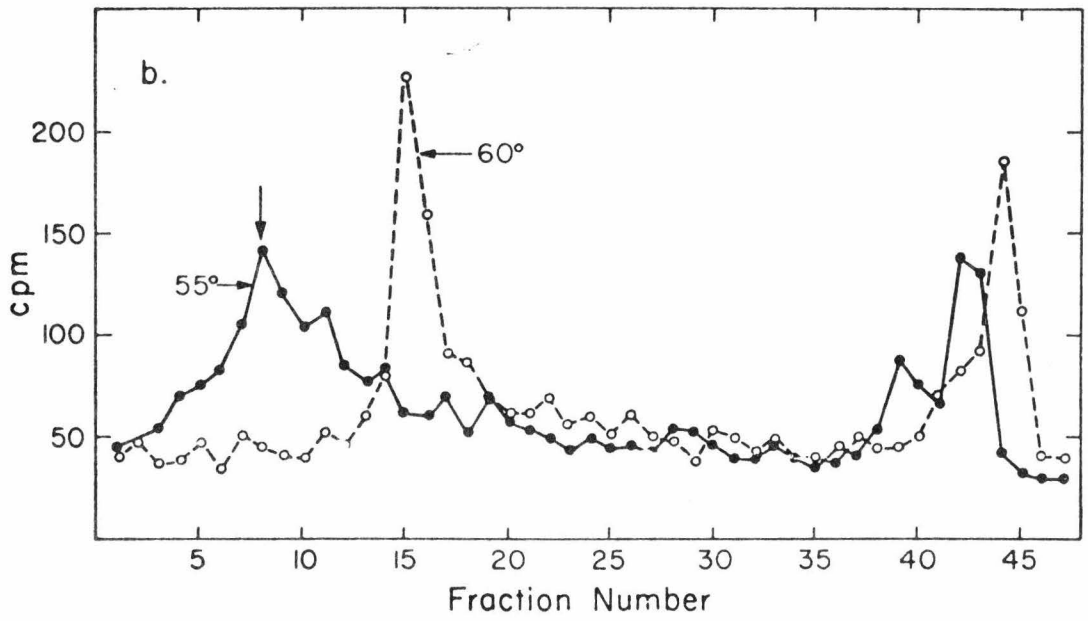
b.
60°
55°
200
150
100
50
cpm
5
10
15
20
25
30
35
40
45
Fraction Number

Fig. 9. A plot of RNA electrophoretic mobility in 5 mM CH_3HgOH 0.8% agarose gels as a function of molecular weight. Marker RNAs, indicated by the filled circles, are 16S and 23S *E. coli* rRNA, 28S HeLa rRNA, and Sindbis virus RNA with respective molecular weights of 0.56, 1.10, 1.90, and 4.67 megadaltons. The mobility and interpolated molecular weight of RD-114 RNA are shown.

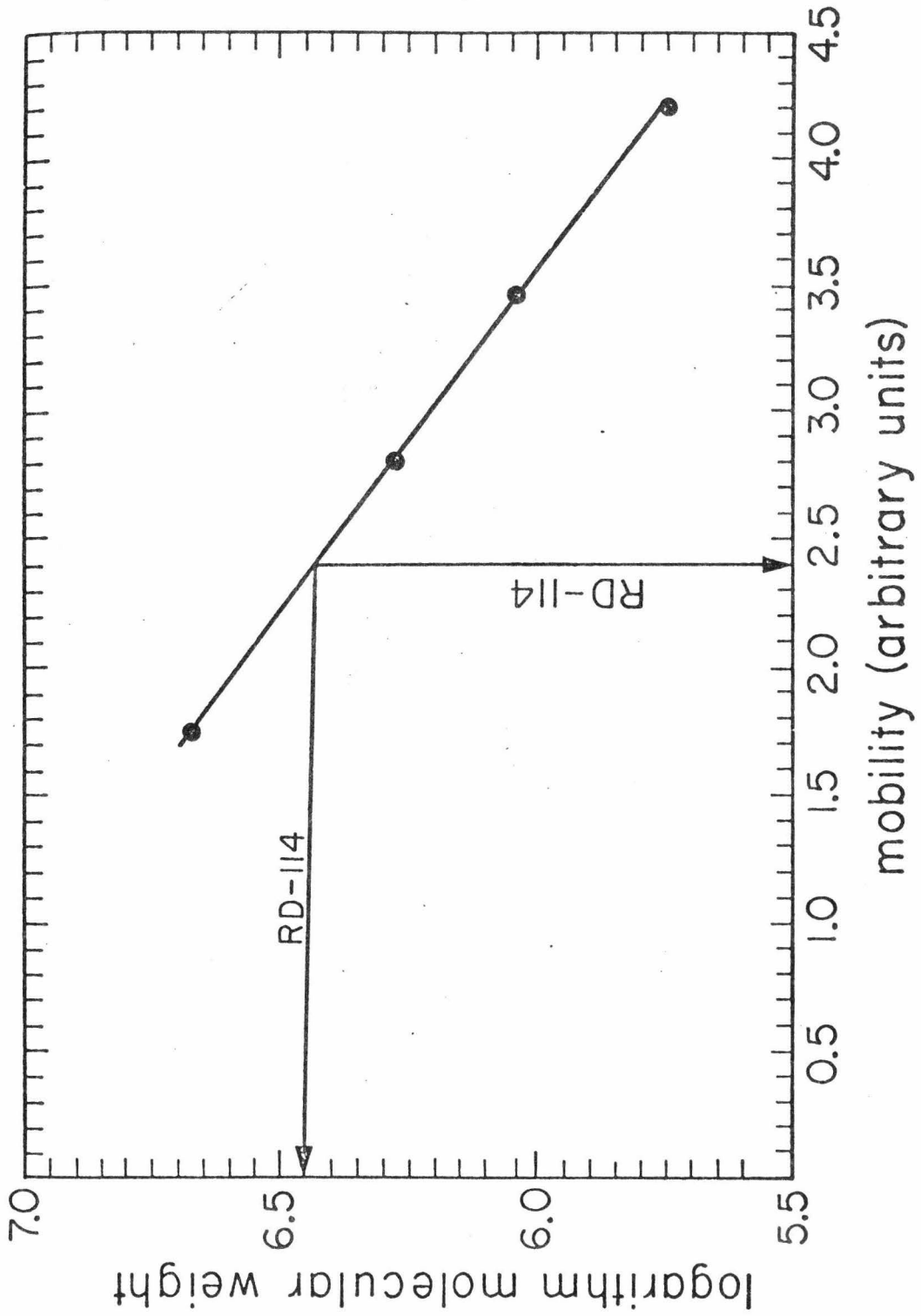
logarithm molecular weight
7.0
6.5
6.0
5.5
mobility (arbitrary units)
0.5
1.0
1.5
2.0
2.5
3.0
3.5
4.0
4.5
RD-114
RD-114

A more precise study of the thermal dissociation of 52S RD-114 RNA (mol. wt. 5.7×10^6 by electron microscopy and sedimentation analysis) into half-size subunits was made using a gel electrophoresis assay to observe dissociation. Labeled 52S RD-114 RNA in the 65% (U+F), 0.06 M cation solvent used for the thermal dissociation electron microscope studies, was heated to various temperatures, quenched on ice, and subjected to gel electrophoresis in the nondenaturing E buffer at room temperature. It may be seen from the radioactivity profiles shown in Fig. 8b that there is a pronounced increase in the distance migrated for a sample heated to 60° as compared to a sample heated to 55°. Samples heated to 25°, 40°, and 50°C all migrated with the same velocity as the 55° heat treatment; samples heated to 70°C and 80°C migrated like the 60° sample. Furthermore, a sample of unlabeled 52S RD-114 RNA from an NTE gradient was diluted directly into a twofold dilution of the electrophoresis buffer, subjected to electrophoresis in the standard buffer, and located by ethidium bromide staining. Its position as shown in Fig. 8 is the same as that of the sample heated to 55°C. There is thus a structural transition with a marked increase in mobility between 55° and 60°C.

By interpolation from the values for the electrophoretic mobilities of HeLa 28S rRNA and Sindbis RNA in the same gel system, the molecular weights of the low and high temperature forms of RD-114 RNA are estimated as 6.7×10^6 and 4.2×10^6 daltons. These values are higher than the expected values of 5.7×10^6 and 2.8×10^6. A sample of RD-114 RNA was treated with 10 mM CH_3HgOH in Na_2SO_4, borate buffer and then

dialyzed against 0.1 M NH_4Cl to remove the bound material and studied by electrophoresis in the nondenaturing gel. We believe, from the electrophoresis studies in 5 mM CH_3HgOH that this treatment will cause dissociation of RD-114 RNA into 2.8×10^6 dalton subunits (actually measured as $2.64 \pm 0.1 \times 10^6$ by electrophoresis in a mercurial gel). The mobility of this sample corresponded to an apparent molecular weight of 4.2×10^6 daltons.

Thus, we believe that the 52S RD-114 RNA with a molecular weight of 5.7×10^6 and its half-size subunit with a molecular weight of 2.8×10^6 show anomalously low electrophoretic velocities due to relatively extended configurations, as compared to HeLa 28S rRNA and Sindbis RNA in the nondenaturing E buffer. The data presented here therefore fix the melting temperature of the central rabbit ears feature, which is manifested by dissociation of 52S RNA into half-size subunits, as between 55° and 60° in the 65% (U+F), 0.06 M cation solvent.

As reported in MATERIALS and METHODS, the T_m of calf thymus DNA in the same solvent was measured as 33°C in an optical melting experiment.

DISCUSSION

Fig. 10 summarizes our observations of the structure and properties of RD-114 RNA. The high molecular weight component extracted from the virion has a sedimentation coefficient of 52S and a molecular weight of $5.74 \pm 0.17 \times 10^6$ daltons. It contains a characteristic secondary structure feature that we describe as the central rabbit ears (RE) with a molecular weight of ca. 0.3×10^6 daltons. The

Fig. 10. Structure and interconversion between the several forms of RD-114 RNA described in the text (molecular weights in daltons are shown, and are based on EM length measurements).

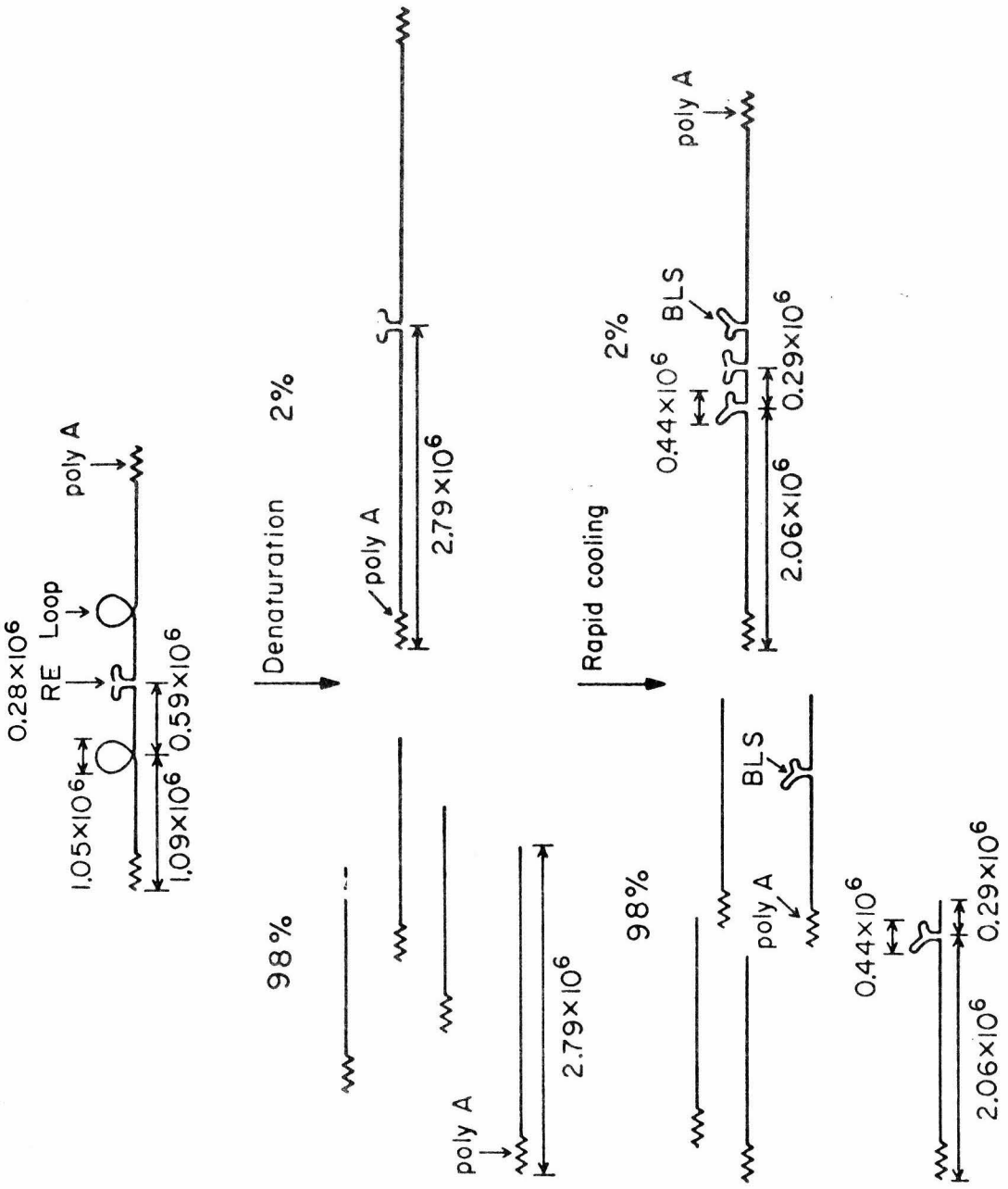
0.28×10⁶
RE
Loop
poly A
1.05×10⁶
1.09×10⁶
0.59×10⁶
Denaturation
2%
98%
poly A
2.79×10⁶
poly A
2.79×10⁶
Rapid cooling
2%
98%
0.44×10⁶
BLS
poly A
0.29×10⁶
2.06×10⁶
BLS
poly A
0.44×10⁶
0.29×10⁶
2.06×10⁶

rest of the molecule is mainly single-stranded, but there are two loops at the symmetrical positions around the RE and with the dimensions indicated in Fig. 10.

The 5.74×10^6 dalton molecule can be dissociated into half-size molecules by sufficiently denaturing conditions (methylmercury-glyxoal, or thermal dissociation in urea-formamide). The RE disappears upon dissociation. We presume, as indicated in Fig. 10, that there is some sort of a base-paired structure between the two subunits giving rise to the RE. Using a gel electrophoresis assay, we have concluded that the melting temperature for dissociation into half-size molecules in 65% (U+F), 0.06 M univalent cation, is between 55 and 60°. By comparison with the melting temperature of 31° for calf thymus DNA in the same solvent, we estimate that the melting temperature of the RE is 108° to 113°C in an aqueous electrolyte containing 0.2 M Na^+. The data collated by Kallenbach (7) on the melting temperature of duplex RNAs as a function of their base composition would then suggest that, if the RE is a simple RNA duplex, its base composition is about 63% G+C.

W. Bender at this laboratory has developed and applied a method of electron microscope mapping of poly-A stretches on polynucleotides by hybridization with poly-dT attached to duplex SV40 circles (as an electron microscope label) (W. Bender, personal communication). This method which is based on a suggestion by Dr. J. Carbon is an extension of one previously reported. Bender finds that there are polv-A stretches on both outside termini of the 5.74×10^6 RD-114 molecule. We presume that the poly-A stretches are located at the 3'-termini of the half-size subunits; therefore the two 5' termini are

contained within the RE, as indicated in Fig. 10. Note that the observation of a poly-A stretch at both of the outside ends demands that the 5.74×10^6 dalton molecule be composed of two subunits, if poly-A stretches occur only at 3′ ends.

We wish to note at this point that in our earlier, preliminary reports(11,12) we drew the tentative conclusion that the 5.74×10^6 dalton molecule was one continuous polynucleotide chain. We now believe that that conclusion was incorrect. At that time we also failed to notice the reproducible presence of the loop structures. It should also be noted that East et al. (1974) had reported that the sedimentation coefficient of the high molecular weight component of RD-114 RNA, as extracted from the virion, was 50S and that thermal dissociation in aqueous electrolyte solution led to the formation of 28S subunits, all in approximate agreement with our present interpretations.

When RD-114 RNA, in 65% (U+F), is heated to temperatures above 60° and then quenched on ice so that the loops disappear a new secondary structure feature, the BLS, is observed. This feature is close to the center, but, as indicated in Fig. 10, a few molecules are observed that contain both the BLS and the RE. This observation strongly suggests that the BLS is a distinct sequence and not part of the RE. The quantitative dimensions, shown in Fig. 10, indicate that the BLS involves some sequences closer to the center than the two loops, but also include some sequences just within the loop.

In spreadings at room temperature from 70% (U+F), almost all full length traceable molecules show the two loops symmetrically

disposed around the RE. In 80% (U+F), about 50% of the loops are seen. A simple interpretation of these results is that the loop is held together by short complementary sequences which are about 50% melted in 80% (U+F) at room temperature. If the loop is not present, the RNA appears to be a simple single strand in this region ; i. e., the BLS is not seen. After heating and cooling in 65% (U+F), the BLS is seen. Since the BLS involves sequences closer to the center of the molecule than is the loop and sequences within the loop, and since the BLS is not seen when a loop is present, we tentatively conclude that the formation of the BLS requires an interaction between sequences within the loop with sequences closer to the center. An alternative possibility is that the loop structure is somehow held together by an additional low molecular weight molecule; the BLS cannot form until this molecule is removed by thermal dissociation.

We propose that two 2.8×10^6 molecules of RD-114 RNA are joined together at their 5' ends to form the rabbit ears feature. Watson-Crick base pairing requires that the two strands be oriented anti-parallel with respect to each other. In the simplest case, this would lead to a linear structure at the junction of the two strands, as shown in Fig. 11. We have been unable to conceive of any simple, anti-parallel scheme of base pairing between two strands that would lead to a Y or T shaped structure. The possibility that an additional low molecular weight RNA component is involved in the cohesion within the RE should also be considered. Since the RNA had been extracted by treatment with phenol, SDS, and pronase, it is unlikely (but not excluded) that any proteins are involved in the cohesion.

Fig. 11. Simplest possible structure for two RNA strands held together by anti-parallel base pairing at their 5′ ends. If the two strands are identical, each one must contain sequence a and its complement a′ as indicated.

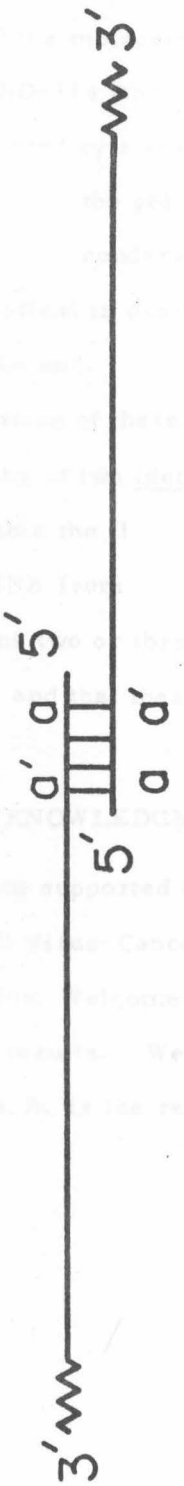
3'
5'
a' a
a a'
5'
3'

We observe that: (1) the molecular weight of the two 2.8×10^6 subunits into which the 52S RD-114 RNA dissociates are identical within experimental error, as indicated by a single sharp peak in both the electron microscope length histogram and the gel electrophoresis pattern of the dissociated subunits; (2) all the secondary structure features observed in these two subunits are identical in position and shape; (3) both subunits contain a poly-A stretch at the end.

One simple interpretation of these results is that the 52S RD-114 molecule is a dimer consisting of two identical subunits, joined together somehow at their 5′ ends within the RE. These observations are consistent with results for the RNA from other tumor viruses, indicating that the 60 to 70S complex contains two or three subunits of molecular weight in the range $2.5 - 3.3 \times 10^6$, and that these several subunits are identical in sequence (1, 3, 4).

ACKNOWLEDGMENTS

This research has been supported by contracts NO-1-CP-43306 and PH 43-68-1030 within the Virus-Cancer Program of the National Cancer Institute. We thank Mr. Welcome Bender for permission to quote his unpublished poly-A mapping results. We also thank Dr. James Casey for helpful discussions. J. M. B. is the recipient of a Helen Hay Whitney Fellowship.

LITERATURE CITED

1. Baluda, M. A., M. Shoyab, P. D. Markham, R. Evans, and W. N. Drohan. 1974. Characterization of avian myeloblastosis virus genome by molecular hybridization. Cold Spr. Harb. Symp. Quant. Biol. 39, in press.

2. Davis, R., M. Simon, and N. Davidson. 1971. Electron microscopic heteroduplex methods for mapping regions of base sequence homology. p. 413-428. In L. Grossman and K. Moldave (ed.), Methods in enzymology, vol. XXI. Academic Press, Inc., New York.

3. Delius, H., P. Duesberg, and W. Mangel. 1974. Electron microscopic measurements of Rous sarcoma virus RNA. Cold Spr. Harb. Symp. Quant. Biol. 39, in press.

4. Duesberg, P. H., P. K. Vogt, M. Lai, and K. Beeman. 1974. Studies on genetic recombination between avian tumor viruses. Cold Spr. Harb. Symp. Quant. Biol. 39, in press.

5. East, J. L., J. E. Knesek, P. T. Allen, and L. Dmochowski. 1973. Structural characteristics and nucleotide sequence analysis of genomic RNA from RD-114 virus and feline RNA tumor viruses. J. Virol. 12, 1085-1091.

6. Forsheit, A. B., N. Davidson, and D. B. Brown. 1974. An electron microscope heteroduplex study of the ribosomal DNAs in Xenopus laevis and Xenopus mulleri. J. Mol. Biol. 90, 301-314.

7. Gruenwedel, D. W., and N. Davidson. 1966. Complexing and denaturation of DNA by methylmercuric hydroxide. J. Mol. Biol. 21, 129-144.

8. Hsu, M. T., H. J. Kung, and N. Davidson. 1973. An electron microscope study of Sindbis virus RNA. Cold Spr. Harb. Symp. Quant. Biol. 38, 843-950.

9. Inman, R. B., and M. Schnös. 1970. Partial denaturation of thymine- and 5-bromouracil-containing λ DNA in alkali. J. Mol. Biol. 49, 93-98.

10. Kallenbach, N. R. 1968. Theory of thermal transitions in low molecular weight RNA chains. J. Mol. Biol. 37, 445-466.

11. Kung, H. J., J. M. Bailey, N. Davidson, M. O. Nicolson, and R. M. McAllister. 1974. Structure and molecular length of the large subunits of RD-114 viral RNA. J. Virol. 14, 170-173.

12. Kung H. J., J. M. Bailey, N. Davidson, P. Vogt, M. O. Nicolson, and R. M. McAllister. 1974. Electron microscope studies of tumor virus RNA. Cold Spr. Harb. Symp. Quant. Biol. 39, in press.

13. Robberson, D., Y. Aloni, G. Attardi, and N. Davidson. 1971. Expression of the mitochondrial genome in HeLa cells. XI. Size determination of mitochondrial ribosomal RNA by electron microscopy. J. Mol. Biol. 60, 473-484.

14. Sharp, P. A., B. Sugden, and J. Sambrook. 1973. Detection of two restriction endonuclease activities in Haemophilus parainfluenza using analytical agarose ethidium bromide electrophoresis. Biochem. 12, 3055-3063.

15. Simpson, R. B. 1963. Association constants of methylmercuric and mercuric ions with nucleosides. J. Am. Chem. Soc. 86, 2059-2065.

16. Trávniček, M. and R. Josef. 1973. Subunits of oncornavirus high - molecular-weight RNA. I. Stepwise conversion of 60S AMV RNA to subunits. Biochem. Biophys. Res. Comm. 53, 217-223.

17. Wellauer, P. K., and I. B. Dawid. 1973. Secondary structure maps of RNA : processing of HeLa ribosomal RNA. Proc. Nat. Acad. Sci. 70, 2827-2831.

18. Wellauer, P. K., I. B. Dawid, D. E. Kelley, and R. P. Perry. 1974. Secondary structure of mouse L-cell ribosomal RNA and variations in processing pathway. J. Mol. Biol. 89, 397-407.

Chapter 3

BKD (Baboon Endogenous Virus)

WoMV (Simian Sarcoma and Leukosis Virus)

RD-114, Baboon and Woolly Monkey Viral RNA's Compared in Size and Structure*

Hsing-Jien Kung, Sylvia Hu, Welcome Bender, James M. Bailey, and Norman Davidson

Department of Chemistry
California Institute of Technology
Pasadena, California 91125

Margery O. Nicolson and Robert M. McAllister

Department of Pediatrics
University of Southern California
School of Medicine
Childrens' Hospital of Los Angeles
Los Angeles, California 90054

* The studies of Baboon viral RNA's were carried out by S. Hu and J. Bailey.

Summary

The molecular weights, subunit compositions and secondary structure patterns of the RNA's from an endogenous baboon virus and from a woolly monkey sarcoma virus were examined and compared to the properties of the RNA of RD-114, an endogenous feline virus. The high molecular weight RNA extracted from each of these three viruses has a sedimentation coefficient of 52S, and a molecular length, measured by electron microscopy, of 16-20kb. Each such RNA is a dimer, containing two monomer subunits of 8-10kb in length (3×10^6 daltons, molecular weight). The two monomer subunits are joined at their non-poly(A) ends in a structure called the dimer linkage structure. The appearance of this structure is somewhat different for the different viruses. The dimer linkage dissociates at the same high temperature in RD-114 and baboon viral RNA's but at a lower temperature in woolly monkey RNA. All three viral RNA's have two large loops of similar size and position symmetrically placed on either side of the dimer linkage structure.

Since the baboon virus is distantly related to RD-114, and the woolly monkey virus is unrelated to either of the other two, the dimer linkage and symmetrical loops are surprisingly similar and may well be common features of type C virus RNA's.

Introduction

The RNA of the endogenous feline type C virus, RD-114, has been extensively studied in this laboratory and has been shown to have a novel structure (Kung et al., 1975). The RNA from the virion is a 20kb dimer molecule with an end of one 10kb monomer noncovalently joined to an end of the other in a secondary structure feature at the middle of the dimer molecule. The name "rabbit ears" was used to describe this central junction feature in RD-114, but, as will be shown here, the detailed shape of this feature differs with different spreading conditions or with RNA's of different viruses under identical spreading conditions. Therefore, we have now adopted the more functional name "dimer linkage structure." RD-114 dimer RNA also has a large loop in each monomer half, and these loops are symmetrically placed with respect to the dimer linkage structure. Poly(A) mapping has located poly(A) sequences on both free ends of the dimer (Bender and Davidson, 1976). If the poly(A);s are on the 3' ends of the monomer RNA's, then the two 5' ends must be joined in the dimer linkage structure.

Initial electron microscopic studies had shown no RNA secondary structure features similar to those of RD-114 in either Rous sarcoma virus or Gardner-Arstein Feline leukemia virus (Kung et al., 1973). Therefore we chose to examine the endogenous baboon virus, BKD (Todaro et al., 1974), which is partially related to RD-114, to see if the RD-114 features would be conserved. We found that the structure and physical properties of BKD RNA were quite similar to those of RD-114 RNA. We therefore studied the RNA of another primate

derived virus, denoted WoMV, which is the simian sarcoma virus isolated from a woolly monkey (Theilen et al., 1971). This virus is not endogenous in primates and is not related to either RD-114 or BKD viruses by serological or nucleic acid hybridization tests. Nevertheless, it, too, shows a dimer structure strikingly similar to that of RD-114 and BKD.

Results

I. Baboon Endogenous Virus

A. Sedimentation analysis. Total RNA extracted from the baboon endogenous virus, BKD, was sedimented in a sucrose gradient containing 0.1 M NaCl and RD-114 RNA was sedimented in a parallel tube. RD-114 RNA was shown to have an S value of 52 under these conditions (Kung et al., 1975). Both RNA's sediment with the same velocity (Figure 1a), and so BKD RNA has a sedimentation coefficient of 52S in 0.1 M NaCl. BKD RNA also sediments identically to RD-114 RNA in a low salt (0.6 mM cations) sucrose gradient (data not shown), or on a glyoxal-sucrose gradient (Figure 1c). The latter two sedimentation media are moderately denaturing and cause dissociation of some (but not all) secondary structure. Therefore, these observations suggest that the RNA's of RD-114 and BKD have the same molecular weight.

B. Gel electrophoresis. It has been shown that the high molecular weight RNA of RD-114 is actually a dimer that can be dissociated into monomers only after treatment with strongly denaturing conditions (65% urea plus formamide, 0.06 M cations, 60°, Kung et al., 1975). As will be shown in the results of electron microscope observations,

Fig. 1. Sedimentation profiles of BKD and WoMV RNA as extracted from the virion centrifugation was carried out in SW50.1 rotor at 4°. Arrows indicate RD-114 RNA marker. (a) BKD RNA in NTE-sucrose gradient, 44,000 rpm, 1.25 hr. (b) WoMV RNA in NTE-sucrose gradient, 45,000 rpm, 1.75 hr. (c) BKD RNA in glyoxal-sucrose gradient, 45,000 rpm, 5 hr. (d) WoMV RNA in glyoxal-sucrose gradient, 45,000 rpm, 5.5 hr. All sediemntations are from right to left.

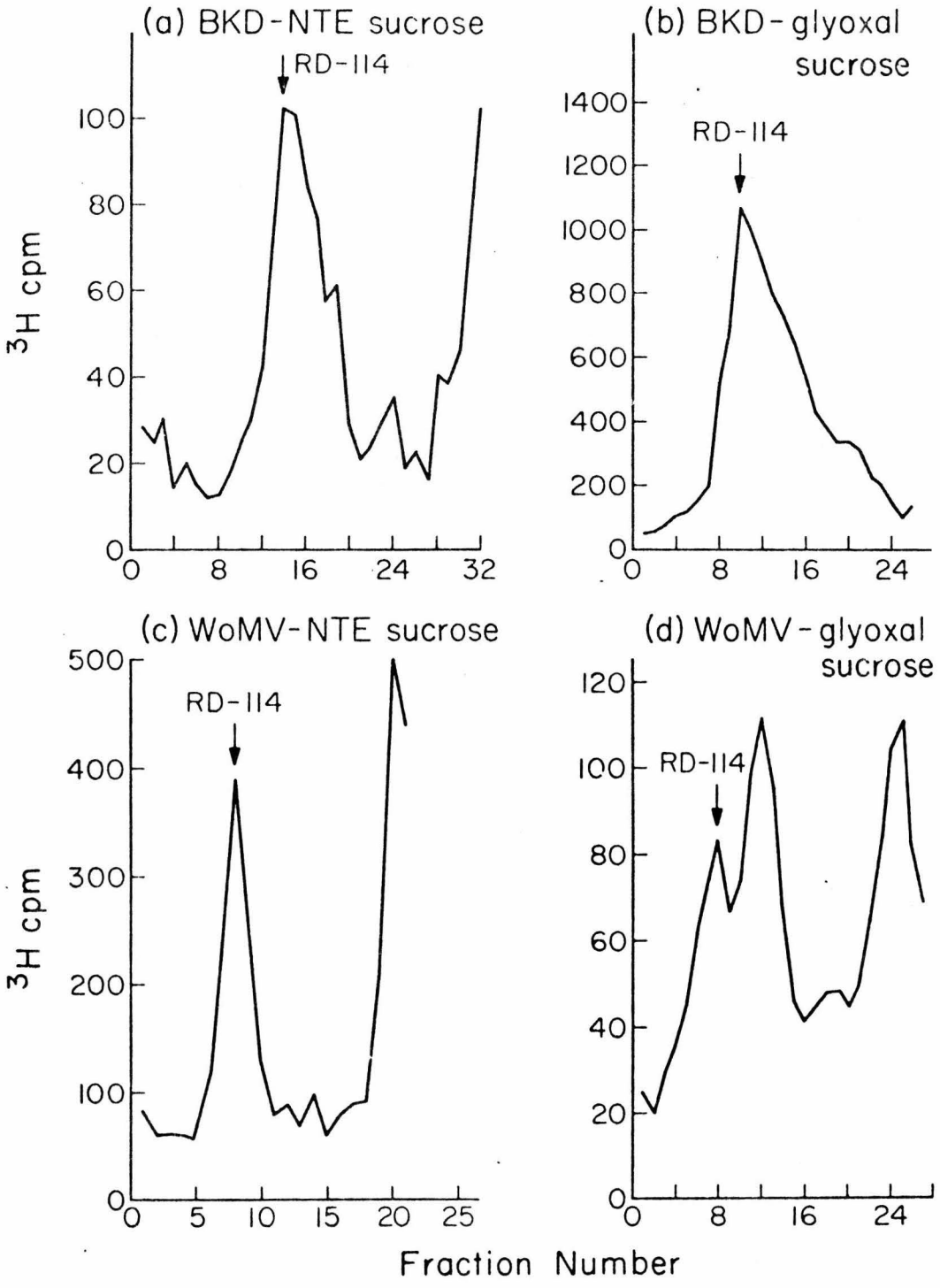
(a) BKD-NTE sucrose
RD-114
(b) BKD-glyoxal sucrose
RD-114
(c) WoMV-NTE sucrose
RD-114
(d) WoMV-glyoxal sucrose
RD-114
^{3}H cpm
Fraction Number

the BKD high molecular weight RNA is also a dimer. We wished to determine the melting temperature of the dimer linkage as compared to that of RD-114. Samples of BKD RNA in 67% urea plus formamide, 0.024 M cations, were heated to various temperatures, cooled, and applied to a non-denaturing agarose gel for electrophoresis. As shown in Figure 2a, samples heated to 40° or less give a single high molecular weight peak; samples heated to 50° are partially dissociated into a lower molecular weight peak, and samples heated to 60° were completely dissociated to the lower molecular weight. It will be shown below that the high molecular weight peak is an RNA dimer and the lower molecular weight peak is monomer RNA. Making slight corrections for the different solvent conditions used in the melting experiments for RD-114 and BKD RNA's, we conclude that the BKD dimer linkage has about the same stability as the RD-114 dimer linkage.

We have found that methylmercury hydroxide can be used to completely denature RNA molecules, so that agarose gel electrophoresis of RNA in the presence of methylmercury hydroxide can be used to determine the molecular weight (Bailey and Davidson, 1975). As shown in Figure 3a, BKD RNA monomers on a methylmercury hydroxide agarose gel comigrated with RD-114 RNA at a mobility corresponding to 3×10^6 daltons (or 9kb).

C. Electron microscopy. (i) Glyoxal treatment is an easy and effective way to disrupt most RNA secondary structure (Hsu et al., 1973) and we consider length measurements in the electron microscope of glyoxal treated RNA to be our most reproducible method for determining molecular weights. BKD RNA was taken from the high molecular weight

Fig. 2. Agarose gel electrophoresis of viral RNA's showing dissociation of the high molecular weight complex. (a) BKD RNA in 67% (U+F), 0.024 M cations. Unheated (——), heated to 40° (--), heated to 50° (-·-), and heated to 60° (····). (b) WoMV RNA at room temperature with 0.015 M cations and 0% (U+F) (——), 65% (U+F) (--), and 75% (U+F) (-·-).

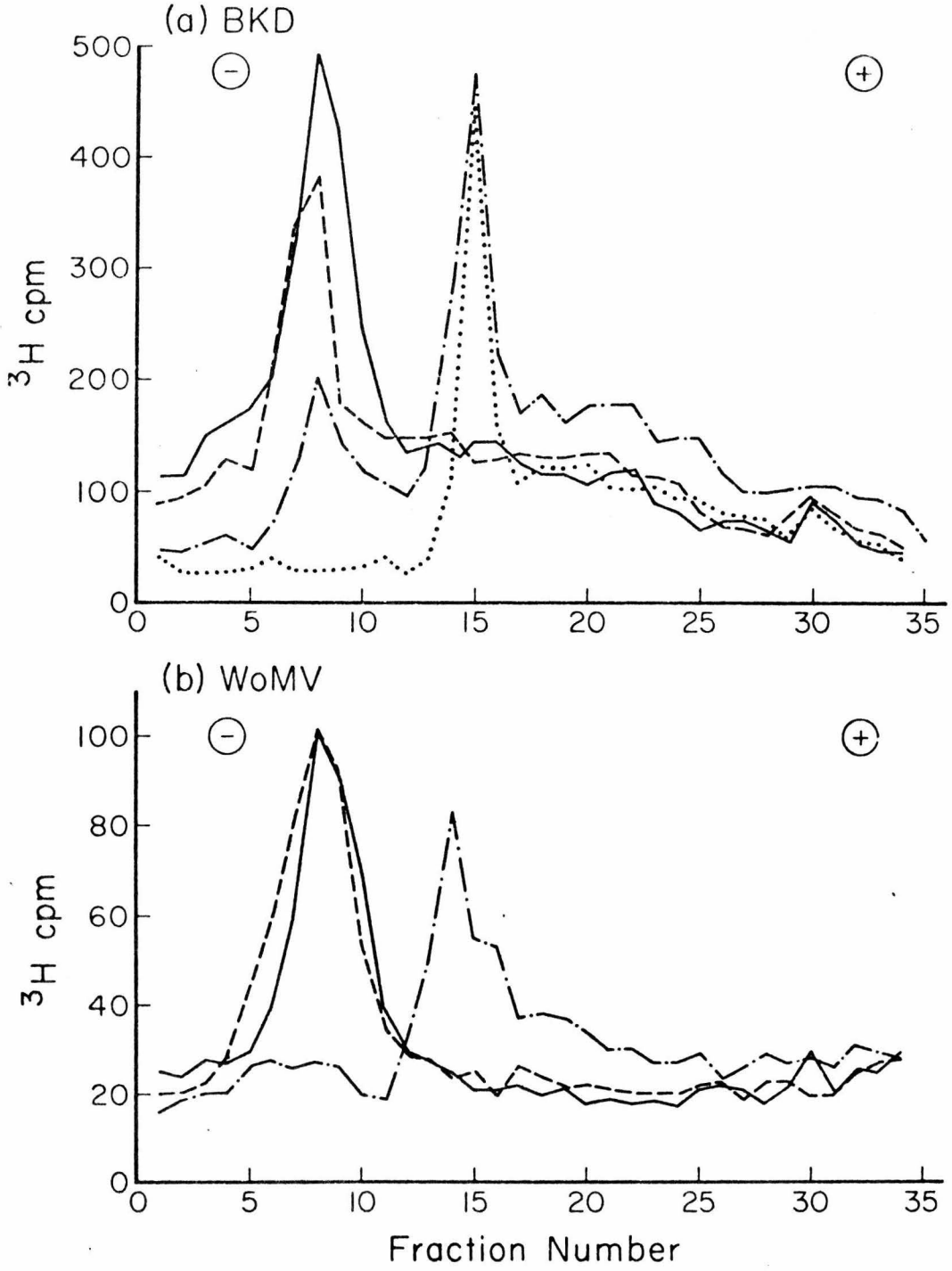
(a) BKD
⊖
⊕
500
400
300
200
100
0
^{3}H cpm
0
5
10
15
20
25
30
35
(b) WoMV
⊖
⊕
100
80
60
40
20
0
^{3}H cpm
0
5
10
15
20
25
30
35
Fraction Number

Fig. 3. Electrophoresis of viral RNA on denaturing methylmercury hycroxide gels (a) BKD viral RNA, run at 5mA per gel for 3 h. The positions of HeLa 18S and 28S rRNA markers and of RD-114 viral RNA (run in a separate tube) are shown. (b) WoMV viral RNA, run at 5 mA per gel for 5 h. The positions of HeLa 18S and 28S and E. coli 23S rRNA markers and of BKD RNA (in a separate tube) are shown.

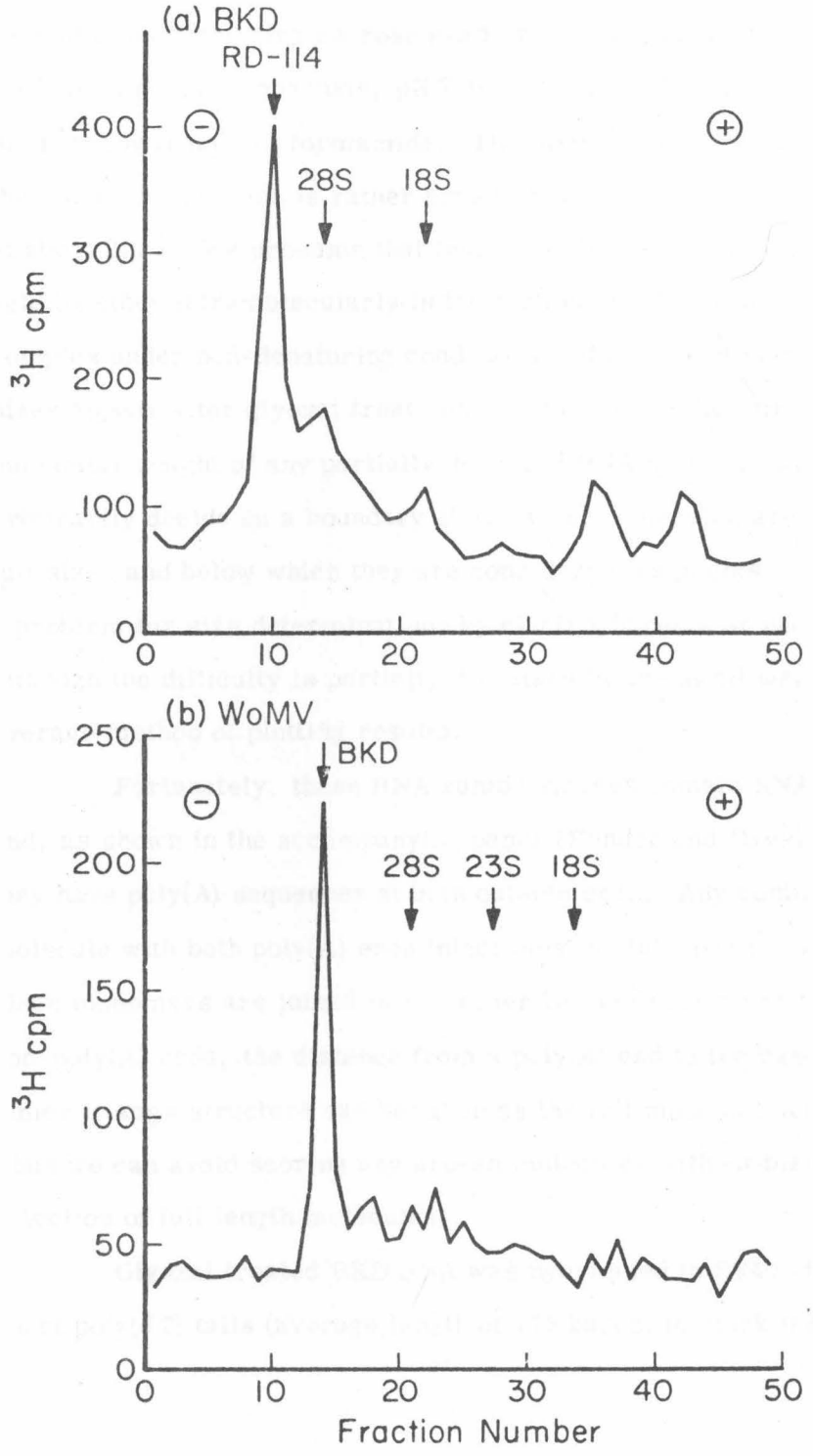
(a) BKD
RD-114
28S
18S
400
300
200
100
0
^{3}H cpm
0
10
20
30
40
50
(b) WoMV
BKD
28S
23S
18S
250
200
150
100
50
0
^{3}H cpm
0
10
20
30
40
50
Fraction Number

peak of a nondenaturing sucrose gradient, incubated with 1M glyoxal, 0.01 M potassium phosphate, pH 7.0 for 1 hr at 37°, and spread for microscopy from 55% formamide. The histogram in Figure 4a shows that the length distribution is rather broad, although there is a maximum at about 20kb. We presume that there are many nicked molecules held together intramolecularly in the high molecular weight RNA complex under non-denaturing conditions and these fragments of all sizes appear after glyoxal treatment. To estimate the full size molecular weight of any partially degraded RNA or DNA, one must arbitrarily decide on a boundary above which molecules are considered full size, and below which they are considered fragments. This is also a problem for size determinations by electrophoresis or sedimentation, although the difficulty is partially disguised by the usual weight average method of plotting results.

Fortunately, these RNA rumor viruses contain RNA dimers, and, as shown in the accompanying paper (Bender and Davidson, 1976), they have poly(A) sequences at both outside ends. Any continuous dimer molecule with both poly(A) ends intact must be full length. Likewise, since monomers are joined in the dimer linkage very close to their non-poly(A) ends, the distance from a poly(A) end to the base of the dimer linkage structure can be taken as the full monomer length. Thus we can avoid scoring any broken molecules without biasing our selection of full length molecules.

Glyoxal treated BKD RNA was hybridized to SV40 circles with short poly(dT) tails (average length of 175 bases) to mark the poly(A)

Fig. 4. Histogram of total lengths of glyoxal-treated viral RNAs. (a) BKD 52S RNA treated with 1M glyoxal for 1 hr and spread from 55% formamide. All molecules were measured. (b) BKD 52S RNA treated with 1 M glyoxal for 1 hr at 37°, dialyzed against 10 mM Tris, 1 mM EDTA fpr 24 hr, hybridized with SV40 circles with short poly(dT) tails to mark the poly(A) ends, and spread from 40% formamide. Dimers (solid bars) were scored as unbroken molecules with two poly(A) ends marked by the SV40-poly(dT). The lengths are measured from one SV40 attachment point to the other (excluding the dimer linkage structure). Monomers (open bars) were scored as molecules continuous from poly(A) end to dimer linkage; contour lengths were measured from the SV40 attachment site to the base of the dimer linkage. (c) WoMV 52S RNA treated with glyoxal, dialyzed 24 hr, hybridized with SV40-poly(dT) and spread, as above. Dimers (solid bars) and monomers (open bars) were scored and measured as above.

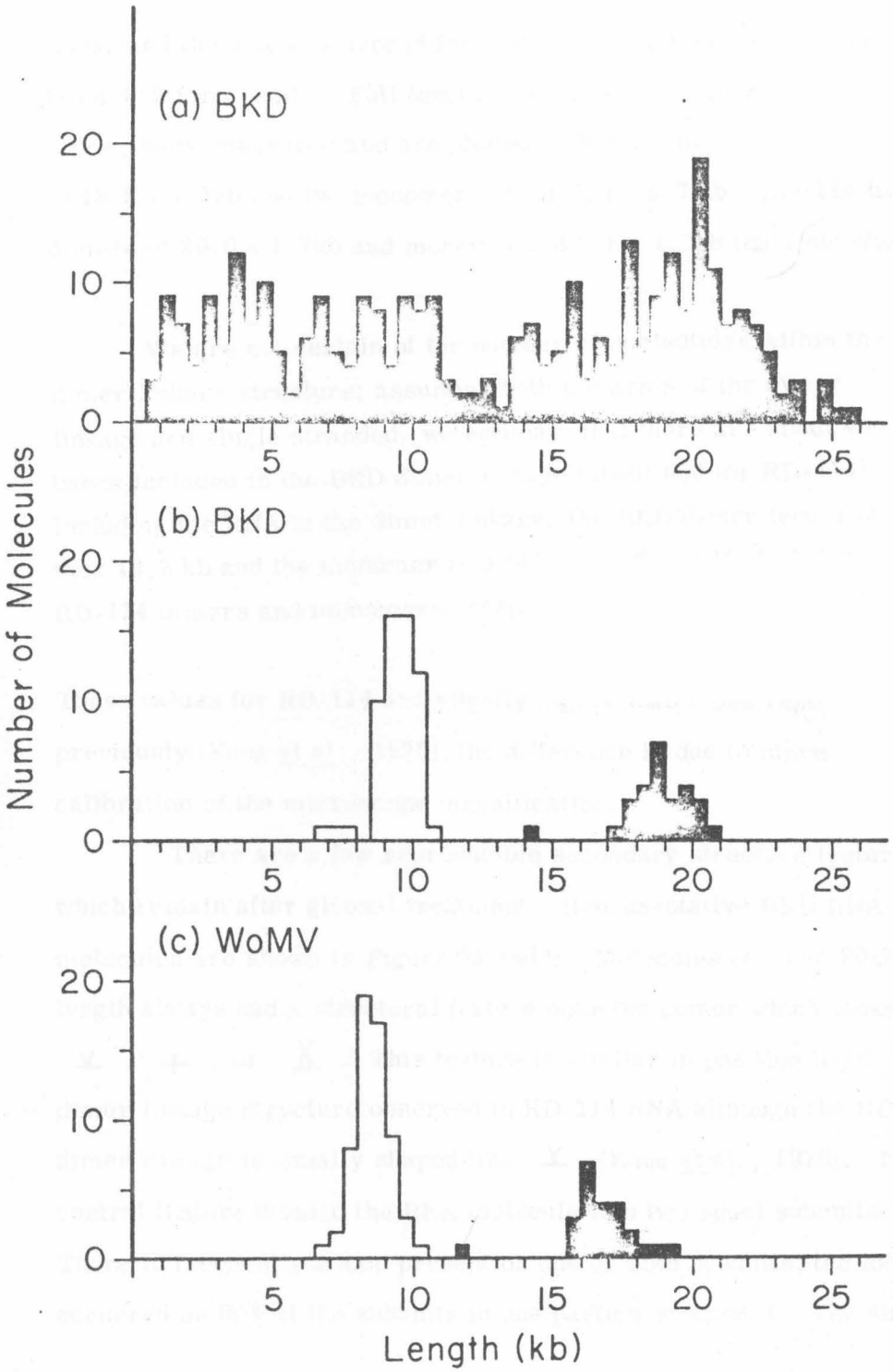
(a) BKD
(b) BKD
(c) WoMV
Number of Molecules
Length (kb)
0
10
20
5
10
15
20
25

ends, and the mix was spread for microscopy (Bender and Davidson, 1976) from 40% formamide. Full length dimers and monomers, as defined above, were measured and are plotted in Figure 4b. The dimer length is 18.8 ± 1.3kb and the monomer size is 9.4 ± 0.7 kb. RD-114 has dimers of 20.0 ± 1.7kb and monomers of 9.8 ± 1.0kb (data not shown).

We are not certain of the number of nucleotides within the dimer linkage structure; assuming both the arms of the dimer linkage are single stranded, we estimate that there are about 400 bases included in the BKD dimer linkage (about 600 for RD-114) Including the RNA in the dimer linkage, the BKD dimer length is thus 19.2 kb and the monomer is 9.6kb. (20.6 and 10.1 kb for RD-114 dimers and monomers, respectively).

These values for RD-114 are slightly higher than those reported previously (Kung et al., 1975); the difference is due to more accurate calibration of the microscope magnification.

There are a few reproducible secondary structure features which remain after glyoxal treatment. Representative BKD RNA molecules are shown in Figure 5a and b. Molecules of about 20kb length always had a structural feature near the center which looked like , , or . This feature is similar in position to the dimer linkage structure observed in RD-114 RNA although the RD-114 dimer linkage is usually shaped like (Kung et al., 1975). This central feature divided the RNA molecule into two equal subunits. There is frequently a loop present on one or both subunits; the loop occurred on 80% of the subunits in one particular spread. The size and

Fig. 5. Electron micrographs of BKD RNA. (a) and (b) glyoxal treated RNA spread from 55% formamide. (c) and (d) RNA in 67% (U+F) heated to 55°, cooled, and spread at room temperature. (e) RNA in 80% (U+F) spread without prior heating. D indicates the dimer linkage structures, L indicates the loops, SH indicates the small hairpins within the loop region, and LH indicates the new large hairpin that appears under denaturing conditions. The bar lengths are 0.5 μm.

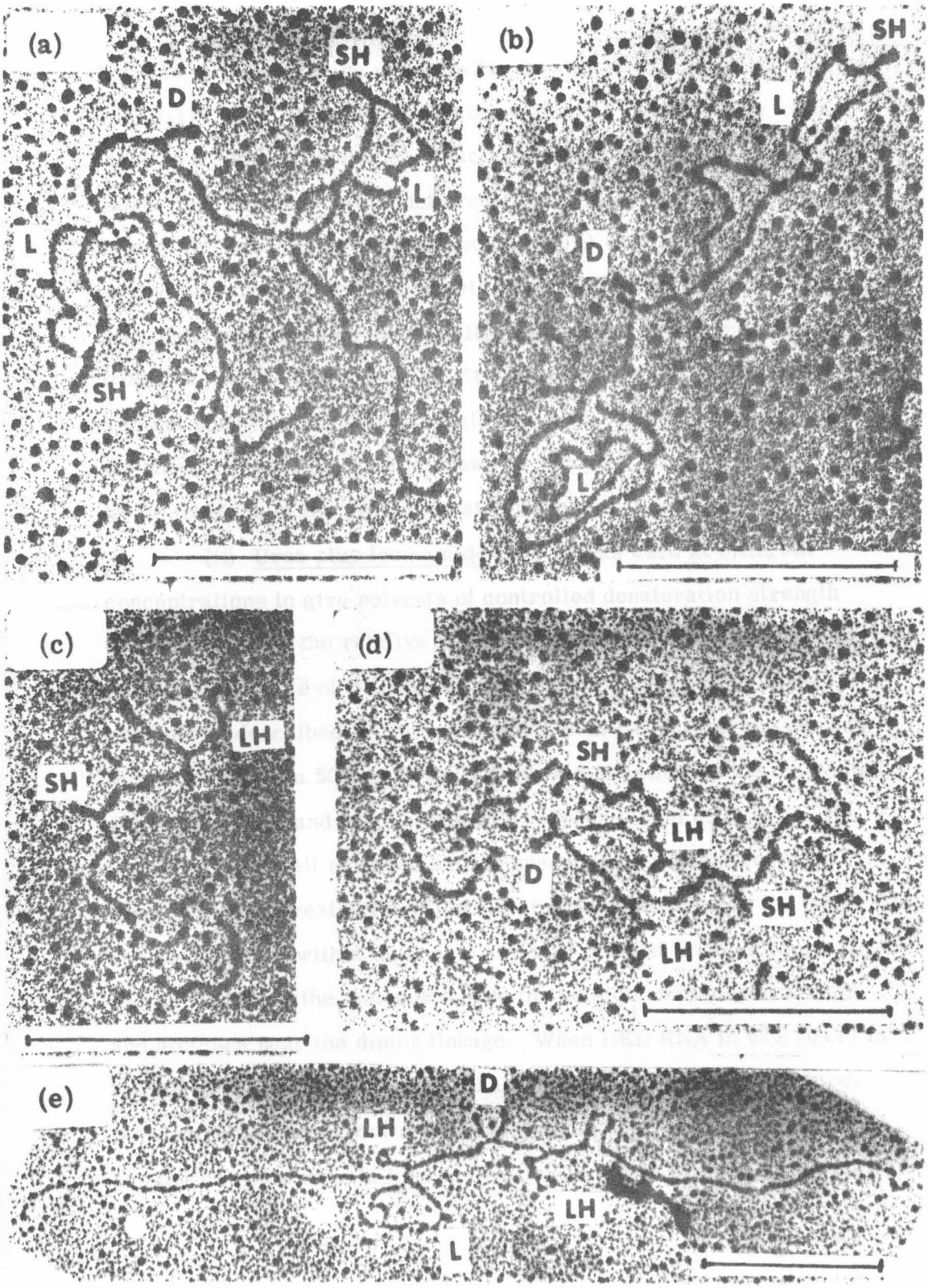
(a)
SH
D
L
L
SH
(b)
SH
L
D
L
(c)
LH
SH
(d)
SH
LH
D
SH
LH
(e)
D
LH
LH
L

location of the loops are very similar to what we observed previously on RD-114. On 70% of the subunits, within the region of the loops, there is a small hairpin-like structure with a length of about 250 base pairs. This structure was not present on RD-114 RNA. The outside ends of the subunits in some molecules (30%) were observed to loop around and attach at a reproducible site. The point which is 0.5kb from the poly(A) end crosses over the RNA of the same monomer at about 1kb from the central dimer linkage structure (Figure 5b). This attachment was not seen in glyoxal treated RD-114 RNA. An overall diagram of the structure of BKD RNA is shown in Figure 7 and the contour lengths of the features of the glyoxal treated molecules are given in Table I.

(ii) Urea plus formamide (U + F) was used at different concentrations to give solvents of controlled denaturation strength in order to study the relative stabilities of the various secondary structure features of BKD RNA. The exact composition of these solvents is described in Methods. When BKD RNA is spread at room temperature from 50% or 70% (U+F) (0.024 M cations), the molecules are still tangled and hardly traceable. Spread from 80% (U+F), the molecules are well extended but the secondary structure features seen in glyoxal treated RNA (the dimer linkage structure, the loops, and the hairpins within the loops) are still present on most molecules and about 15% of the molecules have the outside ends looped around and attached near the dimer linkage. When BKD RNA in 67% (U+F) is heated to 40° briefly, then cooled and spread at room temperature, the loops disappear from most molecules although the dimer linkage and the hairpins remain intact. Heating to 55° in 67% (U+F) causes

most of the dimers to dissociate into monomers; this result is direct confirmation of the dimer melting temperature determined by the agarose gel electrophoresis method. The small hairpin formerly within the loop is still present after brief heating to 55° in 67% (U+F) and it is near the center of the monomer RNA (Figure 5c, d); either it has a very high melting temperature, or it melts on heating but then renatures during the subsequent cooling.

After brief heating BKD RNA to 55° in 67% (U+F), a new secondary structure feature appears in most of the dissociated molecules. This feature, which is not seen in glyoxal treated RNA, looks like a hairpin, usually with a loop at the end of the stem (see Fig. 5c). It measures about 1.3kb in contour length and is about 1kb from the non-poly(A) end. A similar feature was seen in RD-114 RNA after heating and cooling (Kung et al., 1975). Rarely, we find an intact dimer after the above heating procedure with two of these new large hairpins symmetrically placed about the dimer linkage (Figure 5d). These molecules show that the new hairpin is formed in a region close to the dimer linkage end of the monomer, and near the region that is normally the loop. We have also seen that in spreads from 80% (U+F) at room temperature, where almost all molecules are still dimers, about 20% of the monomer subunits have these new large hairpins instead of the usual large loop. Under these conditions, there are a few cases (about 1%) in which both the new hairpin and the large loop appear to be present on the same RNA subunit; in these molecules the base of the hairpin is immediately adjacent to the base of the loop (Figure 5e).

II. Woolly Monkey Virus

The WoMV virus preparation (called SSV-1 by some authors) contains mostly nontransforming helper virus (Wolfe et al., 1972) so that these studies deal with the RNA of this nontransforming virus

A. Sedimentation Analysis. The sedimentation of high molecular weight RNA extracted from WoMV was compared with RD-114 RNA on a sucrose gradient in 0.1 M NaCl. As shown in Figure 1b, the WoMV RNA cosediments with the 52S RD-114 RNA. WoMV RNA also cosediments with RD-114 RNA in gradients containing 0.01 M NaCl (data not shown). When WoMV RNA is first treated with glyoxal under our standard conditions and then run on a glyoxal sucrose gradient, two peaks appear (Figure 1d). In addition to the peak cosedimenting with glyoxal treated RD-114 RNA, there is a more slowly sedimenting peak. The electron microscope analysis, reported below, showed that the fast peak contained RNA dimers and the slow peak contained monomers. Since glyoxal treated RD-114 RNA or BKD RNA gave only the dimer peak, the WoMV RNA dimer linkage is less stable to glyoxal treatment than that of RD-114 or BKD.

B. Gel electrophoresis. We used electrophoresis on non-denaturing agarose gels to follow the dissociation of the WoMV dimer. High molecular weight RNA was dissolved at room temperature in a solvent containing 0.015 M cations and varying concentrations of urea plus formamide and was then applied to the gel. Figure 2b shows that RNA treated with 65% (U+F) at room temperature, migrated with the untreated sample, and molecules in 75% (U+F) moved significantly faster. Heating the RNA to 40° in 88% (U+F) did not produce any

further dissociation. As will be shown, the slow peak contains dimer length RNA molecules and the fast peak contains RNA monomers. BKD RNA dimers melted apart in 67% (U+F) at about 50°; the dissociation of WoMV at 25° in 75% (U+F) demonstrates that the dimer linkage is considerably less stable in WoMV RNA than in BKD or RD-114 RNA's.

To get a size determination of the WoMV RNA monomer we ran the RNA on an agarose gel in the presence of methylmercury hydroxide. The WoMV RNA migrates as a single peak corresponding to a molecular weight of about 3×10^6 daltons or 9kb (Figure 3b).

C. Electron microscope studies. (i) Glyoxal treated WoMV RNA sedimented as two separate peaks on a glyoxal sucrose gradient (Figure 1d) and these peaks were each isolated and spread from 30% formamide. The slower sedimenting peak gave molecules of about 9kb contour length (Figure 6b) and the faster peak contained molecules which had a dimer linkage structure similar to those of RD-114 and BKD and which were about 17kb in length (Figure 6a). We conclude that the slow and fast peaks of the glyoxal sucrose gradient contain monomers and dimers of WoMV RNA, respectively.

Again we attempted to get an accurate estimate of the RNA size by using the poly(A) mapping technique. Full length dimers are defined as continuous molecules with poly(A) sequences at both outside ends; full-length monomers are molecules continuous from a poly(A) end to a clear dimer linkage structure. A histogram of the monomer and dimer lengths is plotted in Figure 4c; the dimer length is 16.7 ± 1.4kb and the monomer length is 8.5 ± 0.7kb. If the dimer linkage sequences (about 300 bases) are included, the dimer and monomer lengths are adjusted to 17.0 and 8.7 kb, respectively.

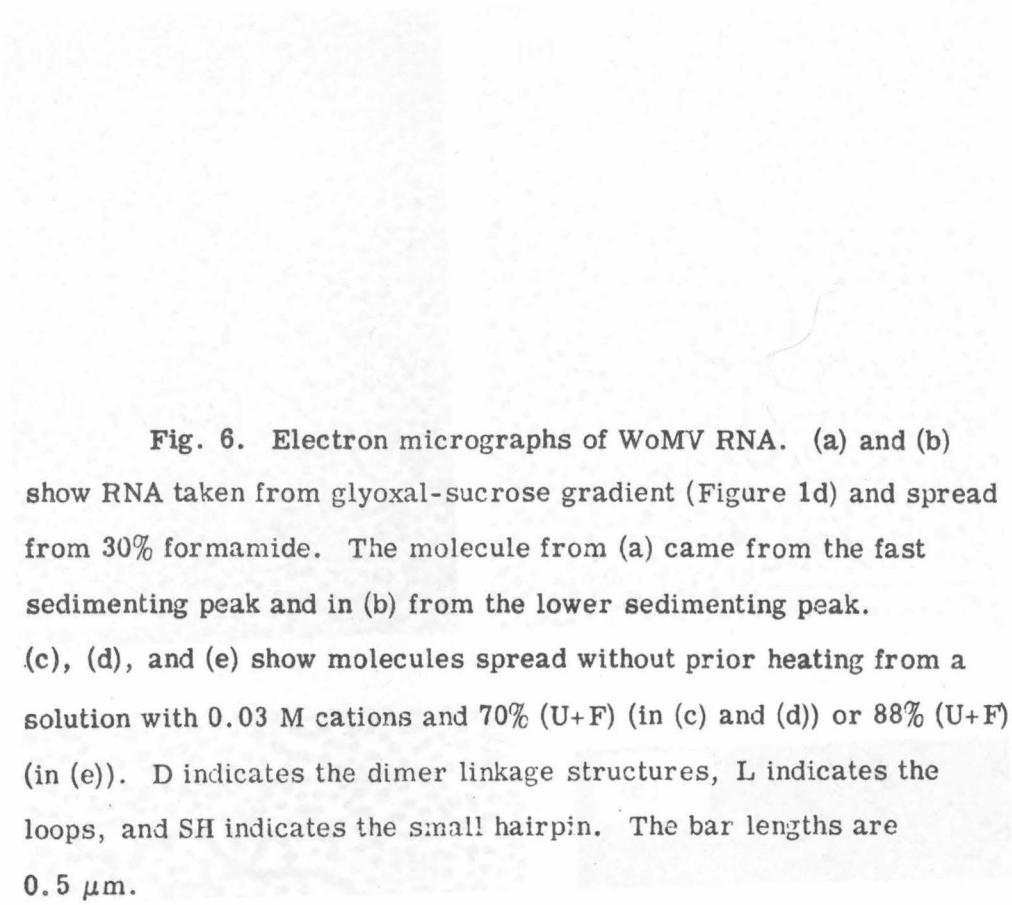

Fig. 6. Electron micrographs of WoMV RNA. (a) and (b) show RNA taken from glyoxal-sucrose gradient (Figure 1d) and spread from 30% formamide. The molecule from (a) came from the fast sedimenting peak and in (b) from the lower sedimenting peak. (c), (d), and (e) show molecules spread without prior heating from a solution with 0.03 M cations and 70% (U+F) (in (c) and (d)) or 88% (U+F) (in (e)). D indicates the dimer linkage structures, L indicates the loops, and SH indicates the small hairpin. The bar lengths are 0.5 μm.

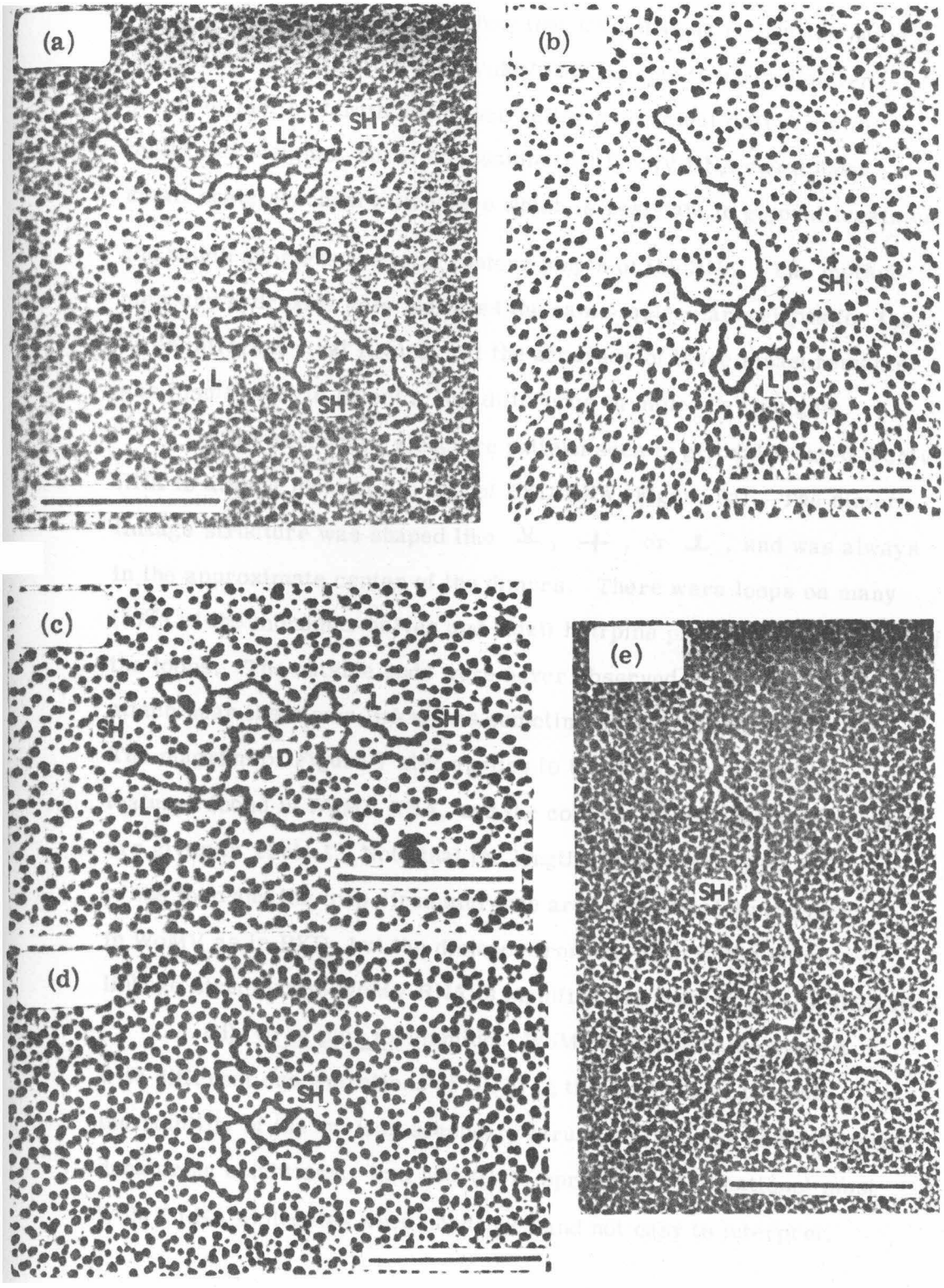
(a)
L
SH
D
L
SH
(b)
SH
L
(c)
SH
L
SH
D
L
(d)
SH
L
(e)
SH

The data in Table 1 show that BKD RNA is nearly the same size as RD-114 RNA but that WoMV RNA is significantly smaller. We presume the length difference reflects an actual difference in molecular weights, but it is possible that WoMV RNA could have small scale secondary structure which is resistant to glyoxal treatment and which shortens the total contour length of the RNA. The methylmercury hydroxide gels indicated the same molecular weights for the three different viral RNA's, but the accuracy of these measurements was insufficient to detect a 10% difference in molecular weights.

The secondary structure pattern seen in glyoxal treated WoMV RNA is almost identical to that of BKD RNA (Figure 6a). The dimer linkage structure was shaped like $\curlyvee$, $+$, or $\perp$, and was always in the approximate center of the dimers. There were loops on many (50%) of the monomer halves and small hairpins present in most (70%) of the loops. The outside ends were never observed to fold back and attach near the dimer linkage as sometimes happened with BKD RNA. The diagram of Figure 7 also applies to the secondary structure features found in WoMV RNA, and the contour lengths of these features are given in Table I. Note that the lengths from the poly(A) end to the loop and the loop circumference are approximately the same in WoMV as in BKD, but the distance from the loop to the dimer linkage structure in WoMV RNA is significantly shorter than in BKD RNA.

(ii) Urea plus formamide. WoMV RNA was also spread with different concentrations of (U+F) in the hyperphase to study the stability of the various secondary structure features under varying denaturing conditions. In a 50% (U+F) spread (0.04 M cations) most WoMV RNA molecules were condensed and not easy to interpret.

Table 1

The lengths and standard deviations of the features marked by the letters a - i in the diagram of Figure 7. The small hairpin feature (SH) is not present in RD-114, and its length (g) for BKD and WoMV is given in kilobases of single strand RNA (twice the apparent double strand length). As discussed in the text, our estimates of the full lengths, including the sequences in the dimer linkage structure, are a+2i for dimers and b+i for monomers. We assume 1 kb equals 0.256 μm for glyoxal treated RNA.

	a	b	c	d	e	f	g	h	i
RD-114	20.0	9.8	3.9	3.8	2.4				0.3
	±1.7	±1.0	±0.7	±0.4	±0.4				±0.07
BKD	18.8	9.4	3.9	3.7	1.9	1.2	0.5	1.9	0.2
	±1.3	±0.7	±0.4	±0.4	±0.1	±0.1	±0.1	±0.3	±0.04
WoMV	16.7	8.5	3.5	3.9	1.4	1.0	0.8	2.1	0.14
	±1.4	±0.7	±0.5	±0.4	±0.3	±0.3	±0.4	±0.4	±0.04

Fig. 7. General diagram of secondary structure features in viral RNA dimers of RD-114, BKD, and WoMV. Contour lengths of various features (A through I) are given in Table I. The dimer linkage structure (DLS) is not always shaped as drawn here, and the small hairpin (SH) with the loop is found in BKD and WoMV but not RD-114. Structures seen under denaturing conditions are shown separately for BKD and WoMV RNA's. LH indicates the new large hairpin seen in BKD under denaturing conditions.

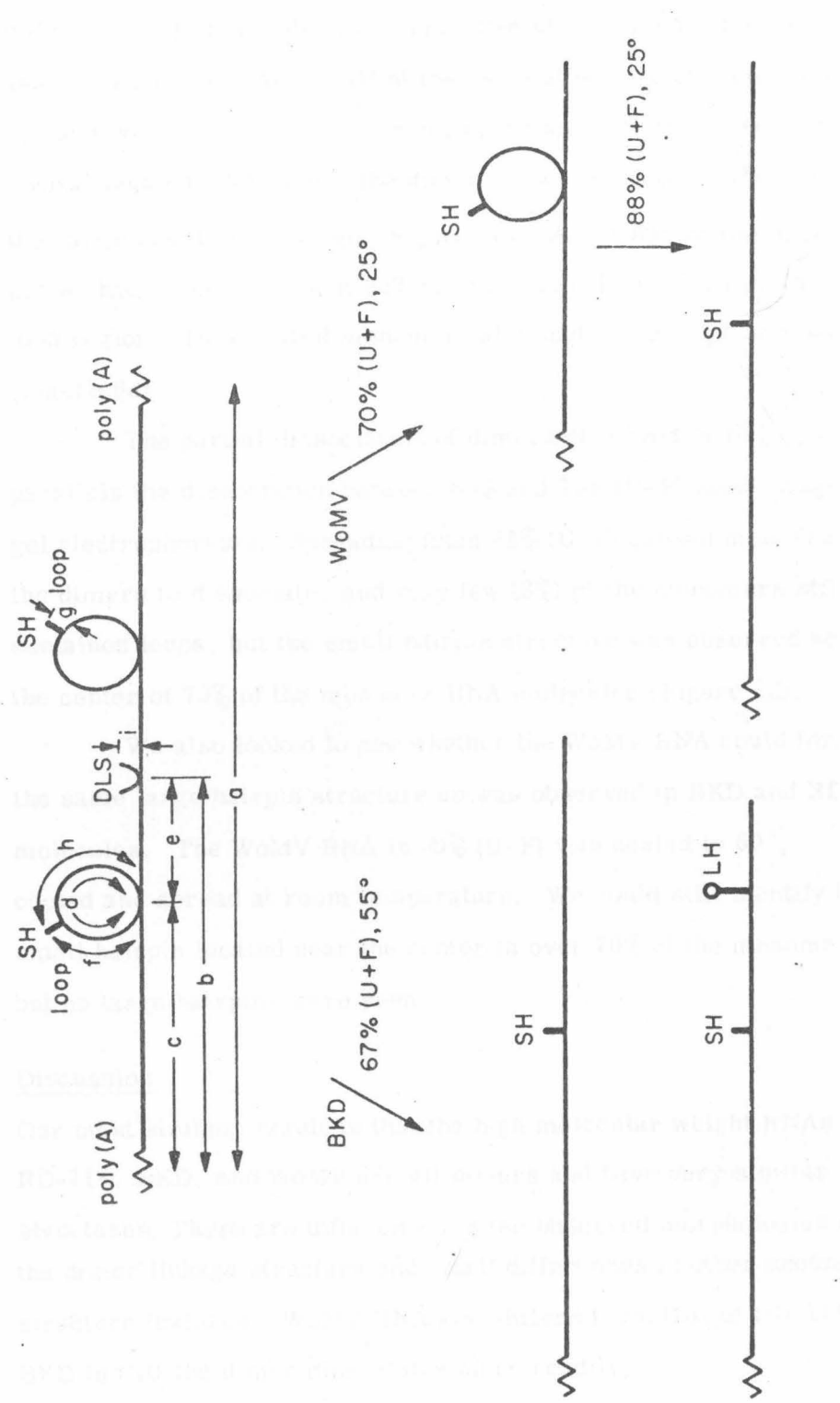
poly(A)
SH
loop
g
DLS
i
h
d
e
f
c
b
a
poly(A)
SH
loop
WoMV
70% (U+F), 25°
SH
88% (U+F), 25°
SH
BKD
67% (U+F), 55°
SH
SH
LH

With 70% (U+F) the molecules were often still tangled but were usually traceable. About half of the molecules were of dimer length (about 17kb) and showed the secondary structure features seen in glyoxal treated RNA, i.e., the dimer linkage structure, the loops, and the hairpins within the loops (Figure 6c). About 80% of the monomer halves had a loop and about 80% had the small hairpin within the loop region. Dissociated monomers also had these loops and hairpins (Figure 6d).

The partial dissociation of dimers observed in 70% (U+F) parallels the dissociation between 65% and 75% (U+F) seen by agarose gel electrophoresis. Spreading from 88% (U+F) caused most (85%) of the dimers to dissociate, and very few (8%) of the monomers still contained loops, but the small hairpin structure was observed near the center of 75% of the monomer RNA molecules (Figure 6d).

We also looked to see whether the WoMV RNA could form the same large hairpin structure as was observed in BKD and RD-114 molecules. The WoMV RNA in 30% (U+F) was heated to 60°, cooled and spread at room temperature. We could still identify the small hairpin located near the center in over 70% of the monomers, but no large hairpins were seen.

Discussion

Our most striking result is that the high molecular weight RNAs from RD-114, BKD, and WoMV are all dimers and have very similar structures There are differences in the observed morphologies of the dimer linkage structure and small differences in other secondary structure features. WoMV RNA also differs from that of RD-114 and BKD in that the dimer dissociates more readily.

RD-114 virus was isolated from a human rhabdomyosarcoma after an in vivo passage in a fetal cat brain (McAllister et al., 1972).

It is thought to be an endogenous feline virus because it shows close sequence homology to the infectious type C virus that can be induced from a cat cell line in culture (Livingston and Todaro, 1973; Fischinger et al., 1973; Sarma et al., 1973), and because it shows sequence homology with cat cellular DNA (Baluda and Roy-Burman, 1973; Neiman, 1973; Ruprecht et al., 1973).

BKD virus was isolated by cocultivation of normal baboon kidney with a dog thymus cell line, and it appears identical to several other isolates of endogenous type C baboon viruses (Melnick et al., 1973; Benveniste et al., 1974a; Todaro et al., 1974). BKD shows partial antigenic relationship to RD-114 with regard to viral reverse transcriptase and the viral core protein, p30 (Hellman et al., 1974; Sherr et al., 1974). The sequence homology between RD-114 and BKD, determined by hybridizing a cDNA probe made from one virus to an excess of RNA from the other, is 10-20% (Benveniste et al., 1974a; Todaro et al., 1974). Thus, by several criteria, BKD and RD-114 are likely to be evolutionarily related. Todaro et al. (1974) have suggested that the CCC/RD-114 family of endogenous cat viruses was introduced into the cat germ line by horizontal transmission of a primate virus, related to the baboon virus.

WoMV is the simian sarcoma virus isolated from a woolly monkey fibrosarcoma (Theilen et al., 1971). There is no detectable sequence homology between WoMV RNA and the RNAs of either RD-114 or BKD as measured by hybridization of labeled reverse transcriptase products to excess viral RNA (Benveniste and Todaro, 1973; East et al., 1975). Likewise, there is no antigenic cross reaction between WoMV

and either RD-114 and BKD for either the viral polymerase or the gs-1 determinents of the p30 protein (Sherr et al., 1974, 1975). WoMV does appear by both antigenic and sequence homology tests to be closely related to the gibbon-ape leukemia virus, and more distantly related to several murine type C viruses and an endogenous pig virus (Sherr et al., 1974, 1975; Benveniste and Todaro, 1973).

That such similar structures appear in the RNA's of RD-114, BKD and WoMV suggests that all type C RNA viruses have RNA dimers with loops. However, these features were very rarely observed in Rous sarcoma virus (Bender and Davidson, 1976). We have observed that the 60-70S RNA of Rous sarcoma virus dissociates to 30-35S RNA at lower temperatures than are required to dissociate WoMV dimers. Thus, it is likely that if dimer structures exist in Rous sarcoma virus, it would be difficult to observe them since denaturing conditions are required to extend the RNA for electron microscopy. If loops exist, they must also be easily disrupted.

The RNA that we observe has been through phenol extraction, ethanol precipitation, and spreading in denaturing solvents. We cannot be certain that what we see represents the "native" structure, i.e., that which exists in the virion. It is unlikely that virions contain single RNA monomers which associate into dimers after extraction, since we have never observed reassociation of dimers after they have been dissociated by heating. Comparisons of the relative sedimentation velocities of RD-114 RNA and several marker RNAs in non-denaturing and glyoxal sucrose gradients support the view that the 52S RNA complex is a single dimer molecule (Kung et al., 1975). By analogy, the same

is true for BKD and WoMV 52S RNAs. Our data say nothing about the number of 52S dimers per virion.

It seems clear that the loops and dimer linkage structures are formed by processes more complicated than simple association of complementary sequences. When the loops are dissociated by heating viral RNA in a low concentration (U+F) the loops never reappear when the solution is cooled. If there were two complementary sequences at the base of the loop, they should reanneal very quickly since they are always in close proximity. Likewise the dimer linkage structure does not reform after heating and cooling. We have heat denatured 52S RD-114 RNA and incubated it at a high RNA concentration in order to allow reassociation of dimer linkages, but reassociation has never been observed. The large hairpin structure of RD-114 and BKD is also peculiar in that it never appears until the virus is subjected to very denaturing conditions, and then it is present on only some of the molecules.

Several alternative models may be suggested for how the monomers are joined in the dimer linkage structure; similar models could account for the structure at the junctions of the loops. There may be a protein binding the two subunits together. Such a protein would have to be resistant to the phenol-SDS extraction used here to prepare all viral RNAs, and also resistant, in the case of RD-114, to pronase-SDS extraction (Kung et al., 1975). If dissociation of the dimers occurs upon heat denaturation of a protein linker, the monomers would probably not reassociate.

Models in which the two monomers are held together by

antiparallel Watson-Crick base pairing are subject to some probable constraints. The poly(A) sequences of mRNAs and some tumor viral RNAs are at the 3' end (Wang and Duesberg, 1974; Quade et al., 1974; Rho and Green, 1974). Our poly(A) mapping shows that the dimer linkage joins two non-poly(A) ends. Oligonucleotide fingerprint evidence suggests that all subunits of Rous sarcoma virus RNA are identical in sequence (Duesberg et al., 1974; Weissmann et al., 1974). Thus we assume for the following discussion that the dimer linkage structures contain two identical 5' monomer ends.

Figure 8a shows a structure with two identical monomers base paired to each other. All such structures require the presence of inverted repeat sequences on each strand. Figure 8b illustrates how a small RNA molecule might serve as a linker. The RNA linker could be the same tRNA that serves as a primer for the in vitro reverse transcriptase reaction (Dahlberg et.al., 1974; Taylor and Illmensee, 1975). In both these models, the monomers would not be expected to reassociate after thermal dissociation. In Figure 8a, the inverted repeats would form base pairs intramolecularly, and the linker of Figure 8b would anneal completely to just one monomer strand. Both models, therefore, require special in vivo mechanisms to cause intermolecular base pairing for dimer formation. Figure 8c gives another possible structure with a small RNA linker which contains a tandem direct repeat so that it can base pair with the two identical monomers. This structure could reform after heat dissociation. Models for the dimer linkage similar to these were independently conceived and communicated to us by Dr. Andrew King of the University of Wisconsin.

Fig. 8. Diagrams of possible structures for the dimer linkage in which the binding is through normal complementary base pairing. (a) shows a model in which identical monomers bind to each other at inverted repeat sequences. In (b), a small RNA linker joins two identical monomers; a second linker of the same sequence could be added to the diagram to give double bonding. (c) is a model in which the linker contains a tandem repeat. In all cases the letters (A-E) indicate base sequences and the primed letters (A' - E') indicate their complementary sequences.

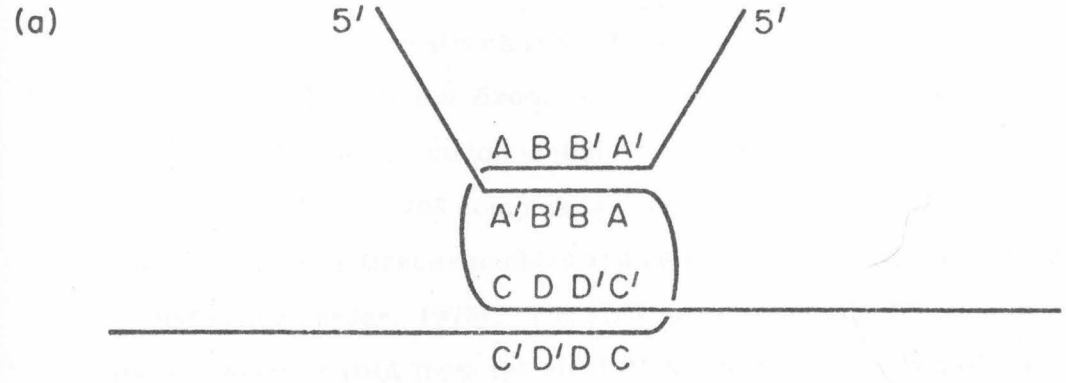
(a)
5′
5′
A B B′ A′
A′ B′ B A
C D D′ C′
C′ D′ D C

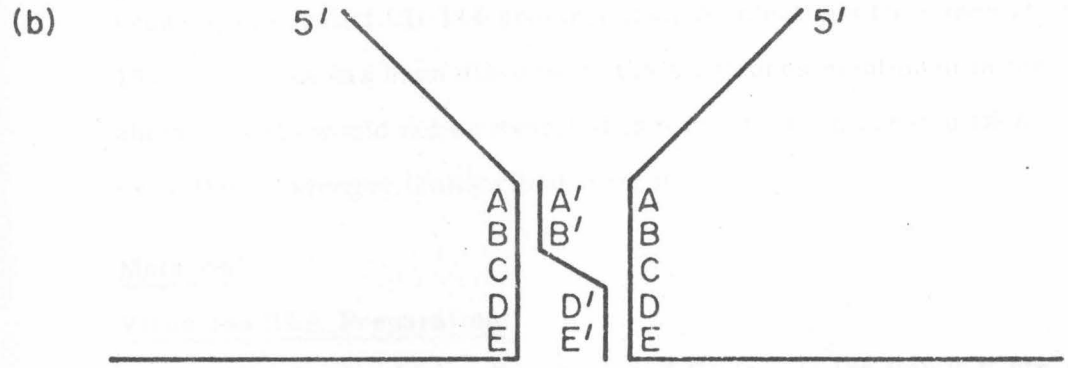
(b)
5′
5′
A
B
C
D
E
A′
B′
D′
E′
A
B
C
D
E

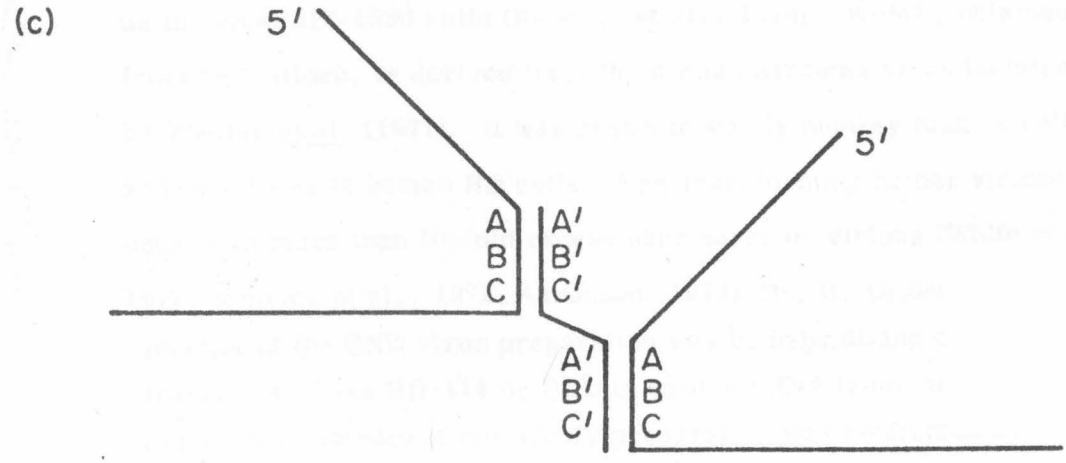
(c)
5′
5′
A
B
C
A′
B′
C′
A′
B′
C′
A
B
C

We can only guess at the functions of the dimer linkage structure and the loop structures. They could have some role in packaging the RNA in the virus. The dimer linkage, for instance, may insure that every virion is diploid. However, it has been reported that the 60-70S complex in avian sarcoma virus is unstable when the virus is first assembled and released (Canaani et al., 1973; Stoltzfus and Snyder, 1975). The structures could also function in the synthesis of DNA from the viral RNA. It is less likely that the dimer linkage structures affect RNA synthesis or protein synthesis because integrated RD-114 proviral DNA is infectious (Nicolson et al., 1975), and, as has been discussed, the structures mentioned in the above models would not be expected to form in the integrated DNA or in the messenger transcribed from it.

Methods

Virus and RNA Preparation

BKD virus, obtained from Dr. Raymond Gilden, is the Bab 8-K strain (Todaro et al., 1974). It was grown in dog thymus cells and then by us in human HT-1080 cells (Rasheed et al., 1974). WoMV, obtained from Dr. Gilden, is derived from the simian sarcoma virus isolated by Theilen et al. (1971). It was grown in woolly monkey muscle cells and then by us in human RD cells. Non-transforming helper virions are usually in more than 10-fold excess over sarcoma virions (Wolfe et al., 1972; Scolnick et al., 1972; Aaronson, 1973). Dr. R. Gilden confirmed the identity of the BKD virus preparation was by hybridizing cDNA transcripts from RD-114 or BKD to cellular RNA from our producer cells. The identity of our WoMV preparation was confirmed by R. Gilden in CF tests using antisera to WoMV p30 antigens.

of our WoMV preparation was checked with antisera mode against WoMV p30 antigens.

The viruses were banded in sucrose and the RNA was prepared by phenol-SDS extraction and ethanol precipitation as described previously (Kung et al., 1975).

Sedimentation Analysis

NTE-sucrose gradient: 10-30% sucrose gradients containing NTE buffer (0.1 M NaCl, 0.01 M Tris, pH 7.0, 0.001 M EDTA) were prepared. ^{3}H-labeled RNA samples (in NTE), about 50 μl, were layered onto the gradients and centrifuged in an SW50.1 rotor at 45,000 rpm and 4°.

Glyoxal-sucrose gradient: ^{3}H-labeled RNA samples were treated with glyoxal by dialyzing against 1 M glyoxal in 0.01 M phosphate buffer, pH 7.0, for 1 hr at 37°, then dialyzing against 0.1 M glyoxal in the same buffer for approximately 30 min at 4°. A sample thus treated was sedimented through a 10-30% sucrose gradient in the presence of 0.1 M glyoxal, 0.01 M phosphate buffer, pH 7.2, at 4°, 45,000 rpm in an SW50.1 rotor. RD-114 52S RNA was similarly treated and run in parallel as an external marker.

For preparative purposes, low salt (1 mM Tris, pH 7.2, 0.1 mM EDTA)-sucrose gradients were used to fractionate high molecular weight RNA species. Phenol-extracted RNA samples were dissolved in the low salt buffer and sedimented through these gradients at 4°. Under these conditions, BKD and WoMV RNAs both sediment as single components with the same sedimentation velocity as RD-114

RNA. Samples taken from the peak positions were used for electron microscope studies.

Electron Microscopy

The preparation of RNA samples for electron microscopy and the details of the different spreading techniques have been previously described (Kung et al., 1975). The urea plus formamide (U+F) solvent was prepared by adding 480 g (8 mol) of urea to 1ℓ of recrystallized formamide; this gives a solution about 74% by volume formamide and about 5.9 M in urea. The volume percent of this solvent in a solution of aqueous buffer is quoted as percent (U+F). The techniques for mapping the poly(A) sequences on the viral RNA are presented in the accompanying paper (Bender and Davidson, 1976). For length measurements, SV40 DNA double-stranded circles were compared to a diffraction grating, and SV40 circles were used as internal length standards in the poly(A) mapping experiments to calibrate the lengths of viral RNA monomers and dimers (Figure 4). Lengths were converted to kilobases assuming 0.256 μm/kb, as measured for glyoxal treated E.coli rRNA (Hsu et al., 1973).

Agarose Gel Electrophoresis

BKD 52S RNA samples were dissolved in 67% (U+F) containing 0.033 M Tris, pH 7.3 (0.024 M cations), heated at desired temperature for 1 minute and then quickly cooled in ice. After adding 10% glycerol, the sample solutions were loaded onto 1% agarose gels containg E buffer (0.05 M boric acid, 0.005 M sodium borate [$Na_2B_4O_7 \cdot 10\ H_2O$], 0.01 M sodium sulfate, and 0.001 M EDTA, pH 8.2), all as described

(Kung et al., 1975). WoMV 52S RNA dissociates more readily than BKD 52S RNA, and so to determine the dissociation conditions WoMV RNA samples were not heated but were dissolved in solutions with varying concentrations of (U+F) and with 0.25 M Tris, 0.025 M EDTA, pH 8.5. These solutions were then applied to the gels.

For methylmercury hydroxide-agarose gel experiments, all RNA samples were applied onto the gel in E buffer containing 5 mM CH_3HgOH and 10% glycerol. 23S and 18S unlabeled HeLa rRNA and 23S E. coli rRNA were included as internal markers. In order to visualize rRNA bands after electrophoresis, gels were stained with 1 μg/ml ethidium bromide, 0.5 M NH_4Ac for 30 minutes and examined by illumination with short wavelength UV light. The distances traveled by rRNA markers were recorded. The gels were then sliced into 2 mm fractions and the radioactivity of ^3H-labeled BKD or WoMV RNAs was determined.

Acknowledgments

We are grateful to Dr. Raymond Gilden for his several contributions as noted in the text. This research has been supported by contracts to Norman Davidson and Robert McAllister from the Virus Cancer Program of the National Cancer Institute; James Bailey has been supported by a fellowship from the Helen Hay Whitney Foundation and Welcome Bender by a National Science Foundation fellowship and a training grant from the National Institutes of Health.

References

Aaronson, S., (1973). Virology 52, 562.

Bailey, J.M., and Davidson, N., (1975). Anal. Biochem.

Baluda, M. A. and Roy-Burman, P. (1973). Nature New Biol. 244, 59.

Beeman, K., Duesberg, P., and Vogt, P., (1974). Proc. Nat. Acad. Sci. U.S.A. 71, 4254.

Bender, W., and Davidson, N., (1976). (Accompanying paper.)

Benveniste, R.E., and Todaro, G. J., (1973). Proc. Nat. Acad. Sci. U.S.A. 70, 3316.

Benveniste, R.E., Lieber, M. M., Livingston, D. M., Sherr, C. J., Todaro, G. J., and Kalter, S. S., (1974). Nature 248, 17.

Canaani, E., Helm, K. V. D., and Duesberg, P., (1973). Proc. Nat. Acad. Sci. U.S.A. 72, 401.

Dahlberg, J. E., Sawyer, R. C., Taylor, J. M., Faras, A. J., Levinson, W. E., Goodman, H. M., and Bishop, J. M., (1974). J. Virol. 13, 1126.

East, J. L. Knesek, J. E., Chan, J. C., and Dmochowski, L., (1975). J. Virol. 15, 1396.

Fischinger, P. J., Peebles, P. T., Nomura, S., and Haapala, D. K. (1973). J. Virol. 11, 978.

Hellman, A., Peebles, P. T., Strickland, J. E., Fowler, A. K., Kalter, S. S., Droszlan, S., and Gilden, R. V. (1974). J. Virol. 14, 133.

Hsu, M. T., Kung, H. J., and Davidson, N., (1973). Cold Spr. Harb. Symp. 38, 843.

Kung, H. J., Bailey, J. M., Davidson, N., Vogt, P. K., Nicolson, M. O., and McAllister, R. M., (1974). Cold Spr. Harb. Symp. 39, 827.

Kung, H. J., Bailey, J. M., Davidson, N., Nicolson, M. O., and McAllister, R. M., (1975). J. Virol. 16, 397.

Livingston, D. M. and Todaro, G. J., (1973). Virology 53, 142.

McAllister, R. M., Nicolson, M., Gardner, M. B., Rangey, R. W., Rasheed, S., Sarma, P. S., Huebner, R. J., Hatanaka, M., Oroszlan, S., Gilden, R. V., Kabigting, A., and Vernon, L., (1972). Nature N. Biol. 235, 3.

Melnick, J. L., Altenberg, B., Arnstein, P., Mivkovic, R., and Tevethia, S. S., (1973). Intervirology, 1, 386.

Nicolson, M. O., Hariri, F., Krempin, M., McAllister, R., and Gilden, R. V., (1975).

Nieman, P. E. (1973). Nature New Biol. 244, 62.

Quade, K., Smith, R. E., and Nichols, J. L., (1974). Virology 62, 60.

Rasheed, S., Nelson-Rees, W. A., Toth, E. M., Arnstein, P., and Garnder, M. B., (1974). Cancer 33, 1027.

Rho, H. M., and Green, M., (1974). Proc. Nat. Acad. Sci. U.S.A. 71, 2386.

Ruprecht, R. M., Goodman, N. C. and Spiegelman, S., (1973). Proc. Nat. Acad. Sci. U.S.A. 70, 1437.

Sarma, P. S., Tseng, J., Lee, Y. K. and Gilden, R. V., (1973). Nature New Biol. 244, 56.

Scolnick, E. M., Parks, E. P., Todaro, G. J., and Aaronson, S. A., (1972). Nature 235, 35.

Sherr, C. J., Lieber, M. L., Benveniste, R. E., and Todaro, G. J., (1974). Virol. 58, 492.

Sherr, C. J., Fedele, L. A., Benveniste, R. E., and Todaro, G. J., (1975). J. Virol. 15, 1440.

Stoltzfus, C. M., and Snyder, P. N., (1975). J. of Virol. 16, 1161.

Taylor, J. M., and Illmensee, R., (1975). J. Virol. 16, 553.

Theilen, G. J., Gould, D., Fowler, M., and Dungworth, D., (1971). J. Nat. Cancer Inst. 47, 881.

Todaro, G., Beneviste, R., Callahan, R., Lieber, M., and Scherr, C., (1974). Cold Spr. Harb. Symp. 39, 1159.

Todaro, G. J., Sherr, C. J., Benveniste, R. E., Lieber, M. M., and Melnick, J. L., (1974). Cell 2, 55.

Wang, L., and Duesberg, P., (1974). J. Virol. 14, 1515.

Weissmann, C., Parson, J. T., Coffin, J. W., Rymo, L., Billeter, M. A., and Hofstetter, H., (1974). Cold Spr. Harb. Symp. 39, 1043.

Wolfe, L. G., Smith, R. K., and Deinhardt, F., (1972). J. Nat. Cancer Inst. 48, 1905.

Chapter 4

Friend Virus (Murine Lymphoid-Leukosis and Spleen-Forcus-Forming Viruses)

Size, Subunit Composition, and Secondary Structure of The Friend Virus Genome

ABSTRACT

The properties and subunit composition of the genomic RNA of the Friend virus (FV) complex isolated from a FV transformed cell line FSD-3 have been studied. The FV "50-60"S RNA appears to be a mixture of at least two, perhaps three species whose molecular weights are in the range of 5 to 6 x 10^6. Under denaturing conditions the "50-60"S RNA dissociates (transition temperature 60C in 0.1 M Na^+) into components of three size classes: L, M and S whose molecular weights are approximately 2.8, 2.4 and 2.2 x 10^6 respectively. Electron microscopic studies reveal that each "50-60"S RNA molecule is a dimer in which the two subunits are joined together by a dimer linkage structure (DLS). The DLS looks like a knot in the center of the molecule. In addition, the "50-60"S RNA contains two symmetrically disposed loops on each side of the DLS and at equal distance from the center. When the "50-60"S RNA is spread under conditions very close to its dissociation temperature, molecules of half the length or subunits containing one loop are also seen. The size and the location of the loop in the monomer and dimer molecules are identical. The melting temperature of the loop structure is close to that of the DLS because under slightly more denaturing conditions the subunit molecules are fully extended.

Introduction

Friend virus (FV) (1) preparations are known to contain two viral components with different biological activities (2-4) the spleen focus forming virus (SFFV) and lymphatic leukemia virus (LLV). The SFFV is oncogenic; it transforms erythroid precursor cells, and induces spleen focus formation thus resulting in erythroleukemia in mice. The SFFV is replication defective and needs a helper virus. The helper function is provided by the LLV (3) contained in the FV complex. The helper function can be provided by many murine leukemia viruses, such as Moloney leukemia virus (MoLV) (3) which do not induce erythroid disease. Recently Dube et al. (5) and Ostertag et al. (6) have shown that the endogenous virus released during dimethyl sulfoxide induced differentiation of Friend cells (5) and upon exposure of these cells to bromodeoxyuridine (6) also has helper activity.

Earlier work on the FV genomic RNA carried out in the laboratories of Dube and Ostertag (7) has shown that a) the FV RNA contains two subunits whose sedimentation coefficients are approximately 35S and 32S, b) the amount of larger subunit is $\leq$ 20%, whereas the smaller subunit constitutes 80% of the FV RNA, c) the genomic complexity is approximately 2.5×10^6 daltons, and d) the viral RNA contains poly A and also internal oligo A tracks. In addition, the 35 S and 32S subunits have been tentatively assigned by Maisel et al. (8) to LLV and SFFV RNA, respectively.

Since the FV complex has both transforming and leukemogenic activities and the Friend cells offer a good system to study the mechanisms by which the expression of viral genes modifies with the expression of cellular genes, we have undertaken to study the FV genome in more detail. In this communication we present the results of some of our physical studies in FV RNA. We show that the undissociated RNA is a "50-60"S dimer molecule

and contains in its center a dimer linkage structure (DLS) which holds the two subunits together through hydrogen bonds. A similar DLS has been observed in several other tumor virus RNAs (9,10). It thus appears that the DLS may be a common feature of the secondary structure of all type C tumor RNA viral genomes.

Materials and Methods

Stock solutions: NTE buffer: 0.01 M NaCl, 0.01 M Tris-Hcl pH 7.2, 0.001 M EDTA.

U + F solvent: This solvent was prepared by mixing 480 g urea with 1 ℓ formamide. There was a 1.35-fold volume increase in the final solution which thus contained 5.9 M urea and 74% formamide. This was taken as 100% U + F.

E buffer: 0.05 M boric acid, 0.005 M sodium borate ($Na_2B_4O_7 \cdot 10 H_2O$), 0.01 M Na_2SO_4 and 0.001 M EDTA, pH 8.2.

TE buffer: 0.1 M Tris-HCl 0.01 M EDTA, pH 8.5 (≃ 0.06 M cations)

Cells, virus and RNA. The cell line used in these experiments was FSD-3 which has been described previously (11). Briefly it originated as follows. FV containing cell-free supernatant from a cell culture of one of our FV transformed cell lines FSD-1 (12) clone F_{4-6} was injected intraperitoneally into Balb C mice. Spleen cells from these mice were used to start the cell line FSD-3. FV was isolated from these cells as described (5). FV twice purified by isopycnic banding in a 24 to 48% sucrose gradient was used for RNA isolation. The viral pellet was suspended in 1% SDS and to this an equal volume of a

mixture of phenol, chloroform and isoamyl alcohol (50:2:48) was added. The aqueous phase containing the extracted RNA was concentrated by ethanol precipitation. The viral RNA was purified on a 10-30% NTE-sucrose gradient. The centrifugation was for 75' at 4°C in Beckman SW50.1 rotor. Fractions were collected and monitored for absorbance at 260 mμ. The peak fractions in the "50-60"S region were pooled, precipitated with ethanol and used for the present studies.

Agarose gel electrophoresis. All gel electrophoresis experiments were conducted on 1% agarose gels in E buffer. The preparation of the non-denaturing and strongly denaturing CH_3HgOH-agarose gels has been described (9, 13). In the experiments for studying the dissociation temperature of the 50-60S RNA, RNA samples were mixed with U + F solvent and NTE buffer to the desired concentrations. Samples (ca. 20 μl) were sealed in a capillary tube, incubated for 5 min at the desired temperature, mixed with glycerol and bromophenol blue, and loaded onto the gels. Electrophoresis was performed at 5 mA per tube for 3 hr at room temperature. The gels were then stained with 1 μg/ml ethidium bromide, 0.5 M NH_4Ac for 30 min, and examined by illumination with short wavelength UV light.

For denaturing, CH_3HgOH-agarose gel electrophoresis experiments. RNA samples were mixed with CH_3HgOH in E buffer to a final concentration of 5 mM CH_3HgOH and then loaded onto a 1% agarose gel containing 5 mM CH_3HgOH. Electrophoresis was performed for 5 hr at 25°C. HeLa 28 and 18S rRNAs were similarly treated and run in parallel as markers for estimating molecular weights. After electrophoresis the gels were stained as before.

Electron microscopy. The urea-formamide (U + F) and the glyoxal-formamide spreading techniques have been described previously (9). In the urea-formamide spreading, RNA samples were diluted into the spreading solution which contained about 30 μg/ml cytochrome c and the desired concentration of U + F and electrolyte. The hypophase was double distilled water. To study the structure of undissociated "50-60" S RNA, the spreading was performed in 80% U + F containing 0.15 M TE (∿0.09 M cations). These conditions are inside the melting range of "50-60" S RNA. In the experiments to determine the molecular weights of dissociated subunits, RNA samples were first treated with 85-90% U + F in ≤ 0.05 M TE, then either spread directly from 85% U + F or diluted and spread from 60% U + F. Essentially identical results have been obtained from these spreadings.

In the glyoxal-formamide spreading, RNA samples were first treated with 1 M glyoxal in 0.01 M phosphate buffer, pH 7.5 at 37°C for 1 hr. The glyoxalated RNAs were then diluted and spread from 30% formamide, 0.1 M TE onto 5% formamide, 0.01 M TE.

Results

The RNA Components of FV Complex from FSD 3 Cells

In nondenaturing (i.e., high salt, NTE) sucrose gradients FV RNA sedimented as a single peak (Fig. 1) with a sedimentation coefficient of about 50-60S. When the 50-60S RNA samples were collected and, without further treatment, subjected to electrophoresis in nondenaturing agarose gels, a single diffuse band (Fig. 2a) with an apparent molecular weight of 5 to 6 x 10^6 was

Fig. 1. Sedimentation profile of "50-60"S FV RNA in NTE-Sucrose gradient. The sedimentation direction is from right to left.

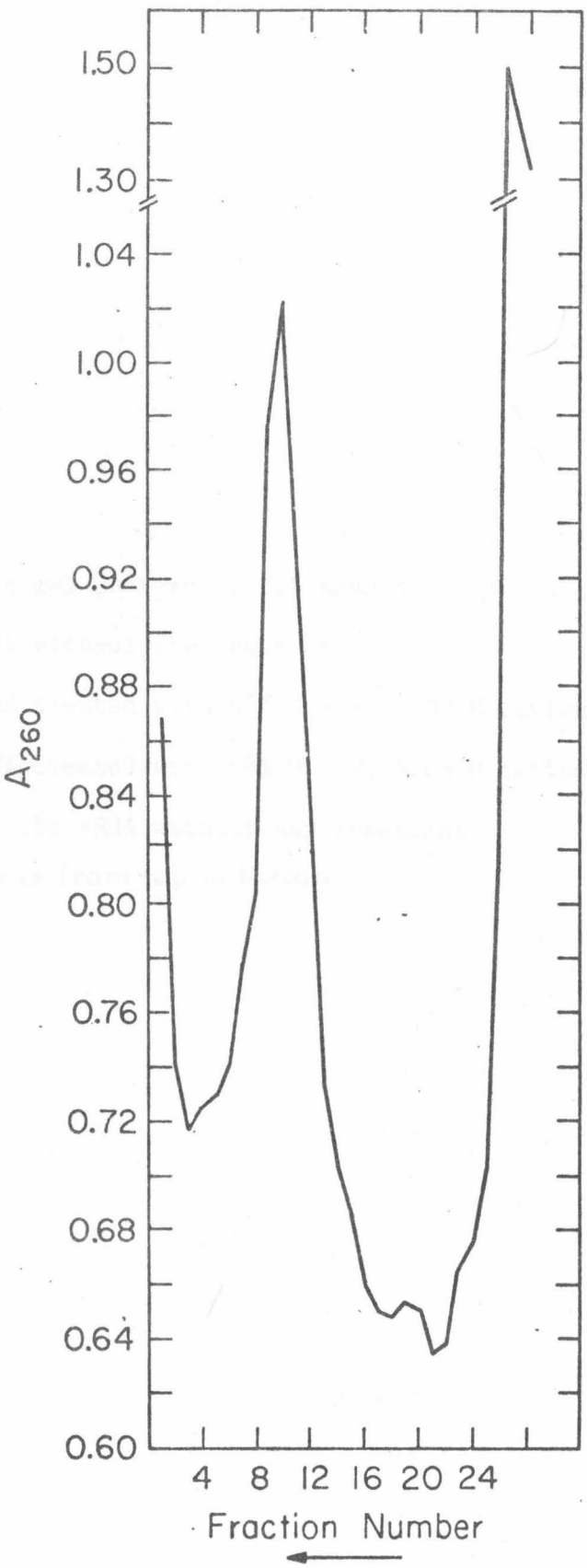
1.50
1.30
1.04
1.00
0.96
0.92
0.88
0.84
0.80
0.76
0.72
0.68
0.64
0.60
A_{260}
4 8 12 16 20 24
Fraction Number

Fig. 2. Electrophoretic gel patterns in 1% agarose.

a) "50-60"S RNA without pretreatment

b) "50-60"S RNA treated with 66% U + F, 0.03 M cations at 25°C

c) "50-60"S RNA treated with 66% U + F, 0.03 M cations at 40°C

d) HeLa 28 and 18S rRNA without any treatment

The migration is from top to bottom.

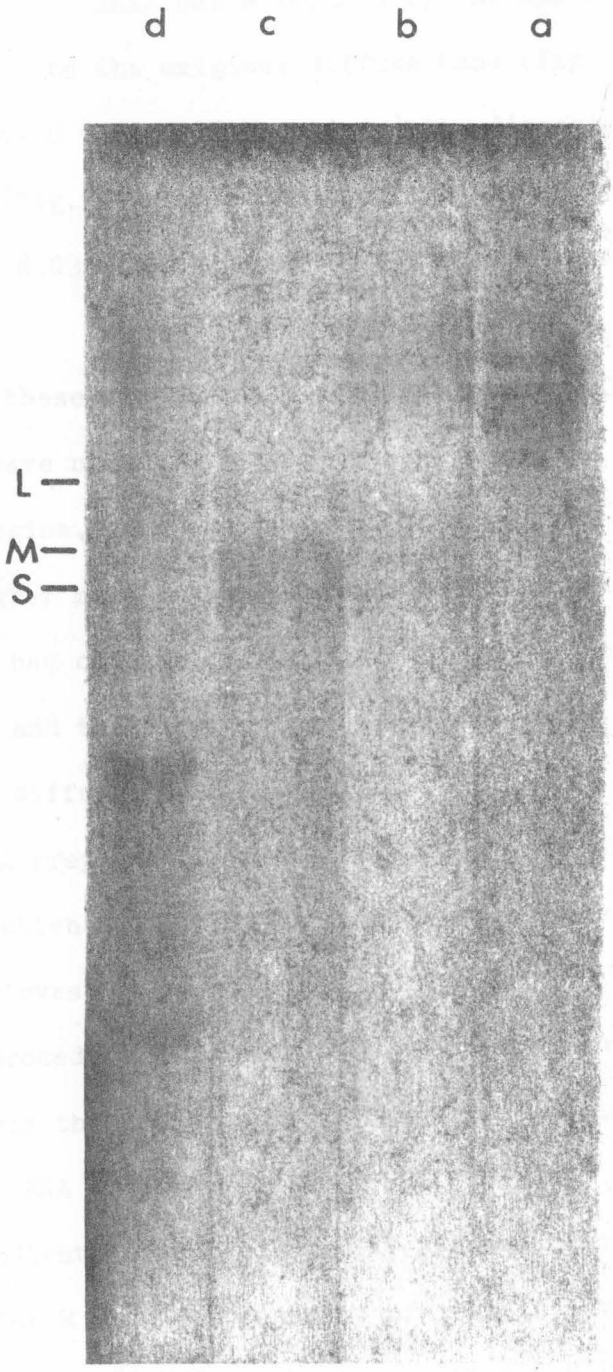
d
c
b
a
L
M
S

reproducibly observed. If, however, the samples were first treated with a denaturing solvent (i.e., dissolved in 66% U + F, 0.03 M cations) at 25°C then applied on to the agarose gel, about 50% of the "50-60" S RNA dissociated into subunits. This was evidenced by the appearance of fast moving bands in addition to the original diffuse band (Fig. 2b). At 40°C in the same solvent (66% U + F, 0.03 M cations) the dissociation into subunits was complete (Fig. 2c). Treatment of RNA with more denaturing conditions (90% U + F, 0.03 M cations) at 40°C did not cause further dissociation.

We have repeated these experiments with different viral preparations from FSD-3 cells and have never failed to observe three well resolved bands in the 30-35S region, corresponding to the dissociated subunits. The two bands with higher mobility referred to as M (for medium) and S (for small) in Fig. 2 had comparable fluorescent intensities when stained with ethidium bromide and the slow moving one, L, was much fainter.

Judging from the diffusiveness of the "50-60" S band, it appears that the "50-60" S RNA preparation is heterogeneous and contains a mixture of molecules which differ slightly in their electrophoretic mobilities. We have investigated this point further using a two dimensional gel electrophoretic procedure (manuscript in preparation) and have obtained evidence which suggests the presence of at least two, perhaps three "50-60" S RNA species in the FV RNA preparations from FSD-3 cells.

The data also indicate that the FSD-3 FV RNA contains subunits of different lengths. The M and S components, present in almost equal proportions, comprise about 80-90% of the total "50-60" S RNA and the L component about 20%. The dissociation of the "50-60" S RNA complexes

into these components takes place at 25°C in 66% U + F, 0.03 M cations, which corresponds to a transition temperature of about 60°C in 0.1 M Na^+ as calculated using the following approximate equation:*

$$\Delta \text{ Tm} \simeq 0.4°\text{C} \times \text{percent(U + F)} + 16.6°\text{C} \log \frac{[\text{cation}]}{0.1}$$

to correct for the melting point depression caused by U + F solvent and salt (14).

The Molecular Weights of RNA Components

In order to demonstrate that the RNA subunits which migrate differently in nondenaturing gels are not conformational variants and, also, to determine more accurately the molecular weights of these components, we have used the strongly denaturing CH_3HgOH - agarose gel electrophoresis system (13). It is believed that, under these strongly denaturing conditions, the electrophoretic mobility or an RNA species depends only on its size. We again observed three discrete bands (Fig. 3). Relative to HeLa 28S [1.76×10^6 daltons (17)] and 18S [0.7×10^6 daltons (17)] ribosomal RNA markers, the molecular weights of FV RNA subunits were found to be 2.8, 2.4 , and 2.2×10^6 for L, M, and S components, respectively.

*Footnote: The effect of U + F solvent on the depression of Tm of ds RNA has not been determined. The effect of 100% U + F is comparable to that of pure formamide (9, 15). Friedrich & Feix(16) have shown that the Tm of ds MS2 RNA (replicative form) is depressed by 0.3-0.5°C per 1% formamide. We have taken 0.4°C as the depression value for our calculation.

Fig. 3. Electrophoretic gel pattern of FV RNA in 5 mM CH_3HgOH-1% agarose. HeLa 28 and 18S rRNA were run in parallel as molecular weight markers. The migration is from top to bottom.

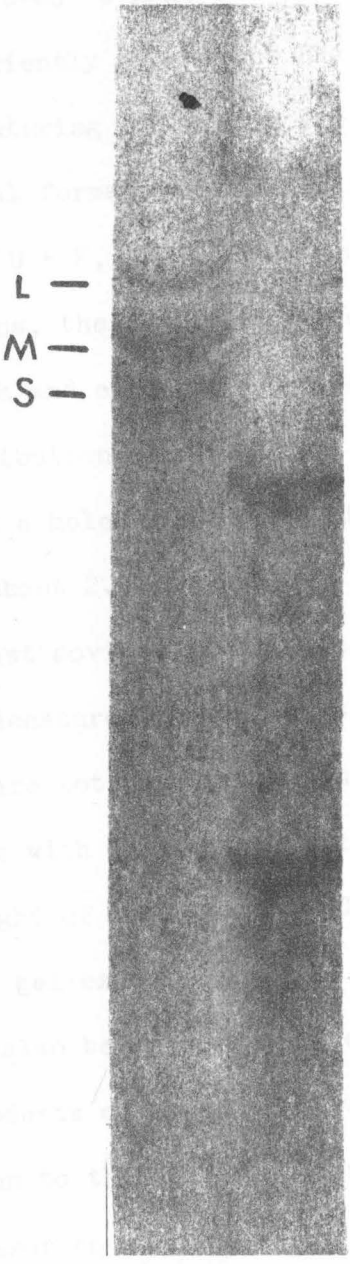
L
M
S

Electron Microscope Studies on FV "50-60" S RNA

Subunit lengths and molecular weights

We wished to characterize the secondary structure as well as determine the molecular weights of the "50-60" S RNAs and their subunits by electron microscopy. In order to sufficiently extend the RNA molecules for good length measurements strong denaturing conditions are usually required. We have applied both the glyoxal formamide (0.1 M glyoxal, 40% formamide) and the urea formamide (85-90% U + F, $\leq$0.03 M cations) methods (9). Under these spreading conditions, the FV "50-60" S RNA is fully dissociated and the molecules appear smooth and extended (Fig. 4a, b).

A histogram of size distribution obtained from such a spreading is shown in Fig. 5a. A peak with a molecular length of 1.7-1.9 μm corresponding to a molecular weight of about 2.2-2.4 x 10^6 is apparent. This peak, we believe, represents the two fast moving bands M and S seen on gels (Figs. 2, 3) when the "50-60" S RNA is denatured. Owing to the small difference in size of these subunits, they are not resolved by this technique. The histogram also shows molecules with molecular lengths of 2.2-2.4 μm corresponding to a molecular weight of 2.8-3 x 10^6. These molecules, we believe, migrate as band L in gel experiments. In the histogram low molecular weight species can also be detected. These molecules probably represent the degradation products of FV RNA. However, owing to their small size, their contribution to the ethidium bromide induced fluorescence is much smaller and for this reason could not be easily picked up in our gel experiments.

Fig. 4. Electron micrographs of FV RNA's.

a) 90% U + F (0.03 M cations) treated, and spread from 60% U+F

b) Glyoxal treated, and spread from 30% formamide (0.06 M cations)

c) and d) 80% U + F (0.09 M cations) treated and spread in the same medium. All spreading procedures are described in Materials and Methods. The length marker is 0.2 μm.

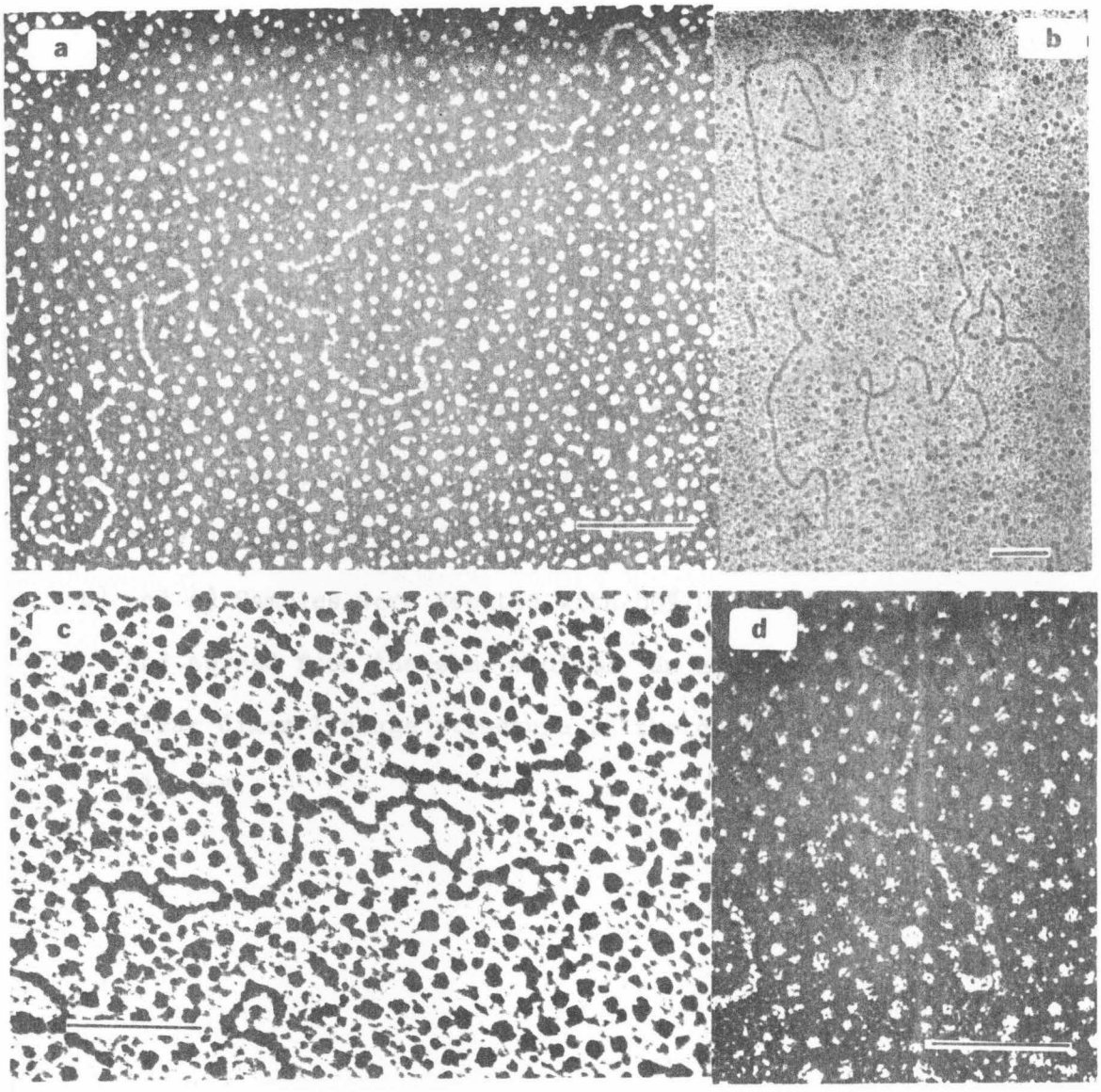
a
b
c
d

Fig. 5. Histogram of size distribution of FV RNA's.

a) Samples were treated with 90% U + F (0.03 M cations) and spread from 60% U + F

b) and c) Samples were treated with 80% U + F (0.09 M cations) and spread from the same medium. In c) molecules with a clear dimer linkage structure in the center were selected and plotted.

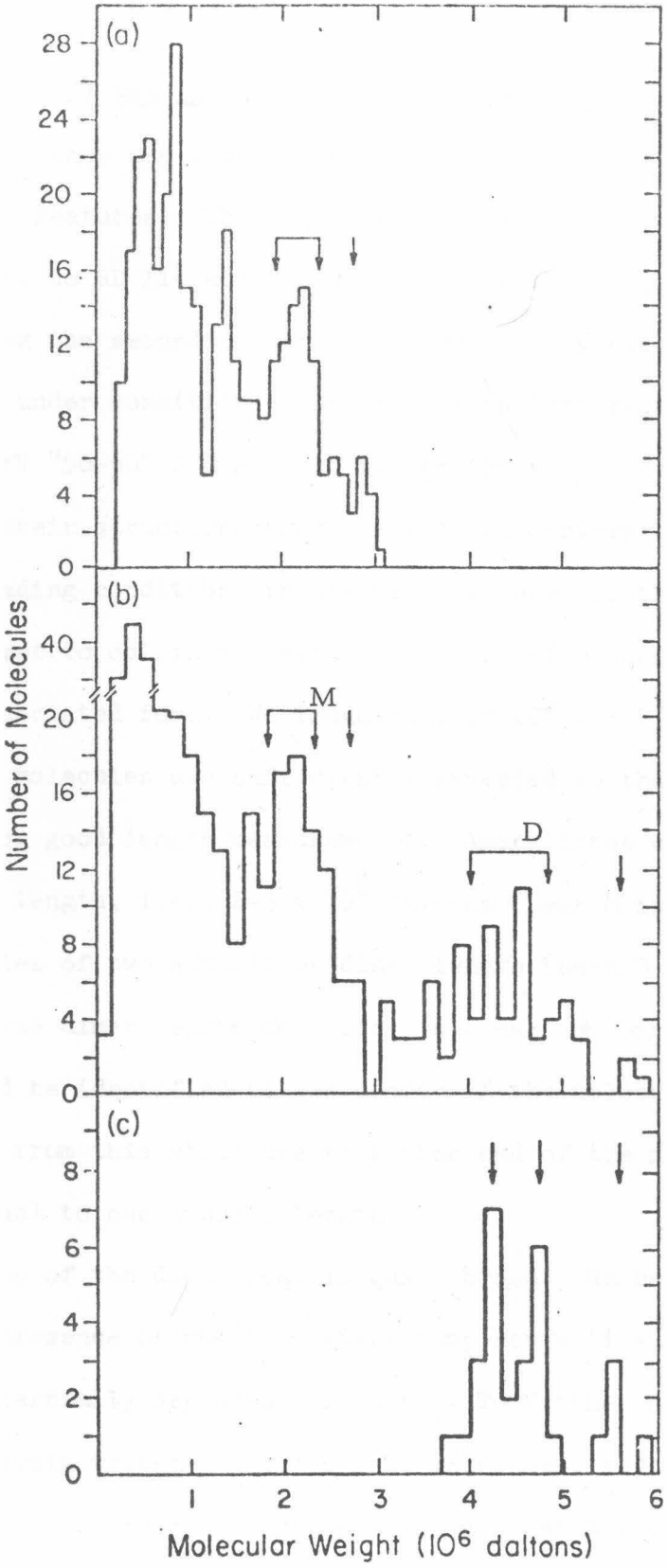
(a)
(b)
(c)
M
D
Number of Molecules
Molecular Weight (10^6 daltons)

Secondary Structure of the "50-60" S RNA

Earlier work on RD 114 (9), BKD and WoMV (10) viral RNAs has shown that in the undissociated state they are dimer molecules containing characteristic secondary structure features. The relatively low melting temperature of FV RNA as compared to RD 114 and BKD viral RNAs poses a difficult problem for characterizing the secondary structure features by electron microscopy. When spread under conditions less denaturing than required for dissociation of the FV "50-60" S RNA, most of the RNA molecules appear to be quite tangled and their structure cannot be properly interpreted. We therefore sought spreading conditions in the melting range of the "50-60" S RNA in an attempt to obtain at least a fraction of molecules in an extended yet undissociated form. We found that in 80% U + F, 0.09 M cations about 70% of the molecules are sufficiently extended so that they could be easily traced for good length measurements. Among these were molecules of one subunit length, i.e., 2-3 x 10^6 daltons (peak M in Fig. 5b) and also molecules of two subunit or dimer length (peak D in Fig. 5b). In many of these dimer length molecules, a clear —•— or —o— secondary structure could be identified at the center of the molecule (Fig. 4c). The distance from this structure to either end of the molecule was found to be about equal to one subunit length.

The size distribution of the dimer peak is quite broad. We believe that this is due to the presence of multiple viral components (i.e., L, M, and S) as well as of partially degraded molecules. To further analyze the data, we have selectively traced molecules (all molecules, regardless of length) in which a clear secondary structure is located at the center

and the lengths of the two halves are close to each other within experimental error ($\sim 0.2 \times 10^6$). The sizes of these molecules are plotted in Fig. 5c. The figure shows three peaks corresponding to the dimer lengths of 2.8, 2.4 and 2.2 x 10^6 dalton components. We believe these homodimers are the intact undissociated "50-60" S RNA molecules of L, M, and S components.

Among these intact molecules another feature of secondary structure was discerned. The molecules were found to contain two loops symmetrically disposed with respect to the DLS (Fig. 4c). Dissociated subunits in the same spreading also contained one loop (Fig. 4d). The size and location of the loops in the undissociated and dissociated molecules was found to be identical (Fig. 6). The distance from the loop joint to the proximal end in the dissociated subunit was equal to that from the loop joint to the DLS in the dimer (Fig. 6a, b). Electron microscopic poly A mapping experiments have shown that the poly A sequences are at both free ends of the dimer molecule (manuscript in preparation).

Discussion

We have demonstrated that the viral RNA from FSD-3 cells contain a mixture of RNA species of sedimentation coefficients ranging between 50 and 60S. The "50-60" S RNA contains subunits of three size classes: L, M, and S. Their respective molecular weights are 2.8, 2.4 and 2.2 x 10^6. The M and S subunits are present in approximately equal amounts and represent about 80-90% of FV RNA. These subunits are derived when the "50-60" S RNA is exposed to denaturing conditions, i.e. $\geq$ 66% U + F,

Fig. 6. The location and size of the characteristic loop observed in the dimer and monomer molecules.

a) Distance from loop joint to DLS in dimer molecule

b) Distance from loop joint to the proximal end in monomer molecule

c) Size of the loop in dimer molecule

d) Size of the loop in monomer molecule

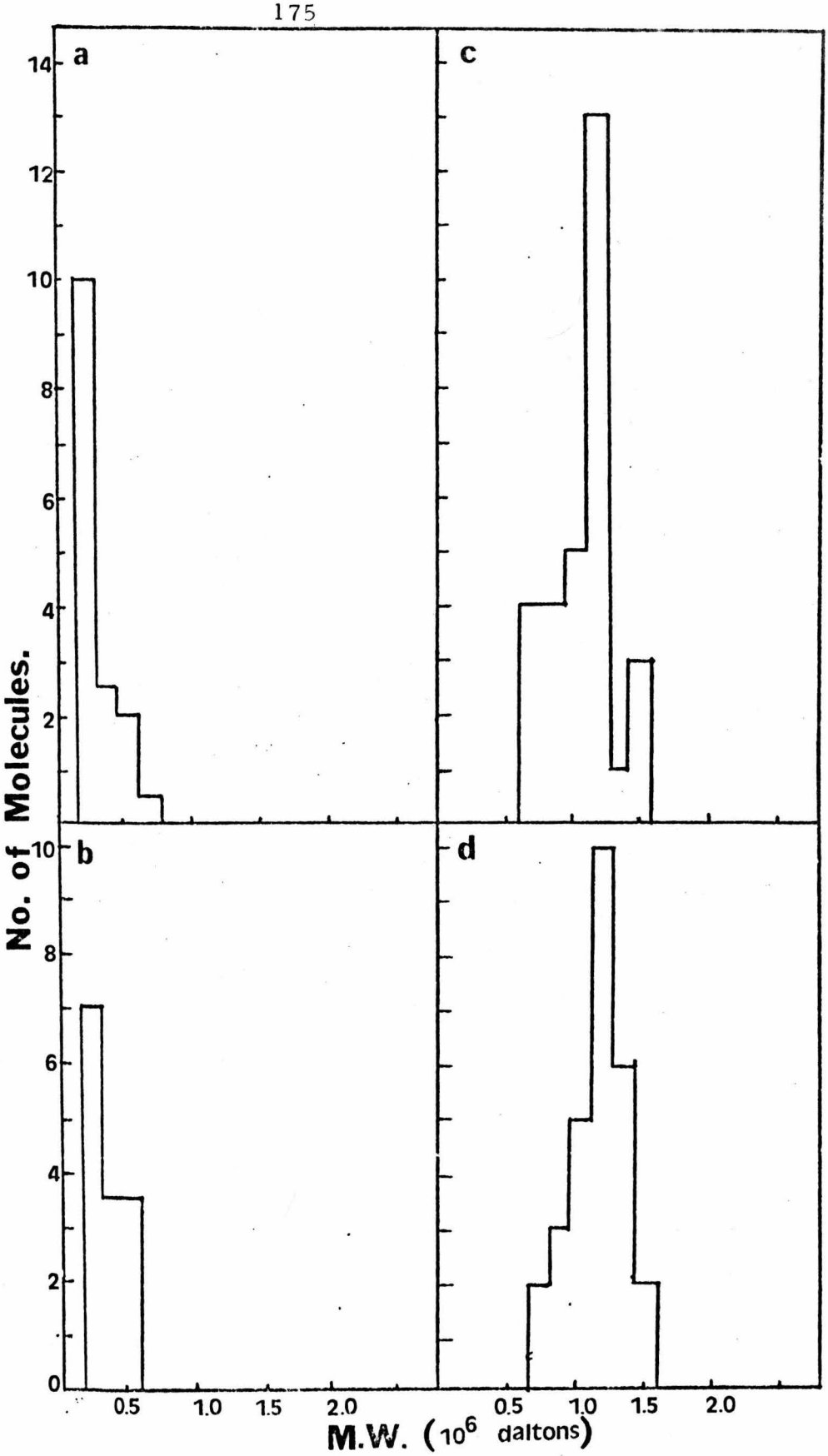
a
c
b
d
No. of Molecules.
M.W. (10^6 daltons)
0
2
4
6
8
10
12
14
0.5
1.0
1.5
2.0

0.03 M cations at 25°C. The calculated transition temperature for dissociation of FV RNA in 0.1 M salt is about 60°C.

The undissociated "50-60" S RNA is a dimer molecule. It is composed of two subunits and contains in its center a dimer linkage structure (DLS) which holds the two subunits together through hydrogen bonds. In addition to this secondary structure feature the dimer molecule also contains two loops symmetrically disposed with respect to the DLS. The loop is present also in the dissociated subunits indicating that the loop joint is at least as stable as the DLS. It is interesting to note that whereas in FV RNA these two features of secondary structure, i.e., the DLS and loops are of equal stability, in the case of RD 114 (9) and BKD (10) RNAs, the DLS is far more stable (dissociation temperature ∿30°C higher) than the loops. In fact, in the dissociated RD 114 and BKD RNA subunits the loops are no longer observed, suggesting that the stability of loops in FV, RD 114 and BKD RNAs is very similar. It seems not unlikely that the degree and the type of base pairing involved in the formation of secondary structure loops may be very similar in these RNAs. Indeed both in this respect and in having a DLS all type C tumor viral RNAs may have a common denominator and these features of secondary structure may have evolved for a common biological purpose. It is perhaps worthy of mention at this point that in addition to DLS there is considerable secondary structure in viral RNA which is not discernible by electron microscopy. This is evidenced by the fact that we have reproducibly obtained large discrete fragments (unpublished results) when FV and other viral RNAs are digested with nucleases indicating that not all regions in the molecule are equally accessible to nucleases.

The presence of three RNA subunits together with the finding that the undissociated "50-60" S RNA is a dimer molecule raises several important questions: How many viral components are present in FSD-3 FV isolates or how many "50-60" S RNA components are present in the FV RNA? How are the three classes of RNA subunits distributed among the "50-60" S RNA molecules? Do the "50-60" S dimer molecules contain subunits of the same class (i.e., L-L, M-M, and S-S) or of different classes (i.e., L-M, M-S, L-S) which are joined together to form homodimers as in the former case or heterodimers as in the latter? Furthermore, if there are multiple viral components what are the genetic relationships between them and how are these viruses derived?

The diffusiveness of the "50-60" S RNA band as observed in nondenaturing gels suggests that there is more than one "50-60" S component in FV RNA. Biological assays on FV preparations have revealed the presence of at least two viral components, SFFV and LLV (2-4). Biochemical analysis of FV RNA by Dube and colleagues (7) has demonstrated the presence of a 35S and a 32S subunit which have been tentatively assigned to LLV and SFFV RNAs respectively by Maisel et al (8) by comparing with the RNA gel patterns of other murine sarcoma-leukemia viruses.

The fact that the LLV function can be separated from the SFFV by end point dilution (3) suggests, if the above assignment is correct, that the L component is derived from a separate virion - the LLV particle. The unequal representation of L component relative to others in the gel pattern provides supporting evidence. Furthermore, two dimensional gel electrophoretic (manuscript in preparation) and electron microscopic observations showing the presence of intact "50-60" S dimer molecules consisting of two L sized subunits are consistent with the above view.

The genetic sequence relationships between these viruses and hence the nucleotide sequence relationships between the RNA subunits are not yet clear. The L and M subunit classes with relative amounts similar to what we have observed have been consistently found in many other FV transformed cell lines (Dube & Ostertag, unpublished results). The detection of the S component, however, has not been reported previously. The S component could represent an endogenous virus of FSD-3 cells. Indeed, the induction of endogenous virus in FV transformed cells has been reported by Dube et al (5) and Ostertag et al (6). On the other hand, the S component could be derived from L or M components through deletion, mutation or recombination events during the passages of FSD-3 cells in culture. Preliminary nucleotide sequence analysis on these gel-resolved bands indicates that M and S components are closely related and the S component is perhaps a deletion variant of M component.

References

1. Friend, C. (1957) J. Exp. Med. 105, 307-318.

2. Axelrad, A. A. and Steeves, R. A. (1964) Virology 24, 513-518.

3. Steeves, R. A., Eckner, R. J., Bennett, M., Mirand, E. A. and Trudel, P. J. (1971) J. Nat. Cancer Inst. USA 46, 1209-1217.

4. Lilly, F. and Pincus, T. (1973) Adv. Cancer Res. 17, 231-277.

5. Dube, S. K., Pragnell, I. B., Kluge, N., Gaedlicke, G., Steinheider, G. and Ostertag, W. (1975) Proc. Nat. Acad. Sci. USA 72, 1863-1867.

6. Ostertag, W., Roesler, G., Krieg, C. J., Kind, J., Cole, T., Crozier, T., Gaedlicke, G., Steinheider, G., Kluge, N. and Dube, S. K. (1974) Proc. Nat. Acad. Sci. USA 71, 4980-4985.

7. Ostertag, W., Cole, T., Crozier, T., Gaedicke, G., Kind, J., Kluge, N., Krieg, J. C., Roesler, G., Steinheider, G., Weimann, B. J. and Dube, S. K . (1973) in Proc. 4th Symp. Princess Takamatsu Cancer Research Fund, Differentiation and control of malignancy of tumor cells (U. Tokyo Press), pp. 493-520.

8. Maisel, J., Klement, V., Lai, M. M-C., Ostertag, W. and Duesberg, P. (1973) Proc. Nat. Acad. Sci. USA 70, 3536-3540.

9. Kung, H. J., Bailey, J. M., Davidson, N., Nicolson, M. O. and McAllister, R. M. (1975) J. Virol. 16, 397-411.

10. Kung, H. J., Hu, S., Bender, W., Bailey, J. M., Davidson, N., Nicolson, M. O. and McAllister, R. O. Submitted to Cell.

11. Dube, S. K., Gaedicke, G., Kluge, N., Weimann, B. J., Melderis, H., Steinheider, G., Crozier, T., Beckmann, H. and Ostertag, W. (1973) in Proc. 4th Symp. Princess Takamatsu Cancer Research Fund, Differentiation and control of malignancy of tumor cells (U. Tokyo Press), pp. 99-135.

12. Ostertag, W., Melderis, H., Steinheider, G., Kluge, N. and Dube, S. K. (1972) Nature New Biol. 239, 231-234.

13. Bailey, J. M. and Davidson, N. (1975) Anal. Biochem. (in the press).

14. Paul Burnett, J., Frank, B. J. and Douthart, R. J. (1975) Nucleic Acids Res. 2, 759-767.

15. McConaughy, B. L., Laird, C. D. and McCarthy, B. J. (1969) Biochemistry 8, 3289-3295.

16. Friedrich, R. and Feix, G. (1972) Anal. Biochem. 50, 467-471.

17. Wellauer, P. K. and Dawid, I. B. (1973) Proc. Nat. Acad. Sci. USA 70, 2827-2831.

Part II

Structure of Arbovirus RNA

An Electron Microscope Study of Sindbis Virus RNA

by

Ming-ta Hsu, Hsing-Jien Kung,

and Norman Davidson

Department of Chemistry
California Institute of Technology
Pasadena, California 91109

ABSTRACT

Glyoxal reacts preferentially with guanine residues of polynucleotides of G's. Single-stranded RNA, after treatment with glyoxal, appears as an extended filament when prepared for electron microscopy by the formamide-basic protein film method. Good sharp length distributions are obtained for a homogeneous RNA. The molecular weight of Sindbis virus RNA is thus measured as 4.7×10^6 daltons, relative to 23S *E. coli* rRNA taken as 1.07×10^6, in reasonable agreement with sedimentation data. Glyoxal treatment should be useful for electron microscopic mapping of poly(A) sequences on RNA molecules by hybridization with poly U or poly dT, since the RNA can be spread without interfering with the A-U bonding. Preliminary studies suggest that Sindbis virus RNA carries poly(A) sequence at its end. Many circular molecules are seen when RNA is extracted from Sindbis virus, treated gently with glyoxal, and spread for electron microscopy. Under more denaturing conditions, linear molecules are seen. This implies that the two ends of the RNA molecule contain mutually complementary sequences.

We wish to describe electron microscope methods for measuring the molecular lengths of RNA molecules and of mapping any poly-A sequences present. We chose to apply these methods initially to Sindbis virus RNA.

The virion of Sindbis virus contains only 42s RNA (Pfefferkorn et al., 1967) with a molecular weight of $4.3 \pm 0.3 \times 10^6$ daltons, as estimated by DMSO sedimentation and gel electrophoresis (Simmons and Strauss, 1972). Sinbis RNA contains a poly-A sequence (Johnston and Bose, 1972 a, b). For most of the molecules its length is 60 to 80 nucleotides; for a small fraction (20% or less), the length is 150 to 250 nucleotides (Eaton and Faulkner, 1972).

In general, the basic protein film electron microscope techniques that work very well for both duplex and single-stranded DNA are less effective for RNA. The standard spreading conditions of 40 to 50% formamide and ca. 0.06 M ionic strength (Davis et al., 1971) that cause single-strand DNA to be extended without denaturing duplex DNA do not fully extend most RNA species. RNA can be extended by spreading from a strongly denaturing solvent, in which most duplex nucleic acids would also be denatured (Granboulan and Scherrer, 1969; Robberson et al., 1971 Verma et al., 1970; Nanninga et al., 1972). RNA molecules that have been cross linked by glutaraldehyde to gene 32 protein are well extended in standard formamide spreadings (Delius, Westphal, and Axelrod, 1973). This treatment is moderately denaturing for duplex nucleic acids which are rich in A-T or A-U base pairs.

We decided to investigate glyoxal as a reagent that would block some of the hydrogen bonding functions of a nucleic acid and thus increase the ease with which the molecule could be extended, without

affecting the stability of A-T and A-U base pairs. Glyoxal adds to adenosine and cytidine rapidly and reversibly with the rather small equilibrium association constants of 1.4 $\underline{M}^{-1}$ and 5.8 $\underline{M}^{-1}$ respectively at 20°C. It reacts more slowly with guanosine. The equilibrium association constant is about 6×10^3 $\underline{M}^{-1}$. The half-life of the glyoxal-guanosine adduct is directly proportional to the hydrogen ion concentration and is about 50 hours at 20° and pH 7 (Broude and Budowsky, 1971). The probable structure of the adduct is indicated below.

Under proper conditions therefore it should be possible to block the hydrogen bonding functionalities of the G residues of a nucleic acid without interfering with the ability of a poly-A sequence to hybridize to an added poly-dT strand. It seemed to us that this might be the basis of an electron microscope method of mapping the positions of poly-A sequences on RNA molecules.

RESULTS

a) Sedimentation coefficients and length measurements of glyoxal treated RNA E. coli 16s and 23s rRNA and Sindbis virus RNA were prepared as described in the legend to Fig. 1. The sedimentation profiles in Fig. 1 show that in neutral sucrose, the Sindbis virus RNA preparation has a sedimentation coefficient of 43s, by

Fig. I. Sedimentation profiles of Sindbis RNA and of E. coli rRNA. (a) Sedimentation through a 5 to 30% sucrose gradient in 0.01 M phosphate buffer, pH 7, 0.05% SDS at 15°C, 44 K rpm, 0.5 hrs, SW 50.1 rotor; 0.1 ml of 100 µg/ml ^{3}H Sindbis RNA was layered on top of the gradient. Slightly more ^{3}H E. coli rRNA was run in a separate tube at the same time. (b) A mixture of ^{3}H Sindbis RNA and ^{14}C E. coli rRNA was treated with glyoxal as described in the text and sedimented through the same gradient as in (a) but containing 0.1 M glyoxal, same sedimentation conditions, but 5.0 hrs. The velocity ratios between (a) and (b) are: Sindbis RNA, 2.3; 23s, 1.8; 16s, 1.4.

Sindbis virus was grown in a primary culture of chick embryo fibroblasts prepared by Dr. J. Strauss. His procedure (personal communication) for growth and harvest of the virus was used. Virions were purified by sucrose gradient velocity centrifugation and then pelleted. RNA was purified by phenol extraction at 4°C using distilled water aturated phenol containing 0.1% of hydroxy quinoline. The aqueous phase was 0.1 M NaCl, 0.01 M tris, 0.001 M EDTA, pH 7.0, 1.0% SDS. Degradation of the RNA is less if phenol is added to the virus pellet before adding the aqueous SDS buffer (P. Vogt, J. Strauss, private communications).

^{14}C or ^{3}H labeled E. coli rRNA was extracted from ribosomes (a gift from Drs. R. Deonier and A. Forsheit) with phenol-SDS as described above.

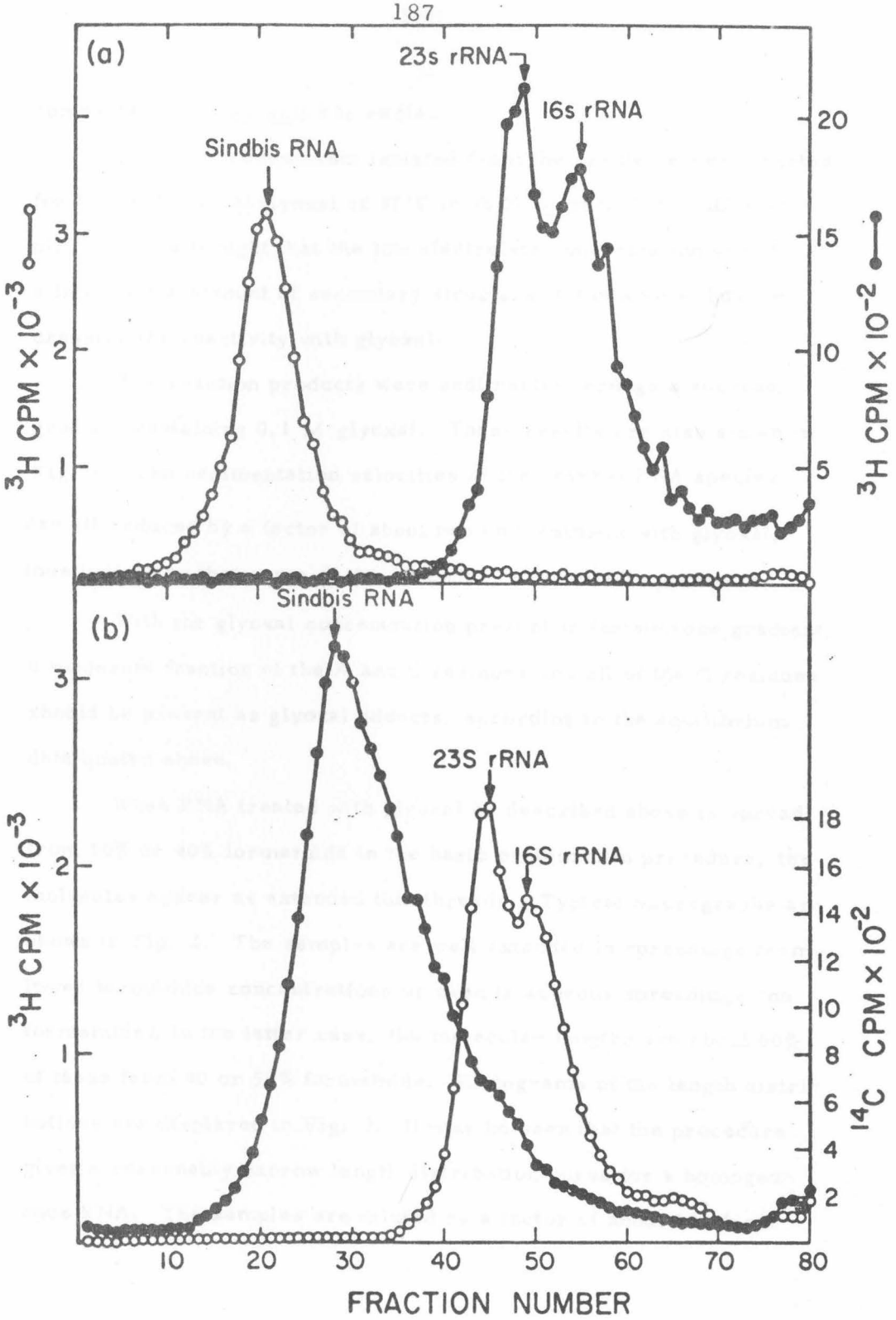
(a)
23s rRNA
16s rRNA
Sindbis RNA
^{3}H CPM x 10^{-3}
^{3}H CPM x 10^{-2}
(b)
Sindbis RNA
23S rRNA
16S rRNA
^{3}H CPM x 10^{-3}
^{14}C CPM x 10^{-2}
FRACTION NUMBER

comparison with E. coli 23s rRNA.

The RNA components isolated from the gradients were treated for 1 hr with 0.5 M glyoxal at 37°C in 0.01 M phosphate buffer at pH 7. It was thought that the low electrolyte concentration would minimize the amount of secondary structure in the RNA's thus increasing the reactivity with glyoxal.

The reaction products were sedimented through a sucrose gradient containing 0.1 M glyoxal. These results are also shown in Fig. 1. The sedimentation velocities of the several RNA species are all reduced by a factor of about two on treatment with glyoxal, thus indicating that some of the secondary structure is disrupted.

With the glyoxal concentration present in the sucrose gradient, a moderate fraction of the A and C residues and all of the G residues should be present as glyoxal adducts, according to the equilibrium data quoted above.

When RNA treated with glyoxal as described above is spread from 50% or 40% formamide in the basic protein film procedure, the molecules appear as extended thin threads. Typical micrographs are shown in Fig. 2. The samples are well extended in spreadings from lower formamide concentrations or even in aqueous spreadings (no formamide); in the latter case, the molecular lengths are about 60% of those from 40 or 50% formamide. Histograms of the length distributions are displayed in Fig. 3. It may be seen that the procedure gives a reasonably narrow length distribution curve for a homogeneous RNA. The samples are diluted by a factor of about 10^2 from

Fig. 2. Electron micrographs of Sindbis RNA and E. coli 23s rRNA after treatment with glyoxal as described in the text. After reaction or isolation from the 0.1 M glyoxal sucrose gradients, the samples were diluted ca. 10^2 fold into 50% formamide, 0.1 M tris, 0.01 M EDTA, pH 8.5 and spread onto 20% formamide with one-tenth the electrolyte concentration (Davis et al., 1971). The relation between the formamide concentration in the hyperphase and the hypophase was: 60% to 30%, 50% to 20%, 40% to 10%, and 30% to 5% (Davis and Hyman, 1971).

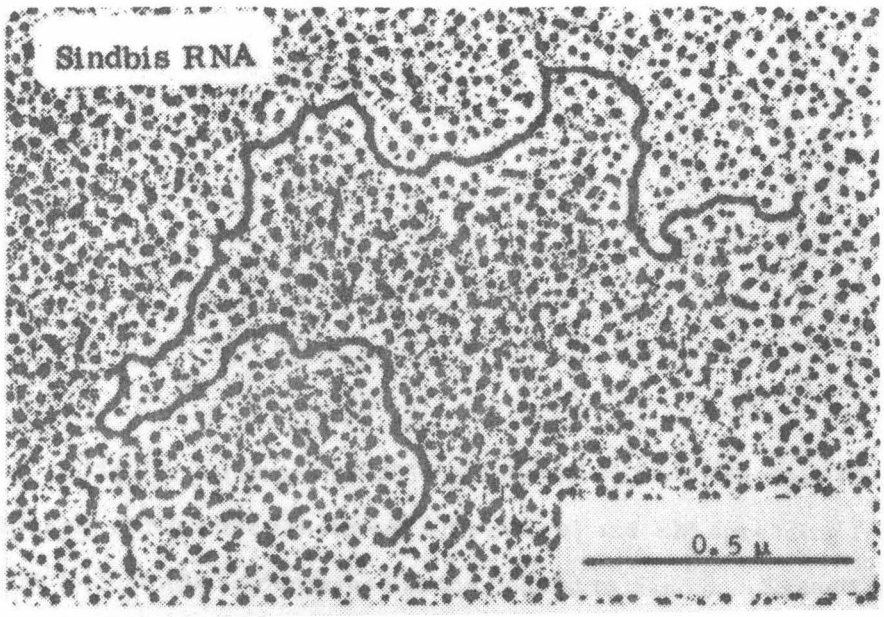
Sindbis RNA
0.5 μ

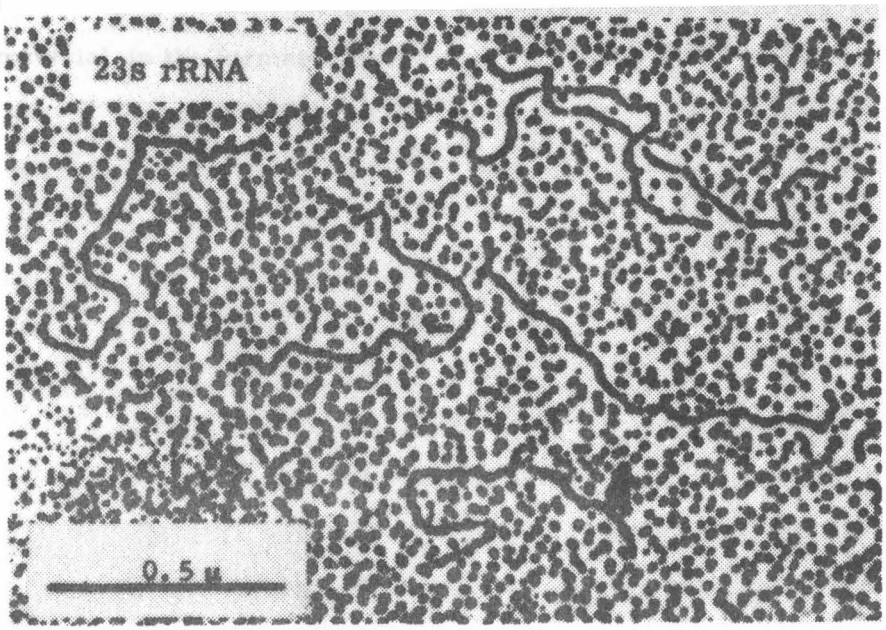
23s rRNA
0.5 μ

Fig. 3. Histograms of length distributions of Sindbis RNA and E. coli rRNA after treatment with glyoxal and EM spreading from 50% formamide as described in the legend to Fig. 2. Essentially the same distribution was obtained by direct dilution of the 0.5 M glyoxal reaction mixture or with the peak samples from the 0.1 M glyoxal sucrose gradient centrifugation, but there is more short degraded material in the former case.

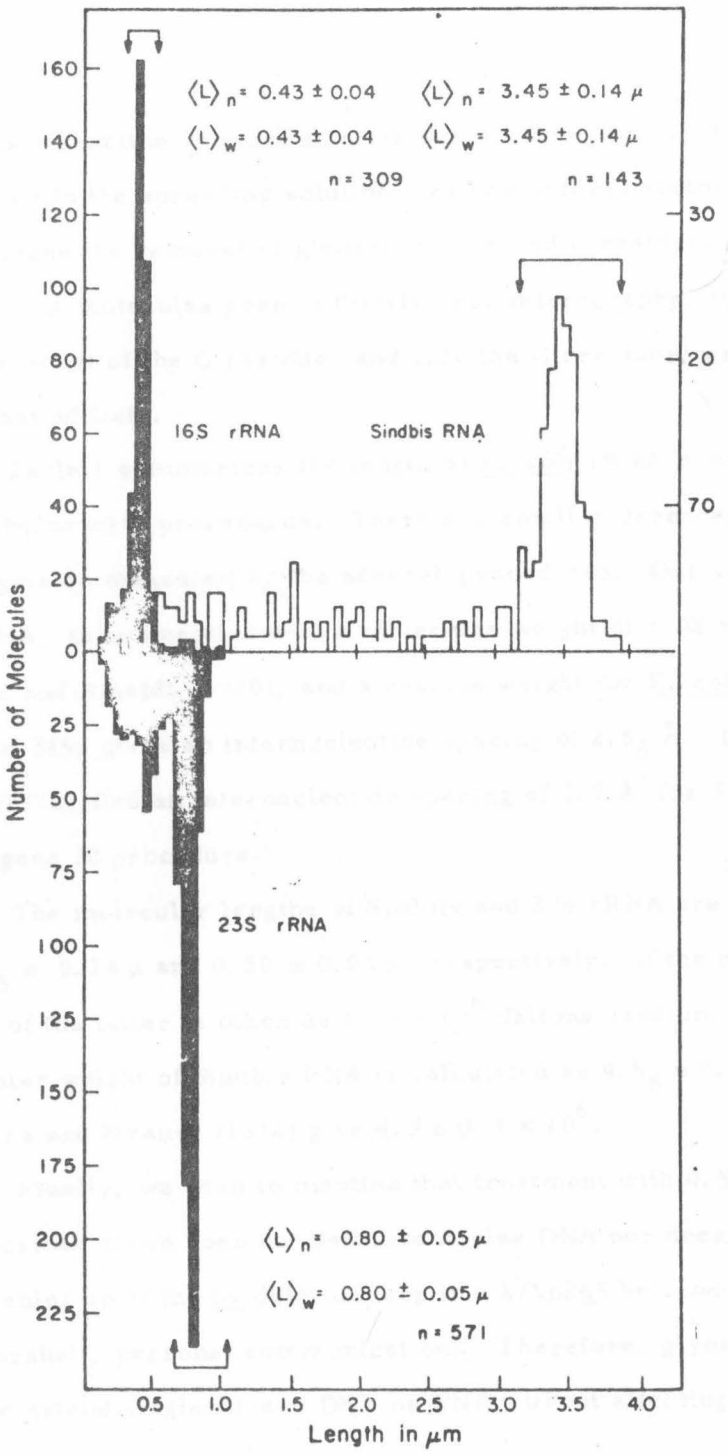
⟨L⟩n = 0.43 ± 0.04
⟨L⟩w = 0.43 ± 0.04
n = 309
⟨L⟩n = 3.45 ± 0.14 μ
⟨L⟩w = 3.45 ± 0.14 μ
n = 143
16S rRNA
Sindbis RNA
23S rRNA
⟨L⟩n = 0.80 ± 0.05 μ
⟨L⟩w = 0.80 ± 0.05 μ
n = 571
Number of Molecules
Length in μm

the glyoxal reaction mixture into the spreading solution. There is tris buffer in the spreading solution. Either of these factors alone should cause the removal of glyoxal from A and C residues. Therefore, in the molecules seen in the electron micrographs, it is probable that most of the G residue, and only the G residues, are present as glyoxal adducts.

Taole 1 summarizes the length of E. coli rRNA molecules as spread by several procedures. There are small differences between the lengths as measured by the several procedures. Our value for 23s rRNA, in conjunction with a molecular weight of 1.08×10^6 (Attardi and Amaldi, 1970), and a residue weight for E. coli Na rRNA of 345, gives an internucleotide spacing of 2.5_6 Å. Delius et al. (1972) find an internucleotide spacing of 3.7 Å for T7 mRNA by the gene 32 procedure.

The molecular lengths of Sindbis and 23s rRNA are measured as $3.4_5 \pm 0.14$ μ and 0.80 ± 0.05 μ, respectively. If the molecular weight of the latter is taken as 1.08×10^6 daltons (sodium salt), the molecular weight of Sindbis RNA is calculated as $4.6_5 \pm 0.4 \times 10^6$. Simmons and Strauss (1972) give $4.3 \pm 0.3 \times 10^6$.

Finally, we wish to mention that treatment with 0.5 M glyoxal as described above does not denature duplex DNA nor does it cause any opening up of the b2 deletion loop in a λ/λb2b5 heteroduplex (A. Forsheit, personal communication). Therefore, glyoxal may be used to extend single-strand DNA or RNA without affecting long, perfect duplex regions.

TABLE 1

rRNA Length Measurements[a] by Several Spreading Procedures

Method	16s E. coli	23s E. coli	18s HeLa
Urea[b]	0.38 ± 0.03	0.79 ± 0.08	0.59 ± 0.04
Urea[c]	0.40 ± 0.01	0.72 ± 0.02	
Formamide/urea[d]			0.51 ± 0.06
Dimethyl sulphoxide[e]	0.43	0.84	
Formamide/glyoxal[f]	0.43 ± 0.04	0.80 ± 0.05	

a) Number average lengths and standard deviations, all in μm.

b) Granboulan and Scherrer (1969).

c) Verma et al. (1970).

d) Robberson et al. (1971).

e) Nanninga et al. (1972).

f) This paper.

b) Sindbis virus RNA has cohesive ends. When Sindbis virus RNA is treated with glyoxal under the extreme conditions described above, almost all of the molecules seen are linear. We have observed that when Sindbis RNA is subjected to any one of several more gentle denaturing treatments, which are sufficient to cause partial extension of the molecules, about 25% to 50% (depending on the preparation) of the RNA molecules in an electron microscope grid are circular, with a duplex "handle" at one point on the circle.

For example, if Sindbis RNA in 0.010 M phosphate buffer, pH 8.0, is treated with 0.010 M glyoxal at 37°C, and then (after ca. 10^2-fold dilution) spread from 30% formamide, 0.10 M tris, 0.010 M EDTA, pH 8.5 onto a hypophase of 5% formamide with one-tenth the electrolyte concentration, the following observations are made as a function of time of incubation with glyoxal. At zero time, the molecules are collapsed bushes. After 20 minutes, they are slightly extended and many are circular. After 75 minutes, the molecules are more extended, and 25 to 50% of the molecules are scored as circles with an apparent handle or duplex stem. The stem has a length of about 0.083μ corresponding to 250 ± 50 nucleotide pairs. Typical micrographs are shown in Fig. 4. The molecules consist of smooth regions, secondary structure bumps of variable position and appearance, and the handle. The measured single-strand contour length, treating all secondary structure features as duplex is 2.76 ± 0.10 μ. Thus the molecules appear to be less extended than those shown in

Fig. 4. Electron micrographs of Sindbis RNA, treated as described in the text, showing circular molecules. In several cases, the duplex handle is identified with an arrow. The top two micrographs are after treatment with 0.010 M glyoxal for 75 minutes, and spread from 30% formamide; the bottom one is a spreading from 40% formamide without prior glyoxal treatment. For other details about the spreading solution and hypophase, see legend to Fig. 2.

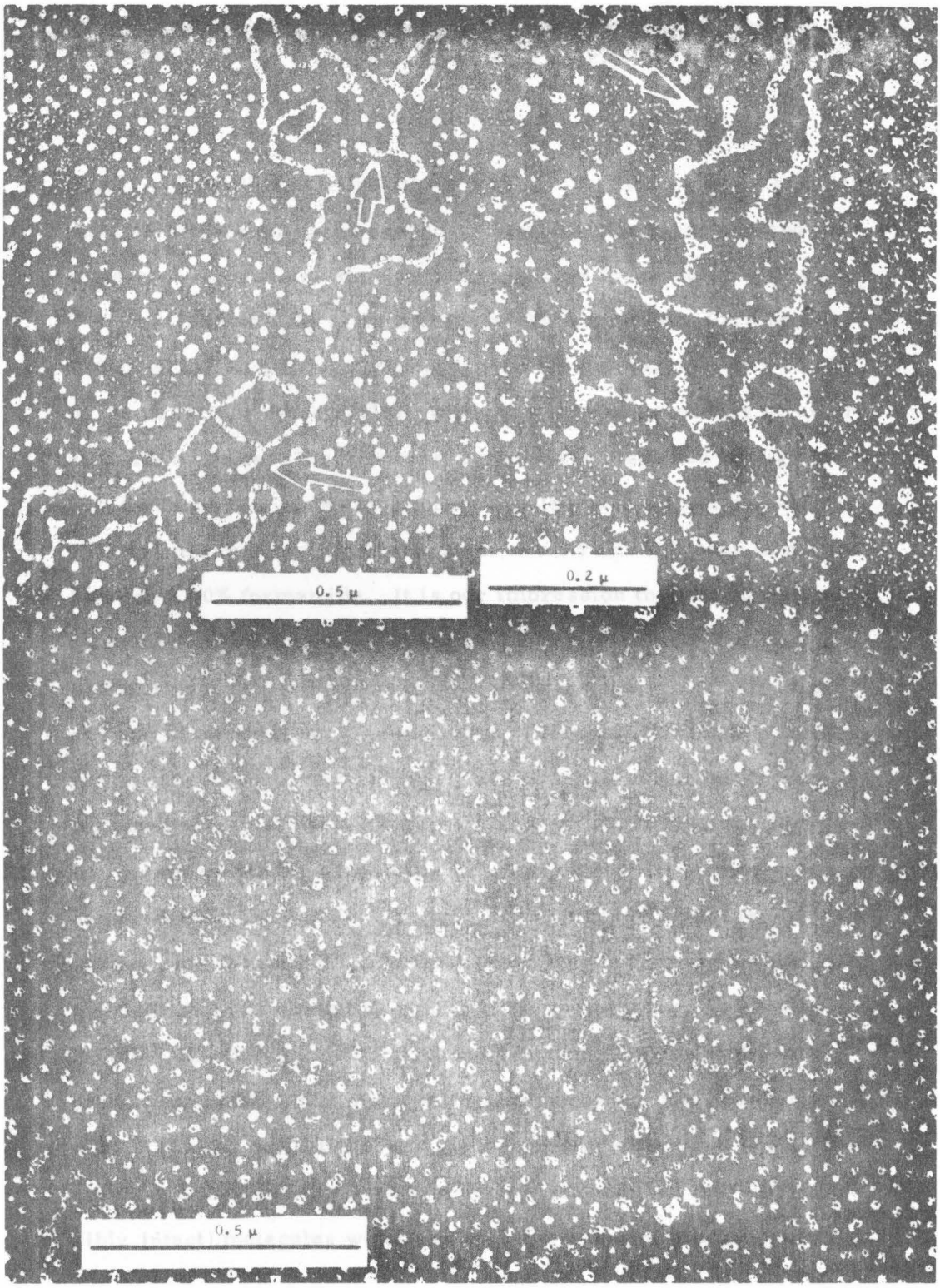
0.5 μ
0.2 μ
0.5 μ

Fig. 2. On still longer treatment with glyoxal, the circular structures open up, before all of the secondary structure is disrupted, and the molecules become as extended and smooth as those shown in Fig. 2.

If Sindbis RNA is spread from 40% formamide, 0.10 M tris, 0.010 M EDTA, pH 8.5, without treatment with glyoxal, 10% to 50% of the molecules are circular, with considerable secondary structure, and with a handle. Electron micrographs are displayed in Fig. 4. If 50% formamide is used, most of the circles have opened up, and the RNA is smoother and more extended. No circles are seen in spreadings from 60% formamide. It is our impression that the 40% formamide solvent represents a delicate balance between the denaturing power needed to partially extend the RNA and that which will cause opening of the circles. The variation of frequency of circles in different experiments may be largely due to small variations in spreading conditions.

Under proper annealing conditions, linear molecules with undamaged ends can reform circles. Thus, if Sindbis RNA is dialyzed against pure formamide at 4°C for one to two hours, and diluted into a 40% formamide spreading solution, the molecules are all linear. If, after dissociation by pure formamide, the RNA molecules are dialyzed into 40% formamide, 0.20 M phosphate buffer, pH 8.0 ($[Na^+]$ = 0.38 M) and incubated at 4°C, and then diluted into the 40% formamide spreading solution, the fraction of the long (and therefore possibly intact) molecules which are circular rises over a period of 4

hours to about 25%. Longer incubations are not useful because of degradation of the RNA.

c) Sindbis RNA has a poly-A sequence at one end. We chose to use poly-dT as a complementary polynucleotide strand to physically label the poly-A sequence of Sindbis RNA for EM mapping. It has several advantages for this purpose. Poly-dT is available as a high molecular weight polymer from General Biochemicals. The rA:dT duplex melts about 7° higher than the rA:rU duplex (Riley et al., 1966). Poly-dT itself gives an extended filament, even from our aqueous spreading solution.

The available evidence suggests that poly-A sequences, if present, are at the 3' end of RNA molecules. A terminal poly-A sequence could base pair with a stretch of T residues anywhere along the poly-dT chain. The complex would then have a Y-shaped structure, with one branch being Sindbis RNA and two branches poly-dT. If there were a poly-A sequence in the middle of an RNA molecule, the complex would have an X shape. A unique interpretation of a Y-shaped structure, for example, is complicated by the facts that many of the Sindbis RNA molecules are fragmented and that the poly-dT has a heterogeneous length distribution. However, it is possible to distinguish between Sindbis RNA and poly-dT by spreading under conditions in which the former has some residual structure whereas the latter does not.

By studying complexes of pure poly-rA with poly-dT, we observed that in our standard electrolyte, the strands are mainly

associated as duplexes in 40% formamide but significantly dissociated into single strands in 50% formamide. This observation is reasonably consistent with the report by Riley et al. (1966) that the rA:dT complex melts at 64° in 0.15 M Na^+.

Hybridization of poly-dT with Sindbis RNA was carried out by denaturing the mixture with pure formamide, renaturing at 37°C in 0.1 M NaCl, 0.01 M tris, 0.001 M EDTA, pH 7.0 for several hours. Each polynucleotide concentration was about 100 μg/ml. The samples were diluted and spread from 40% formamide. A large number of Y-shaped structures were observed. The RNA branch can be distinguished from the two dT branches because the former has scondary structure knobs and, even where it appears extended, is thicker. Typical micrographs are shown in Fig. 5.

Alternatively, Sindbis RNA was treated with 0.5 M glyoxal as described above. It was dialyzed against 0.10 M phosphate buffer, pH 8.0, at 37°C for three hours. Poly-dT was added and the mixture incubated at 37° for several hours. It was then spread from 30% or 20% formamide (hypophase, 5% and 0% formamide). Typical micrographs are shown in Fig. 6. In 30% formamide, the distinction between glyoxal treated Sindbis RNA and dT is rather subtle; the RNA is thicker and smoother. In 20% formamide, the RNA is more curved and shows some secondary structure knobs. The structures seen are Y-shaped. We conclude that the poly-A sequence on Sindbis RNA is at one end.

A small number of circular Sindbis RNA molecules with dT attached to the handle were seen. An example is shown in Fig. 5.

Fig. 5. Poly-dT hybridized to the ends of Sindbis RNA in 40% formamide spreadings without glyoxal as described in the text. The bottom micrograph shows a circular RNA molecule attached at the handle to poly-dT. The poly-dT had a length distribution ranging from 1 to 6 μm. It was obtained from the General Biochemicals Company, Chagrin Falls, Ohio 44022.

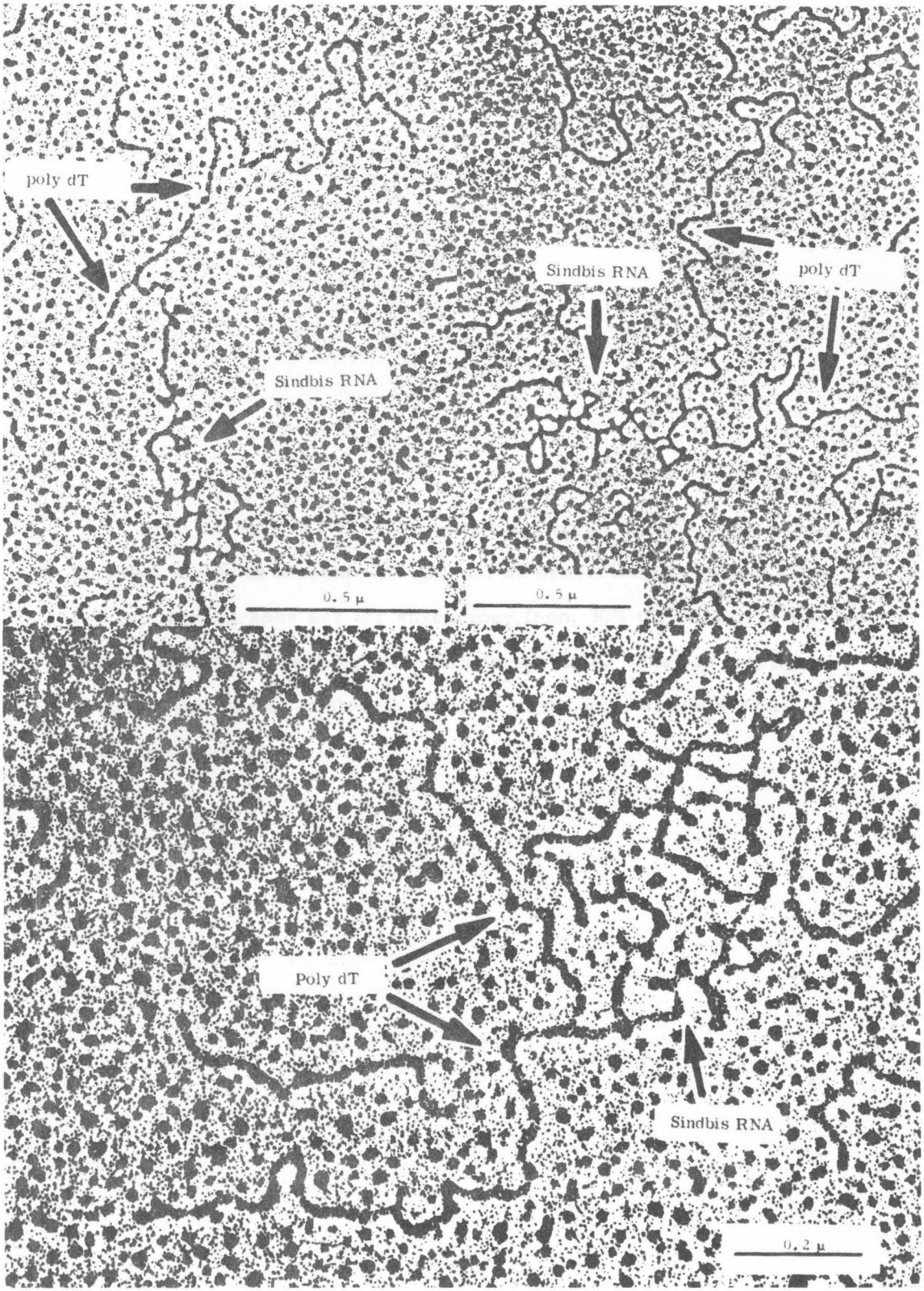
poly dT
Sindbis RNA
poly dT
Sindbis RNA
0.5 μ
0.5 μ
Poly dT
Sindbis RNA
0.2 μ

Fig. 6. Poly-dT hybridized to the ends of Sindbis RNA after the RNA has been treated with glyoxal as described in the text. The two top micrographs are for spreadings from 30% formamide. The bottom one is a spreading from 20% formamide. The top left micrograph shows one dT molecule attached to the ends of two Sindbis RNA molecules.

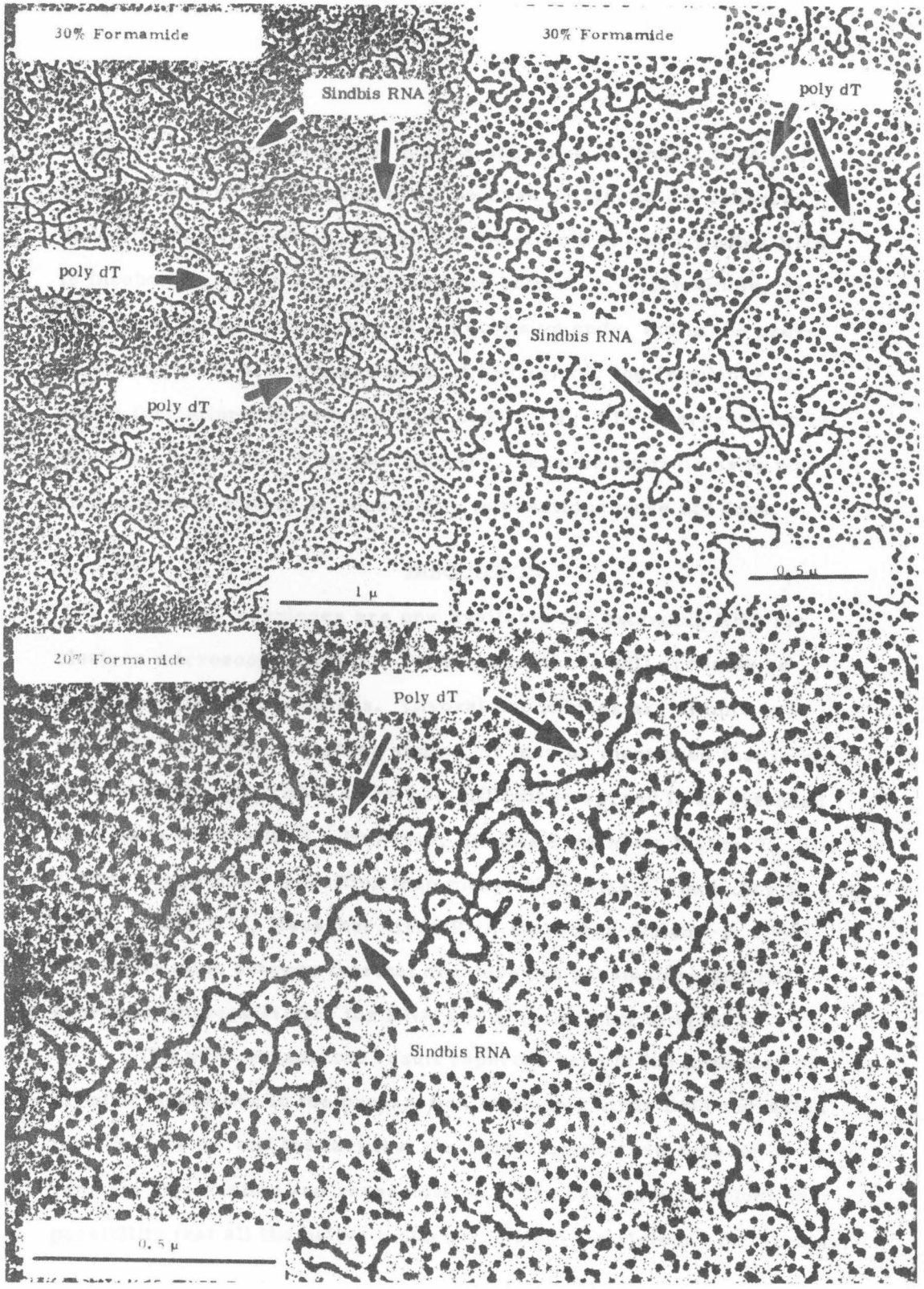
30% Formamide
Sindbis RNA
poly dT
poly dT
poly dT
1 μ
30% Formamide
poly dT
Sindbis RNA
0.5 μ
20% Formamide
Poly dT
Sindbis RNA
0.5 μ

This result suggests that the poly-A sequence of Sindbis RNA is not at all or only partially involved in the base pairing of the cohesive ends. In this connection, we wish to mention that when Sindbis RNA is incubated at 4° in 0.20 M phosphate buffer, 40% formamide, as described for the reannealing of the cohesive ends, but in the presence of poly-dT at a concentration of 150 μg/ml, the frequency of circle formation was reduced from 26% to 7%. The interpretation of this observation is not certain however, because controls as to possible nuclease effects or nonspecific interactions were not done.

DISCUSSION

Several techniques are now available for extending RNA for electron microscope studies. Different methods will probably be useful for different purposes. Glyoxal procedures are simple and versatile and deserve further study. It may be mentioned that in our experience E. coli rRNA is just as difficult to spread in an extended form as is Sindbis RNA. However, Sindbis RNA has a higher T_m and a more cooperative transition than many other RNA's, including E. coli rRNA, TMV, R17, Rauscher virus RNA (Sprecher-Goldberg, 1966). The correlation between thermal denaturation parameters and EM spreading characteristics for RNA's is evidently not simple.

The most unexpected result reported here is the presence of circular molecules in the preparation of Sindbis virus RNA extracted from the virion and the fact that the cohering ends are capable of reversible dissociation and reassociation. The data do not exclude the possibility that all the native molecules within the virions are circular,

and the linear molecules observed are due to degradative effects. The RNA had been deproteinized with phenol and SDS. It is unlikely that the cohesion of the ends is due to an attached protein.

The observed handle in the circular molecule could be a secondary structure feature in the middle of the linear molecule. We believe that this is incorrect and that the handle is due to the cohesive sequences very close to the ends. The observation of circular molecules with poly-dT attached to the handle (Fig. 5) supports this interpretation. Furthermore, we see a very low frequency of circles in Sindbis RNA after the 0.5 M glyoxal treatment. These molecules always have a handle. The linear molecules are smooth with no handle or other secondary structure features. Thus the handle is due to the duplex formation leading to cyclization. The handle structure is consistent with inverted repeat sequences close to the ends that are paired in a standard antiparallel Watson-Crick structure. We have estimated that the length of the handle corresponds to 250 ± 50 base pairs. Evidently, one of the cohesive sequences is not quite at the end of the molecule, because there is a poly-A sequence beyond it.

It may be recalled that the single strands of several types of adeno virus and of adeno-associated virus have cohesive ends (Garon et al., 1972; Wolfson and Dressler, 1972; Koczot et al., 1973). In the case of Sindbis RNA, the circular structure with the handle may be significant for replication and/or translation.

ACKNOWLEDGMENT

This research has been supported by NIH grant GM-1991. We are deeply grateful to Professor James Strauss and Dr. Ellen Strauss for generous assistance and loan of facilities for growing Sindbis virus, and their counsel as to the preparation and properties of the RNA.

REFERENCES

ATTARDI, G., and F. AMALDI. 1970. Structure and synthesis of ribosomal RNA. Ann Rev. Biochem. 39:183.

BROUDE, N. E., and E. I. BUDOWSKY. 1971. The reaction of glyoxal with nucleic acid components. III. Kinetics of the reaction with monomers. Biochim. Biophys. Acta 254: 380.

DAVIS, R. W., and R. W. HYMAN. 1971. A study in evolution: the base sequence homology between coliphages T7 and T3. J. Mol. Biol. 61: 287.

DAVIS, R. W., M. SIMON, and N. DAVIDSON. 1971. Electron microscopic heteroduplex methods for mapping regions of base sequence homology in nucleic acids. In (L. Grossman and K. Moldave, eds.) Methods in Enzymol. Academic Press, New York XXI, p. 413.

DELIUS, H., H. WESTPHAL, and N. AXELROD. 1973. Length measurements of RNA synthesized in vitro by E. coli RNA Polymerase. J. Mol. Biol. 74: 677.

EATON, B. T., and P. FAULKNER. 1972. Heterogeneity in the poly-A content of the genome of Sindbis virus. Virology 50: 865.

GARON, C. F., K. W. BERRY, and J. A. ROSE. 1972. A unique form of terminal redundancy in adenovirus DNA molecules. Proc. Nat. Acad. Sci. USA 69. 2391.

GRANBOULAN, N, and K. SCHERRER. 1919. Visualization in the electron microscope and size of RNA from animal cells. Europ. J. Biochem. 9: 1.

REFERENCES (continued)

JOHNSTON, R. E., and H. R. BOSE. 1972a. Adenylate-rich segment in the virion RNA of Sindbis virus. Biochem. Biophys. Res. Commun. 46: 712.

JOHNSTON, R. E., and H. R. BOSE. 1972b. Correlation of messenger function with adenylate-rich segments in the genomes of single-stranded RNA viruses. Proc. Nat. Acad. Sci. USA 69: 1514.

KOCZOT, F. J., H. J. CARTER, C. F. GARON, and J. A. ROSE. 1973. Self-complementarity of terminal sequences within plus or minus strands of adenovirus-associated virus DNA. Proc. Nat. Acad. Sci. USA 70: 215.

NANNINGA, N., M. MEYER, P. STOOF, and REIJNDERS, I. 1972. Electron microscopy of Escherichia coli ribosomal RNA: spreading without a basic protein film. J. Mol. Biol. 72: 807.

PFEFFERKORN, E. R., B. W. BURGE, and H. M. COADY, 1967. Intracellular conversion of the RNA of Sindbis virus to a double-stranded form. Virology 33: 239.

RILEY, M., B. MALING, and M. J. CHAMBERLIN. 1966. Physical and chemical characterization of two- and three-stranded adenine-thymine and adenine-uracil homopolymer complexes. J. Mol. Biol. 20: 359.

REFERENCES (continued)

ROBBERSON, D., Y. ALONI, G. ATTARDI, and N. DAVIDSON. 1971. Expression of the mitochondrial genome in HeLa cells. XI. Size determination of mitochondrial ribosomal RNA by electron microscopy. J. Mol. Biol. 60: 473.

SIMMONS, D. T., and J. H. STRAUSS. 1972. Replication of Sindbis virus. I. Relative size and genetic content of 26s and 49s RNA. J. Mol. Biol. 71: 599.

SPRECHER-GOLDBERGER, S. 1966. Differences between the structures of poliovirus and Sindbis virus infectious ribonucleic acids. Arch. Gesamte Virusforsch. 20: 225.

VERMA, I. M., M. EDELMAN, M. HERZBERG, and U. Z. LITTAUER. 1970. Size determination of mitochondrial ribosomal RNA from Aspergillus nidulans by electron microscopy. J. Mol. Biol. 52: 137.

WOLFSON, J., and D. DRESSLER. 1972. Adenovirus-2 DNA contains an inverted terminal repetition. Proc. Nat. Acad. Sci. USA 69: 3054.

PROPOSITIONS

Proposition I.

An Electronmicroscopic Method for Mapping Genes and Studying Genetic Sequence Relationships of RNA Tumor Viruses: An Application to the Study of Transformation Gene in Rous Sarcoma Virus.

The information content, genetic organization and structures of the genomes of RNA tumor viruses have recently been the subject of intensive investigation. At least 5 viral specific proteins, identified by SDS gel electrophoresis (1), appear to be viral gene products. Among these, two are glycoproteins with which the type specific antigens are associated, the remaining three are located within the virion and give rise to group specific antigenicity of the viruses. In addition to these structural proteins, each virion contains an RNA-directed DNA polymerase and possibly enzyme(s) responsible for transformation. Information for all these viral specific products can be grouped into four genetic elements - env (genes for envelope proteins), pol (genes for polymerase), gag (genes for gs antigens) and onc (genes for transformation) (1).

All these genes are contained in a $3x10^6$ dalton RNA genome. At present, very little is known about the arrangements of these genetic elements in the genome. There have been recent reports which indicate that in the avian system the onc gene is located near the 3' end (2) and the env gene at 25% fractional length from the 3' end (3).

It is proposed that the electronmicroscopic heteroduplex method

can be used for mapping these genes. Basically, the tumor RNA genome from a deletion or substitution mutant is hybridized to the complementary strand of the provirus DNA isolated from cells infected with wild type viruses. When the heteroduplex is examined in the electronmicroscope, the deletion (or substitution) loop or tail(s) (if the gene of interest is located at the end) locates the deletion (or substitution) gene. The provirus DNA has been successfully isolated and purified from RSV-infected duck or quail cells (4). The strand complementary to the RNA genome has been shown to be ~$3x10^6$ daltons, about the size of a 35S RNA. Presently the purified proviral DNA cannot be obtained in large quantities (~50ng/preparation). However, we have developed a "drop" spreading technique, which requires only ~1ng of nucleic acid sample for examination in the electronmicroscope. This method is therefore very useful in these studies. Several deletion mutant viruses such as td RSV-PRC (for onc gene) SN-8R RSV (for env gene) and possibly RSV_α (for pol gene) are available (5-7). The heteroduplex mapping procedure is summarized as follows:

(1) The proviral DNA (pDNA) is isolated and purified by the procedure of Varmus et al. (4).

(2) The wild type linear duplex pDNA, is denatured and allowed to anneal with a large excess of 35S RNA's from deletion mutant viruses. The resulting RNA:DNA hybrid molecules are then purified by Cs_2SO_4 gradient centrifugation.

(3) Samples of RNA:DNA heteroduplex for electromicroscopy

can be prepared by the drop technique in the standard formamide conditions (8). Depending on whether the deleted gene is located internally or not, either a deletion loop or a tail would be observed. This loop or tail would indicate the position of the gene of interest along the RNA genomes.

(4) To further locate the deleted gene relative to the 3' (or 5') end of the genome, 35S RNA of mutant virus is first subjected to limited digestion with 3'-exonuclease (9) (an RNA piece about $1x10^6$ daltons is removed) and then employed for heteroduplex experiment described above. The 3'-exonuclease digestion introduces a new (if the deleted gene is located internally or at 5' end of the RNA) or a longer tail (if the gene is at 3' end) on the heteroduplex. These tails would indentify the 3' end of the genome.

In addition to the gene mapping studies described above, the proposed method can also provide ways to analyze the relationship between viruses of different subgroups or different species. Of particular interest was the detetion of interspecies homologous sequences between feline RD-114 and baboon endogenous viruses (10), between murine (M. musculus) and woolly monkey viruses (11) and between rat (NRK) and murine (kirsten) viruses (12). Locating these homologous region in the viral genome would undoubtedly be very important in the understanding of the evolution, the mechanism of recombination and mutation of these viruses.

References

1. Baltimore, D. (1974) Cold Spr. Harb. Symp. Quant. Biol., 39, 1187.
2. Wang, L.H., P. Duesberg, K. Beemon and P.K. Vogt (1975) J. Virol., 16, 1051.
3. Duesberg, P., S. Kawai, L.H. Wang and H. Hanafusa (1975) Cold Spr. Harb. RNA Tumor Virus Meeting Abstract, p. 24.
4. Varmus, H.E., R.V. Guntaka, C.T. Deng and J.M. Bishop (1974) Cold Spr. Harb. Symp. Quant. Biol., 39.
5. Martin, G.S. and P.H. Duesberg (1972) Virology, 47, 494.
6. Duesberg, P.H., S. Kawai, L.H. Wang, P.K. Vogt, H.M. Murphy and H. Hanafusa (1975) P.N.A.S., 72, 1569.
7. Hanafusa, H. and T. Hanafusa (1971) Virology, 43, 313.
8. Davis, R., M. Simon and N. Davidson (1971) p. 413 In L. Grossman and K. Moldave (ed.), Methods in Enzymology, Vol. 21.
9. Singer, M.F. and G. Tolbert, (1965) Biochemistry, 4, 1319.
10. Benveniste, R.E. and G.J. Todaro (1973) P.N.A.S., 70, 3316.
11. Benveniste, R.E., R. Heinemann, G.L. Wilson, R. Callahan and G.J. Todaro (1974) J. Virol., 14, 56.
12. Benveniste, R.E., G.J. Todaro, E.M. Scolnick and W.P. Parks (1973), J. Virol., 12, 711.

Proposition II

Physical Mapping of Reverse-Transcription Primer Binding Site on Tumor Viral RNA Genome

An essential step in the replication of the RNA tumor viruses is the reverse transcription of genomic RNA to provirus DNA (1). This step requires not only a special enzyme, and RNA template, but also a primer molecule for initiating DNA synthesis (2). The nature and properties of the primer molecule in the transcription reaction *in vitro* have been a subject of intensive research. These *in vitro* primers have been characterized to be tRNA molecules ($tRNA^{Trp}$ for RSV (3) and $tRNA^{Pro}$ for MuLV (4)). The position where the primer associates with the genomic RNA presumably is the initiation site of the DNA synthesis. By analyzing the radioactive counts associated with the tRNA on alkali-treated RSV RNA fragments, J. Taylor and R. Illmensee (5) have recently located the primer binding site to be near the 5'-terminus of the 35S RNA. We propose a simpler and more precise way of mapping the primer molecule by electronmicroscopy. This work is important because the mapping of the primer site would give us much insight into the mechanism of tumor virus RNA replications.

Our method is based on the findings that, first, the 35S viral RNA contains in average one tRNA primer binding site per molecule (3) and secondly, most, if not all, of the 35S RNA's have a stretch of poly(A) sequence at their 3'-terminus (6). We wish to enzymatically synthesize a molecule containing both the tRNA primer and a poly dT sequence. This small tRNA-poly dT molecule,

when annealed with a 35S viral RNA, can serve as a linker molecule to hold the tRNA binding site and the 3' terminal poly(A) sequence together, through hybridization with their complementary sequences. This procedure is illustrated below:

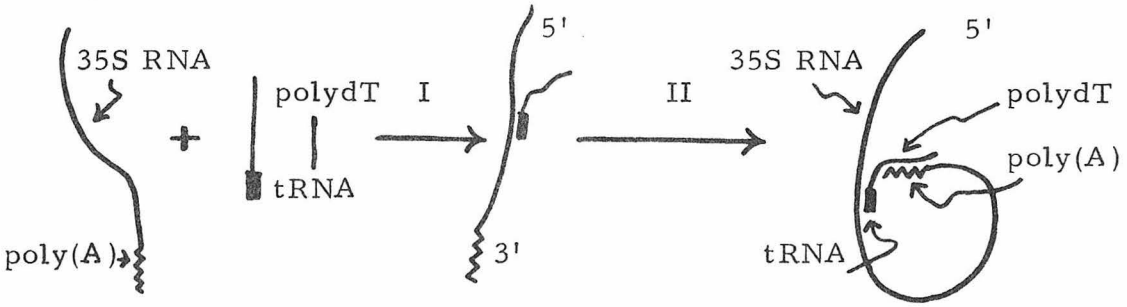

In the first step, a tRNA-polydT molecule is hybridized onto the 35S RNA through the tRNA binding sequences, the 3' terminal poly(A) sequence of the 35S RNA will then subsequently be annealed with the polydT sequence (on the tRNA-polydT molecule) leading to the formation of a circular structure. The second hybridization step is an intramolecular reaction and is expected to be kinetically favorable. Depending on the location of the tRNA binding sites, a σ shaped, circular or linear molecule will be observed.

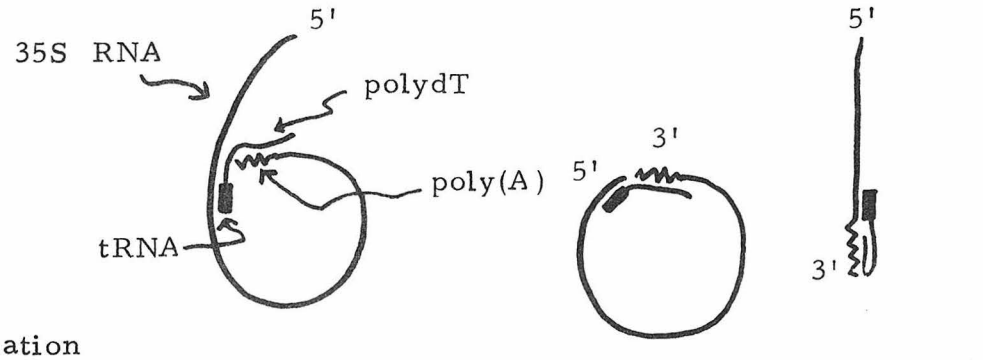

Location of primer: internally binding site | at 5' end | at 3' end

A σ shaped molecule would indicate that the tRNA-binding site is located internally on the 35S RNA. The point where the tail emerges with the circle identifies the tRNA binding site, and the length of the tail maps the position of this site relative to the 5' end. If, on the other hand, circular molecules (without tails) or linear molecules are constantly observed, the tRNA binds at or near the 5' or 3' end of the 35S RNA respectively. Therefore, in either case, the position of the tRNA binding sites can be accurately mapped.

To attach a polydT molecule to the tRNA, the terminal transferase reaction developed by W. Bender and N. Davidson (7) would be employed. This enzyme system has been proven very effective in snythesizing polydT tails(for an average length of 100 to 1000 nucleotides) on DNA primers. Unfortunately, the same reaction cannot be carried out with RNA primer such as a tRNA molecule. To circumvent this problem, we propose to use the viral endogenous reverse transcription machinery to attach one or a few deoxyribonucleotides to the tRNA through limited synthesis. This can be accomplished by conducting the in vitro transcription in the absence of one of the four deoxyribonucleotide precusors (8). The synthesis will then be stopped at the point when the omitted precusor is required for incorporation. The end product, a mono- or oligo-deoxyribonucleotide-attached tRNA, is then available for the terminal transferase reaction as described above.

We briefly summarize the whole EM mapping procedure as follows (using Rous Sarcoma virus as an example):

(1) An *in vitro* reverse transcription reaction is conducted in the presence of dATP, dGTP and TTP (but no dCTP). Under these conditions the first 7 nucleotides synthesized would be dAdAdTdGdAdAdG. This tRNAdAdAdTdGdAdAdG, referred to as tRNA-dG, can be dissociated from the template and isolated by centrifugation or electrophoresis (9).

(2) The tRNA-dG is elongated with dTTP to about 200-300 nucleotides (i.e. tRNA-dG-polydT$_{200}$) by terminal transferase reaction (7).

(3) Purified 35S RNA subunit (deprived of the native primer) is allowed to hybridize with the tRNA-dG-polydT$_{200}$ under conditions described in ref. 9.

(4) To extend the RNA molecule for electromicroscopic observation, the hybrid molecules are treated with glyoxal under conditions in which perfect duplexes are not dissociated (10). The glyoxal is then removed by dialysis at 4° C. RNA molecules, such treated, are in extended form yet contain unmodified poly(A) sequence available for hybridization with polydT molecule (7).

(5) The glyoxal-treated 35S RNA is then incubated under annealing conditions which favor the formation of poly(A): polydT hybrid (7).

(6) The resultant hybrids are analyzed by electronmicroscope as previously described (10).

This procedure, I believe, offers an efficient and promising way for mapping the reverse-transcription primer on tumor viral RNA genome.

References

1. Temin, H. M. (1971) Ann. Rev. Microbiol., 25, 609.
2. Flugel, R. M., U. Rapp and R. D. Wells (1973) J. Virol., 12, 449.
3. Dahlberg, J. E., F. Harada and R. C. Sawyer (1974) Cold Spr. Harb. Symp. Quant. Biol., 39, 925.
4. Waters, L. C. (1975) B. B. R. C., 65, 1130.
5. Taylor, J. M. and R. Illmensee (1975), J. Virol., 16, 553.
6. King, A. M. Q. and R. D. Wells (1975) J. Biol. Chem., in press.
7. Bender, W. and N. Davidson (1975) submitted to Cell.
8. Taylor, J. M., D. E. Garfin, W. E. Levinson, J. M. Bishop and H. M. Goodman (1974) Biochemistry, 13, 3159.
9. Taylor, J. M., B. Cordell-Stewart, W. Rohde, H. M. Goodman and J. M. Bishop (1975) Virology, 65, 248.
10. Hsu, M. T., H. J. Kung and N. Davidson (1973) Cold Spr. Harb. Symp. Quant. Biol., 38, 943.

Proposition III

The Isolation and Characterization of the Dimer-Linkage-Structure of Tumor Viral RNA.

Our finding that oncornavirus such as RD-114 and woolly monkey viruses all contain in their RNA genomes a similar dimer-linkage-structure (DLS) suggested a possible structural and functional importance of this common feature (1, 2). Poly(A) mapping results demonstrate that the linkage is perhaps via the 5' end of each monomer (1, 3). Models have been proposed to account for the formation of such a structure through a linker molecule or through self-complementary sequences of each monomer (2). Isolation and purification of this structure is necessary for the detailed structural analysis. This proposition describes methods to isolate and purify RNA fragments containing the dimer linkage structure and outlines plans for structural studies of this purified fragment. We shall use the most extensively studied RD-114 RNA as an example in the following discussions.

Isolation and Purification

(A) Enzymic Digestion: In order to isolate the DLS, the RD-114 RNA molecule needs to be digested in such a way that the DLS is preserved, while most other exposed sequences are either completely digested away or easily removed by column fractionation. Limited enzymic digestion offers a controlled and specific fragmentation method which is superior to alkaline or thermal degradation. We shall describe two possible enzymes for this digestion.

(1) 3' exonuclease: Since the DLS is perhaps located at the 5' end of each monomer, it will be the last sequence to be digested away if a 3'-exonuclease digestion is conducted. One difficulty frequently encountered in the 3'-exonuclease digestion method is that sometimes endo-activity is associated with the enzyme. Purified RNase II from E. coli (4), however, has been shown to be free from such contamination (5). For this reason we shall use this enzyme. Optimal conditions which allows the isolation of intact fragments enriched in DLS sequence may be found by varying the digestion time, temperature and the enzyme to substructure ratio etc..

(2) T1 RNase: Alternatively, T1 RNase can be used. This enzyme, when incubated at low enzyme concentration, at low temperature in the presence of Mg^{++} or for a short period of time can preferentially digest the exposed single-stranded RNA regions. From the morphology of the DLS in EM, it is estimated that about 600-800 nuc. (or 300-400 base pairs) are in the double-strand like region. This region should be preserved under the limited digestion conditions. Conditions which give the highest yield of DLS relative to other fragments as assayed by electron microscope will be used. Further purification of these DLS fragments are discussed below.

(B) Column Fractionation: The DLS fragments may be purified using either hydroxylpatite or cellulose column chromatography by virtue of the high stability of their intermolecular hydrogen

bonds.

(1) Hydroxylapatite Column: Hydroxylapatite columns have long been used as a simple and efficient way to separate single and double stranded RNA molecules (6). The standard procedure utilizes 0.12 M and 0.4 M phosphate buffer to elute single and double stranded molecules respectively. Molecules containing duplex regions of different stability can be fractionated by eluting at different temperatures or in different concentration of formamide and urea (7).

The DLS represent the most stable secondary structure in the RD-114 molecule. Under conditions such as 66% formamide and urea, 0.12 M cations at 52° C, the DLS is the only unmelted structural feature. Therefore, if the enzyme-digested fragments are loaded onto the column and eluted with 66% formamide and urea solvent containing 0.12 M phosphate buffer at 52° C, the DLS which has double-stranded character will remain bound to the column while fragments corresponding to other part of the molecule should come out. Elution with 0.4 M phosphate then washes the DLS down. A decent separation is expected.

(2) Franklin Column: Whatman CF-11 cellulose chromatography, first developed by Franklin, has been proven effective in separating single and double stranded RNA molecules (9, 10). Basically, single-strand RNA species are eluted in buffer containing 15% ethanol, double-strand RNA or RNA with high content of stable secondary structures elutes with buffer alone.

It has been suggested that by varying the elution temperature, this column can be used to fractionate RNA species according to their secondary structure content and stability (9,10). It is our hope that the separation of the highly stable DLS structure from other fragments in the RNase digestion mixture can be facilitated with the use of this column procedure.

Plans for Structural Studies of the Purified DLS Fragments

Our ultimate goal would be to determine the complete sequence (~300 base pairs) of the DLS structure. With the present technology this is no longer a formidable problem. Moreover, during the initial stage of these studies, important information about the tumor viral RNA structure can already be obtained. These are briefly discussed below:

(A) Identification of the Reverse Transcription Primer: In the Rous Sarcoma virus system, the primer, a $tRNA^{Trp}$, has been located near the 5' end of the genome (11). It is likely therefore that the DLS of RD-114 also carries one or two primer molecules. If the purified DLS fragments are incubated with purified reverse transcriptase in the presence of three ^{32}P-deoxyribonucleotide triphosphate precusors (one dNTP is left out on purpose, see proposition II). The incorporation of ^{32}P-TCA precipitable counts and hence the initiation of DNA synthesis is the first indication of the presence of the primer. The initial synthesis product, a tRNA primer with oligo-^{32}P-dNTP attached, can be

dissociated from the template and isolated by sedimentation through sucrose. This tRNA can be characterized by fingerprinting studies.

(B) Identification of the Linker Molecule:

If a small nucleic acid molecule is involved in holding the DLS together, it will be necessary to introduce a specific radioactive label to this molecule for its identification. This can be achieved by labeling the intact DLS fragment through kinase and γ^{32}P-ATP reaction (12). Under proper conditions, this procedure labels, and only labels, the 5' termini of the RD-114 RNA monomer and the linker molecule. The ^{32}P-labelled linker, as a separate molecular entity, should have its own characteristic physical and chemical properties such as sedimentation coefficient, gel mobility etc.. Fractionation methods based on these properties will be used for separating the linker from other DLS sequences. Structural analysis on this linker molecule can then be performed.

References

1. Kung, H. J., J. M. Bailey, N. Davidson, M. O. Nicholson and R. M. McAllister (1975), J. Virol., 16, 397.
2. Kung, H. J., S. Hu, W. Bender, J. M. Bailey, N. Davidson, M. O. Nicolson and R. M. McAllister (1975) submitted to Cell.
3. Bender, W. and N. Davidson (1975) submitted to Cell.
4. Singer, M. F. and G. Tolbert (1965) Biochemistry, 4, 1319.
5. Wellauer, P. personal communication.
6. Bernardi, G. (1969) B. B. A., 174, 423 and 449.
7. Tibbetts, C., K. Johansson and L. Philipson (1973) J. Virol., 12, 218.
8. Jakovcic, S., J. Casey and M. Rabinowitz (1975) Biochemistry, 14, 2043.
9. Engelhardt, D. L. (1972) J. Virol., 9, 903.
10. Robertson, H. D. and T. Hunter (1975) J. Biol. Chem., 250, 418.
11. Taylor, J. M. and R. Illmensee (1975) J. Virol., 16, 553.
12. Richardson, C. C. (1965) P. N. A. S., 54, 158.

Proposition IV

Chemical Modification of Alamethicin - A Probe for Studying Membrane Ion-Transportation Mechanism.

Alamethicin, a polypeptide isolated from Trichoderma viride, can induce voltage-gated action potentials in lipid bilayers (1-4). It has been suggested that "pore" formation by alamethicin inside the membrane is responsible for this significant increase in ion-permeabilities through the membrane. The mechanism of pore-formation has been shown to be strongly voltage-dependent. Each pore has more than one discrete conductance states. The cross-sectional area of the pore must necessarily be larger than the cavity of a single alamethicin molecule, judging from the magnitude of conductance of a single pore. Thus the pore is formed by more than one molecule. It is believed that there exist different states of alamethicin pore, which result in the discrete conductance states. However, the molecular structures of these different pore states are not clear.

The amino acid sequence of this polypeptide has been determined (5). The 17 amino acid residuces form a ring structure. An additional glutamine residue which has a free γ-carboxyl group is attached to the glutamic acid residue inside the ring. CPK molecular model suggests that the molecule can be represented as

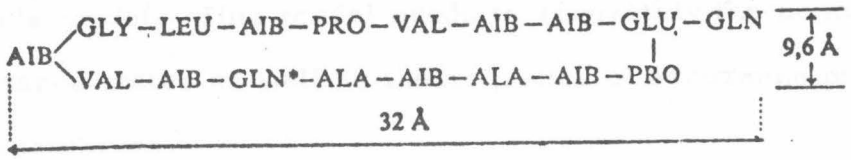

an elongated-flat loop (6). Alamethicins may exist in the form such that the polar groups (i.e. carbonyl groups) are clustered on one side and the apolar groups are on the other. Based on these structural models, G. Boheim has proposed a model to account for the observed discrete conductance states. The model is depicted in Fig. 1a. The pore is formed through lateral aggregation of alamethicin molecules inside the membrane. The hydrophobic residues of the amino acids are pointing outward and in contact with the lipid medium. The interior side is hydrophilic, where the cations are transported. The different conductance states of alamethicin channel are represented by a sequence of aggregates with different number of monomers and therefore different pore sizes.

Eisenberg et. al. (4) when studying the kinetics of pore formation in PE (phosphatidyl ethanolamine) membrane discovered that the stoichiometric-alamethicin concen tration dependence follows the relation expected for decamers in the concentration range tested. It thus suggests that the decamer is likely to be the most probable pore-former. They proposed a model in Fig. 1b. With the same lateral aggregation mechanism described above, the decamer is formed. The pore size (hence the conductance states) is determined by the opening or closing of the dimer molecules, rather than uptake or release of the monomers as proposed in Boheim's model. This model predicts accurately the number of conductance states as well as thefrequence of occurence of each state in PE membrane.

Figure 1.
Proposed models for the formation and interconversion of alamethicin pore states by 1) G. Boheim and b) M. Eisenberg et. al. The ion-conducting channel is shown end-on (perpendicular to membrane surface). Schematic.

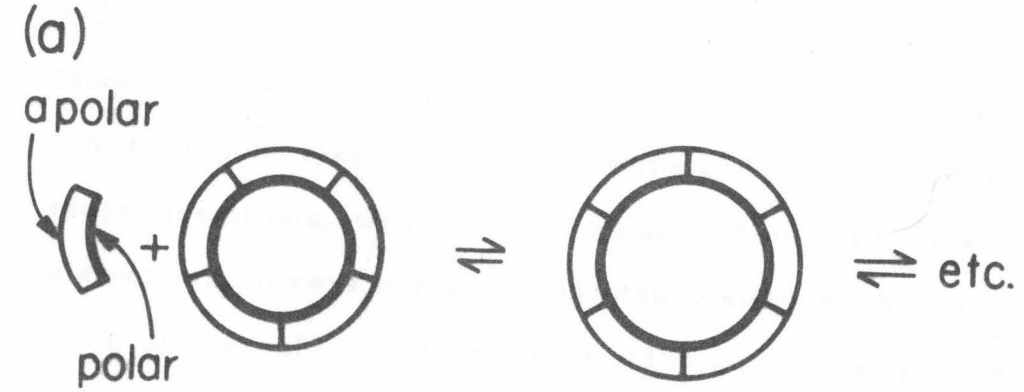
(a)
apolar
polar
+
⇌
⇌ etc.

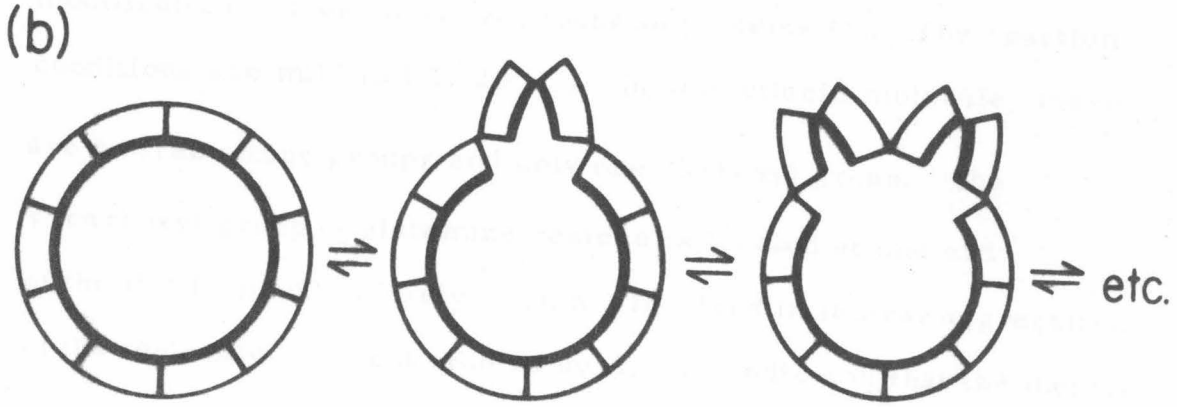
(b)
⇌
⇌
⇌ etc.

The main difference between these two models lies in the mechanism of pore-size transition. In the first model, the uptake and release of monomer is responsible for such transitions. Model II, however, requires an alamethcin dimer to act as a unit to affect the pore size. To gain more insight into the mechanism of these transitions, we propose to employ chemically crosslinked alamethicin dimers in these conductance studies. The alamethicin molecules should be covalently linked in such a way that neither their affinities toward the cations and the membrane, nor their tendency to form lateral aggregation are seriously affected.

Water-soluble carbodiimide has been widely used for specific modification of free carboxyl groups in proteins (7). The reaction conditions are mild (pH 5, 20° C). In alamethicin molecule, there are no free amino groups and only one carboxyl group. The γ-carboxyl group of glutamine residue is located at one end of the flat loop and is likely to be not involved in lateral aggregation of the molecule. Recent studies by A. Lau indicated that the methyl ester of alamethicin (i.e. the carboxyl group of the Glu-17 residue of alamethicin is methylated) exhibits similar voltage-gateable pore-formation as the unmodified species. These results suggest that modification of the carboxyl group does not interfere with the pore formation ability of the antibiotic. If a diamine such as $H_2N-(CH_2)_n-NH_2$, is incubated with alamethicin molecules in the presence of carbodiimide under proper conditions, carbodiimide

catalyzes the amide bond formation between the amino groups of the diamine and the carboxyl groups of alamethicin. The end product will be an alamethicin dimer joined together through a hydrocarbon bridge as depicted below.

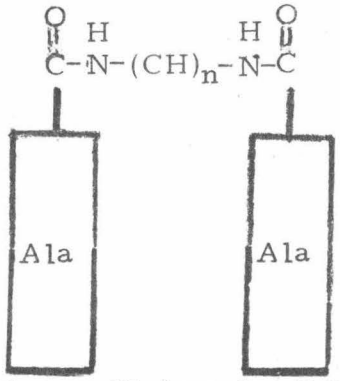

One would anticipate that sufficient flexibility of the hydrocarbon bridge is required for the lateral aggregation to occur. This can be achieved by using a diamine with proper hydrocarbon chain length (i.e. n) as starting material. Studies with diamine bridge of different length can also provide information about the distance between two adjacent alamethicin inside the pore.

The covalently linker dimer molecule can be separated from the unreacted monomers either by gel filtration
These purified dimer molecules are then used in the membrane-conductance experiments. If the conductance level as well as the probability of occurence do not change appreciably from those of the uncrosslinked molecules, it would then imply that dimer molecule indeed participate as a single unit in the pore formation

as Eisenberg et al's model predicts. On the other hand, if a two fold or more change of the conductance level of each state are observed, it tends to support but not prove the mechanism proposed by G. Boheim.

References

1. Pressman, B. (1968), Fed. Proc., 27, 1281.

2. Muller, P., and D.O. Rudin (1968), Nature, 217, 713.

3. Gordon, L.G.M., and D.A. Haydon (1972), BBA, 255, 1014.

4. Eisenberg, M., J.E. Hall and C.A. Mead (1973), J. Memb. Biol., 14, 143.

5. Payne, J.W., R. Jakes and B.S. Hartley (1970) Biochem. J., 117, 757.

6. Boheim, G. (1974) J. Memb. Biol., 19, 277.

7. Means, G.E. and R.E. Feeney (1971) p. 144-148, In Chemical Modification of Proteins, Holden-Day, Inc.

Proposition V

Application of Fluorescence Studies to the Alamethicin-Membrane System

Fluorescence Spectroscopy is one of the most sensitive and versatile of the optical techniques for structural studies of macromolecules such as polypeptides and lipid membranes (1,2). When a fluorescent dye is introduced into a specific site of a macromolecule, its fluorescence properties such as emission spectra, fluorescence polarization, quantum yield and decay times can provide information about the immediate environment around the binding site. Thus it can also be used as a sensitive probe for monitoring the conformational change of macromolecules (2). Applications of these techniques to the studies of structural and biochemical properties in protein and membrane have been quite rewarding.

In an effort to gain more insight into the ion-transporting mechanism by alamethicin (see Proposition IV), we wish to describe here fluorescent approaches for studying the interactions between alamethicin and lipid membrane and providing information about their molecular structures.

Fluorescent Studies of Alamethicin

Alamethicin is known to aggregate extensively. This aggregation is much enhanced with increase in the concentrations of alamethicin and/or salt in the solution (2). When the aggregates come in contact with the lipid bilayer membrane, most of them become

adsorbed onto the bilayer surface (4). Upon the application of a transmembrane voltage with the appropriate sign and magnitude the adsorbed aggregates of alamethicin are driven into the membrane interior, creating an entity called a pore (5, 6). It has been speculated that alamethicin conformations are different in the various states (3-6). The different forms of alamethicin may be summarized as follows:

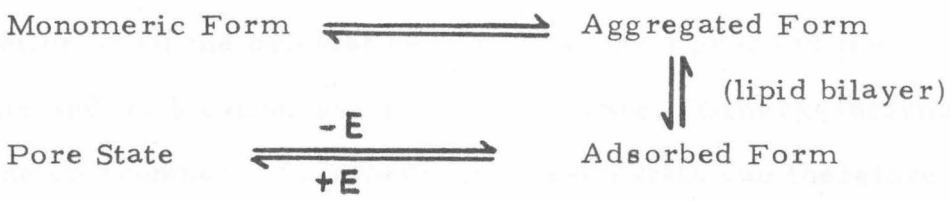

We propose that a fluorescent chromophore be covalently attached to a specific site of the alamethicin molecule and such chromophore be used as an internal probe to study the environmental and structural changes of alamethicin associated with the transitions. Compounds I and II will be employed (7).

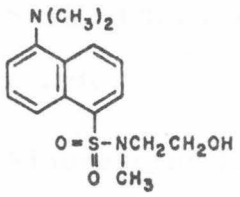

I

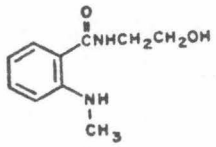

II

I. β - (N-methyl-dansyamide)-ethanol

11. β - (N_b-methyl-anthranilamide)-ethanol

These compounds contain hydroxyl groups which can be covalently linked to the carboxyl group of alamethicin's Glu-17 residue through carbodiimide catalytic reaction (see proposition IV). They also have fluorescent properties quite sensitive to the medium around them (7, 2). Variation of quantum yield and shift in λ max are induced as the polarity of the microenvironment around them changes. These properties can thus help identifying the surroundings of the carboxyl group, which in turn can provide information about the orientation of the carboxyl group in the molecule and its location inside the membrane. General information about the environment of alamethicin in each state can therefore be obtained. Furthermore, if different spectral properties can be demonstrated for each conformational state, they are very useful in the kenetic and equilibrium studies on the structural transitions of alamethicin molecules. It should be pointed out that two compartment-quartz cells suitable for conducting electrical experiments on lipid bilayers have been successfully applied in fluorescent studies of membrane (8, 9). This enables the alamethicin in its pore state to be similarly studied.

(II) Fluorescent Studies of Lipid Bilayer Membrane

It has been shown that in the adsorbed state without a transmembrane voltage, the main interaction between alamethicin and phosphatidyl bilayer is essentially confined to the water lipid interface. As the alamethicin aggregates are pulled into the membrane interior to form ion-conducting pore (i.e. in the pore state), the hydrophobic region of alamethicin are in close contact

with the hydrocarbon interior of the bilayer (6). The formation of ion-conducting pore requires not only the interaction between alamethicin molecules but also their interactions with lipid molecules in the membrane. Knowledge about the conformational change of membrane associated with such processes are the basis for the understanding of the ion-transportation mechanism. These studies have not yet been reported.

Recently several fluorescent analogs of membrane lipids have been synthesized (10). They have selected affinity for different

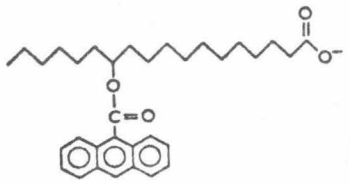

III

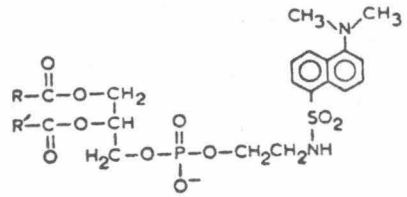

IV

V

III, anthroyl stearic acid (AS)
IV, dansyl phosphatidyl ethanolamine (DPE)
V, octadecyl naphthylamine sulfonate (ONS)

transverse regions of phosphatidyl choline bilayers. Compound III, IV and V are specific for the hydrocarbon, glycerol and aqueous interface regions respectively. Proper amounts of each dye, when

incorporated individually into the membrane, can serve as an indicator for the particular region it is located. The structural change of lipid bilayers resulted from interactions with alamethicin molecules can be accordingly followed by the fluorescent properties of each indicator. Furthermore, through fluorescent polarization studies, the flexibility of each region, before and during ion-transporting process, can be measured and compared. Information obtained from such studies, I believe, has great value in the understanding of the membrane active-transport system.

References

1. Brand, L. and J. R. Gohlke (1972) Ann. Rev. Biochem., 41, 843.
2. Edelman, G. M. and W. O. McClure (1968) Accounts Chem. Res. 1, 65.
3. McMullen, A. I. and J. A. Stirrup (1971) B. B. A., 241, 807.
4. Lau, A. L. Y. and S. I. Chan (1974) Biochemistry, 13, 4942.
5. Eisenberg, M., J. E. Hall and C. A. Mead (1973) J. Memb. Biol., 14, 143.
6. Boheim, G. (1974) J. Memb. Biol., 19, 277.
7. Yang, C. H. and D. Soll (1973) Archives Biochem. Biophys., 155, 70.
8. Smekal, E., H. P. Ting, L. G. Augenstein and H. T. Tien (1970) Science, 168, 1108.
9. Alamuti, N. and P. Lauger (1970) B. B. A., 211, 362.
10. Waggoner, A. S. and L. Stryer (1970) P. N. A. S., 67, 579.